PhD Thesis

Interaction and disorder in helical conductors

Anders Ström

GÖTEBORGS UNIVERSITET

Department of Physics
University of Gothenburg
September 2012

Front cover: The Kondo temperature as a function of the Rashba interaction strength (horizontal axis) and the Luttinger liquid parameter (vertical axis) on the edge of a quantum spin Hall system with magnetic impurities. The scale is logarithmic and lighter colour corresponds to higher Kondo temperature.

ISBN 978-91-628-8535-9

Ale Tryckteam
Bohus 2012

Interaction and disorder in helical conductors

Anders Ström

Department of Physics
University of Gothenburg
SE-412 96 Göteborg, Sweden

Abstract

Different effects from electron-electron interactions and disorder in helical and quasi-helical conductors are studied using bosonisation and renormalisation group methods.

The combined effects of Rashba spin-orbit interaction and magnetic Kondo-type impurities in the helical edge liquids of quantum spin Hall insulators, are investigated. The Kondo temperature is shown to depend on the strength of the Rashba coupling, which allows for electrical control of the Kondo physics by an external electric field.

Anderson localisation due to disordered impurity backscattering in a quasi-helical conductor is also studied. A quasi-helical conductor is a one-dimensional system in which half of the available states are effectively removed from the system with the combination of spin-orbit interaction and magnetic or electric fields. The resulting conductor have counterpropagating modes that are approximately, but not completely, spin-filtered. It is shown that an applied magnetic field can be tuned to make the system pass through two metal-insulator transitions at different magnetic fields, allowing for a conducting quasi-helical phase for intermediate field strengths.

Furthermore, biased and unbiased point contact tunnelling between two quantum spin Hall edges are investigated, in addition to the study of combined effects of electron-electron interaction and different types of Rashba interactions on the quantum spin Hall edges. A disordered Rashba coupling is shown to localise the electrons for sufficiently large Rashba and electron-electron interaction strengths.

The thesis also contains a quick introduction to one-dimensional physics, bosonisation and renormalisation group theory, to set the stage for the topics to be discussed.

Acknowledgments

I thank Anna, Hugo and Stina, for filling my world with love. Without you, physics would be too difficult for me.

My supervisor, Henrik Johannesson, is one of the most inspiring people I have ever met. Regardless of what I need to hear, you always seem to come up with just that. Thank you.

It is a pleasure also to thank my coworkers. First of all I thank Gia Japaradize, both for being a great physicist and collaborator, but also for being a great person in general. It has also been great working with one of my officemates, Erik Eriksson. Thank you for the collaboration and the discussions. A big thank you too, Bernd Braunecker, who always seems to ask the right questions. I also thank Girish Sharma for the collaboration.

There are also two people who stayed in the physics buildings of Gothenburg almost as long as I did. Thanks a lot for making these eleven years even more enjoyable than they otherwise would have been, Carl Borgentun and Joakim Nyman.

Finally, I want all the people on the third floor of Soliden to know that you have been very important to me. You are slightly too many for me to risk forgetting one of you, so I thank you collectively.

Contents

1

Introduction

In this thesis we will explore how interaction and disorder influence the physics in a helical conductor. Helical conductors appear at the edge (or surface) of topological insulators, a newly discovered state of matter, but similar systems mimicking helical conductors can also be constructed from different types of one-dimensional conductors. To set the stage, let us therefore begin by introducing and briefly discussing the notions of interaction, disorder, and topological insulators.

1.1 Interactions in condensed matter physics

Interactions between the electrons in a solid state system may seem like the first thing one needs to consider when setting up a mathematical description of the system. Many properties of for instance metals can, however, be described by considering the conduction electrons as non-interacting and free to move around in the metal, like the atoms that constitute an ideal gas. A non-interacting electron system is called an ideal *Fermi gas*. In a Fermi gas, all available states with energy lower than the Fermi energy are occupied. This picture is not good enough when electron-electron interactions become important. The most successful and useful theory that properly describe solid state systems with electron-electron interaction is the so called Fermi liquid theory, first proposed by Landau [1]. The basic idea is that interactions are accounted for by regarding the elementary excitations as *quasiparticles*, i.e. the microscopically complicated system behaves as if it were made up of particles interacting only very weakly with each other. The situation is similar to the one in quantum electrodynamics, where a charged particle is travelling with a cloud of photons, thereby changing it's effective charge. In

close analogy, the conduction electrons in a metal will stir up density fluctuations around it as it travels through the system, thereby changing for instance its effective mass. The quasiparticles will share some properties with the "bare" electrons from which they are made, while other properties will be determined by collective effects of the system. Remarkably, many observable properties of a normal metal or semiconductor can be predicted from Landau's Fermi liquid theory, neglecting collective effects, and replacing the electrons by quasiparticles with a new effective mass, and, a finite life time.

However successful, there are many examples of physical systems that cannot be described by Fermi liquid theory. Throughout this thesis, we will consider one of these examples, namely systems of interacting electrons in one dimension, in their standard setting often well modelled by the so called *Luttinger liquid theory* [2, 3].

Physics in one dimension - realised for instance by electrons confined to a quantum wire, a carbon nanotube or the edge of a two-dimensional quantum well - is often radically different from physics in higher dimensions. Put simply, the difference most often lies in the fact that it is no longer possible for a single electron to move through the system without significantly influencing the surrounding electrons. In one dimension, any moving electron will bump into other electrons and any movement of an electron in one dimension will therefore have to be a collective phenomenon. Some of these are quite counterintuitive. For instance, the charge and spin attached to a single electron that is inserted into the system (e.g. via tunnelling from an STM tip) will break up and be split into two separate collective excitations carrying spin and charge individually. The fact that the electrons will only have two directions to choose from will also have dramatic consequences. In particular, the Fermi level will consist of two points in the Brillouin zone, at $k = \pm k_F$ and the low-energy excitations around these points will be limited, so that any particle-hole excitation will have a well-defined energy and momentum, implying that electrons in one dimension can effectively be described as a system of bosons. As we shall see in this thesis, this remarkable feature can be taken advantage of to probe the physics with powerful analytical methods.

1.2 Disorder

It was shown by Anderson over 50 years ago that a disorder potential, i.e. a randomly distributed scattering potential, can cause a metallic system to undergo a transition into an insulator [4]. This effect is known as

Anderson localisation. Real systems are not perfect, so disorder and, potentially, Anderson localisation, is something that has to be accounted for.

Anderson localisation is a quantum effect that can be understood in terms of the electron waves. If one regards the electron system as a system of standing waves, each confined in space to a lattice site, the electrons will have a finite amplitude to tunnel between the sites. In a disordered system, the potential energy experienced by the electrons will be randomly distributed between the sites, and thus, the phases of the quantum interference between the possible tunnelling paths for the electrons vanish on average.

In a three-dimensional system, Anderson localisation is a rather weak and subtle effect that comes into play only if the disorder is strong enough. In two dimensions, the scattering against the disorder potential becomes more important, and a free electron system in two dimensions is always localised. However, the *localisation length*, the characteristic length with which the extension of electron wave functions decay, can be very large. Anderson localisation is most dramatic in a one-dimensional electron system, though, where the localisation length is often of the same order of magnitude as the mean free path.

Since the individual effects of both interactions and disorder are most pronounced in one dimension, the combined effect of these become very interesting. As we shall see, in a helical liquid - the type of one-dimensional electron system that we study in this thesis - the interplay between interactions and disorder indeed lead to some fascinating and unexpected phenomena.

1.3 Topological insulators

Ever since the important work on phase transitions by Landau [5] in the 1940's, different states of matter have typically been classified according to which symmetries are spontaneously broken. It has been realised, however, that there is a large class of states that can be characterised not by what symmetries they break, but by the value of some topological invariant. These matter states are said to be topologically ordered [6, 7]. This notion of topological order have sprung from studies of the integer and fractional quantum Hall effects. Recent additions to this family of topologically ordered systems are the two- and three-dimensional topological insulators and the topological superconductors and superfluids. Good reviews on these subjects are found in refs. [8] and [9].

The two-dimensional incarnation of the topological insulator state,

also known as the quantum spin Hall effect, was first predicted to be present in graphene, by Kane and Mele [10] in 2005. It turned out, however, that the spin-orbit interaction in graphene is too weak to produce the large band gap required to sustain a topologically ordered state. In 2006 Bernevig, Hughes and Zhang predicted the quantum spin Hall effect to be present in HgTe quantum wells, which was then experimentally confirmed in 2007 by König et al. [11].

A quantum spin Hall insulator has a band gap in the bulk, just as an ordinary insulator, but with topologically protected edge states with a dispersion crossing in the bulk gap. These states are helical, which means that they move in opposite directions for opposite spins. Possible applications for these materials include dissipationless transport along the edges, which would be useful in all sorts of devices in the future. Since, in the ideal case, the edge transport is spin filtered, one may envision promising applications particularly in spintronics [12].

Three-dimensional topological insulators, with surface states also protected by time-reversal symmetry, were predicted to exist in certain BiSb alloys by Fu and Kane in 2007 [13]. This was experimentally confirmed by Hsieh et al. in 2008 [14] using ARPES. Later, more materials have been predicted and some of them experimentally tested [15, 16]. Though interesting, 3D topological insulators are not treated in the thesis. The same goes for topological superconductors and superfluids, which are other related states of matter [17–20].

This thesis deals with both helical and *quasi-helical* conductors, i.e. one-dimensional conductors where opposite spins move primarily in opposite directions. As we shall discuss, quasi-helical conductors, where the counterpropagating electrons are not completely spin-filtered, can be realised in quantum wires and carbon nanotubes under certain conditions [21, 22].

1.4 Outline

The thesis addresses the problem of interaction and disorder on the edges of quantum spin Hall insulators and in quasi-helical conductors. It is arranged as follows. Chapter 2 provides a very brief introduction to topology in physics and topological insulators, with the focus on the first experimentally realised quantum spin Hall system, the HgTe quantum wells.

In chapters 3 and 4, the investigations of tunnelling at a point contact on the edge of a quantum spin Hall system (chapter 3) and of a spatially disordered Rashba on the edge (chapter 4) is presented in some

detail. One-dimensional field theory and the methods of bosonisation and renormalisation group theory are presented in short introductory sections, with additional details introduced when needed in the applications . The work of these two chapters were published in refs. [23] and [24], respectively. These articles will be referred to as Paper I and Paper II, respectively. Chapter 5 deals with metal-insulator transitions through Anderson localisation in quasi-helical conductors. The RG analysis of Anderson localisation is demonstrated quite thoroughly, and a novel two-fold RG scheme is presented. This work has been submitted for publication and will be referred to as Paper III [25]. In Chapter 6, the combined effect of Rashba and Kondo interactions on a quantum spin Hall edge is discussed. This work is also submitted for publication will be referred to as Paper IV [26]. Papers I-IV are attached to the thesis.

Chapter 7 contains a summary of the work and also a brief outlook on interesting topics that await solutions.

2

Topological insulators

A topological insulator has an insulating bulk, but massless conducting edge modes. The insulating bulk has a certain topological invariant that differs from that of an ordinary insulator. The edge, or surface, constitutes an interface between materials with different topology of their Hamiltonians and it turns out that the bulk energy gap must close precisely when going from a topological to a regular insulator. Thus, gapless states must exist on the insulator surface. A two-dimensional topological insulator is called a quantum spin Hall (QSH) system and its edge is a helical conductor. This means that counterpropagating electrons will have opposite spins, or more correct, they will transform into each other under time reversal symmetry. This is something that turns out to give rise to a multitude of theoretically interesting effects and potential applications. Throughout this thesis, we will investigate different aspects of interactions and disorder in helical conductors, so to understand the context, this chapter gives a brief introduction to topological insulators and the notion of topology in physics.

This chapter follows very closely the exposition in ref. [27]. Other, more extensive reviews, can be found in refs. [9] and [8].

2.1 Homotopy

Before saying anything about topological insulators, we have to know what is "topological" about them. The topological concepts that will be important are those of *homotopy* and *homeomorphisms*, so we will start with the necessary definitions. First, we need to know what topological spaces and manifolds are. A good introduction to the subject of topology in physics is found in Nakahara's textbook [28].

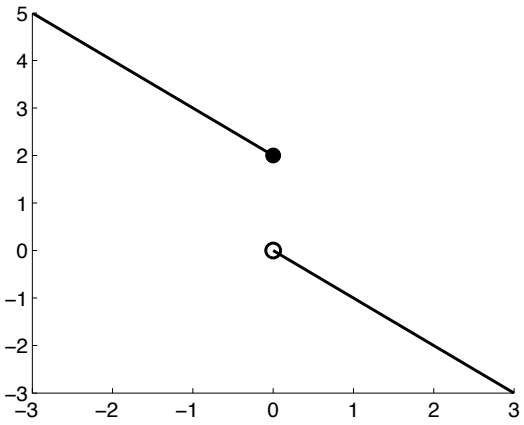

Figure 2.1: $x \in \mathbb{R}$ on the horizontal axis and $f(x) \in \mathbb{R}$ on the vertical axis.

A *topological space* is defined to be the pair $(X, \mathcal{T})$, where X is just a set and $\mathcal{T}$ is a collection of open subsets satisfying:

i. $\emptyset$ and $X \in \mathcal{T}$.

ii. The union of a finite number of the subsets in $\mathcal{T}$ is also in $\mathcal{T}$.

iii. The intersection of a finite number of the subsets in $\mathcal{T}$ is also in $\mathcal{T}$.

We will refer to X alone as a topological space which is given a topology by $\mathcal{T}$.

A map $f : X \to Y$, where X and Y are two topological spaces, is *continuous* if the inverse image of an open set in Y is an open set in X. As an example, consider the map shown in fig. 2.1, $f : \mathbb{R} \to \mathbb{R}$ defined as

$$f(x) = \begin{cases} -x + 2, & x \leq 0 \\ -x, & x > 0 \end{cases} . \tag{2.1}$$

As a function of x, f is clearly discontinuous. We use what is called the *usual topology* on $\mathbb{R}$, i.e. $\mathcal{T}$ consists of all open intervals and their unions. Consider the two open intervals $I_1 = (3, 4)$ and $I_2 = (1, 3)$. The inverse images of I_1 is an open set, $f^{-1}(I_1) = (-2, -1)$, but the inverse image of I_2 is a half-closed set, $f^{-1}(I_2) = (-1, 0]$. Thus, by definition, f is *not* continuous.

The map $f : X \to Y$, is called a *homeomorphism* if it is continuous and has an inverse $f^{-1} : Y \to X$ which is also continuous. An equivalence relation $X \sim Y$ can then be defined if such a homeomorphism exists between X and Y. Two topological spaces can be thought of as

homeomorphic to each other if one can be continuously deformed into the other, that is, without any tearing or pasting being done. A *topological invariant* is a quantity conserved under homeomorphisms. This means that two spaces with differences in their topological invariants are not homeomorphic to each other

An m-dimensional *manifold* is an m-dimensional topological space that is locally Euclidian, i.e. there is a neighbourhood that is homeomorphic to $\mathbb{R}^m$ around every point on it. More exactly, a topological space M is a smooth manifold if it comes with an atlas of charts $\{(U_i, \phi)\}$, where $\{U_i\}$ is a family of open sets covering M, i.e. $\cup_i U_i = M$, and ϕ_i, called a *coordinate function*, is a homeomorphism onto an open subset of $\mathbb{R}^m$.

We are now finally ready to discuss *Homotopy classes*, which are equivalence classes of loops on a manifold. Two loops are equivalent if they can be continuously deformed into one another. To get a clear definition of homotopy, we have to define what a loop is:

Let X be a topological space and $I = [0, 1]$. A *path* is a continuous map $\alpha : I \to X$ with initial point $\alpha(0) = x_0$ and end point $\alpha(1) = x_1$. A *loop* is a path which starts and ends at the same point, $\alpha(0) = \alpha(1) = x_0$, called the base point of the loop.

Now, let $\alpha, \beta : I \to X$ be two different loops on X with the same base point x_0. We introduce an equivalence relation $\sim$, stating that $\alpha \sim \beta$ if there exists a continuous map $F : I \times I \to X$ such that

$$F(s, 0) = \alpha(s), F(s, 1) = \beta(s) \ \forall \ s \in I \tag{2.2}$$

and

$$F(0, t) = F(1, t) = x_0 \ \forall \ t \in I. \tag{2.3}$$

If $\alpha \sim \beta$ under this equivalence relation, they are said to be *homotopic*. The meaning of this definition is just that α and β are homotopic if they have the same base point and can be continuously deformed into one another.

The homotopy classes form the elements of the *first homotopy group*, or the *fundamental group*, of X at x_0, denoted $\pi_1(X, x_0)$. The homotopy group of a manifold is thus defined at each point on the manifold. However, one can show that in most cases, π_1 can be defined on the whole manifold and there is no need for choosing a base point:

An *arcwise connected* topological space is a topological space on which for all pairs of points $x_0, x_1 \in X$ there exists a path α so that $\alpha(0) = x_0$ and $\alpha(1) = x_1$. Let X be an arcwise connected topological space and

let $x, y \in X$. Then $\pi_1(X, x) = \pi_1(X, y)$. A manifold that has a trivial fundamental group, $\pi_1 = 1$, is said to be *simply connected*.

As an example, let us look at the fundamental group of a circle. It is actually easy to understand that $\pi_1(S^1) \simeq \mathbb{Z}$: a loop that goes around the circle $n \in \mathbb{Z}$ times can only be continuously deformed into a loop that goes around the circle $m \in \mathbb{Z}$ times if $n = m$. Furthermore, a loop encircling S^1 n times plus a loop encircling it m times yields a loop encircling S^1 $n + m$ times. Thus, the loops can be characterised with an integer, up to homotopy.

We can also calculate the fundamental groups of manifolds that are products of arcwise connected topological spaces, using the following theorem:

Let X and Y be arcwise connected topological spaces. Then $\pi_1(X \times Y) \simeq \pi_1(X) \oplus \pi_1(Y)$.

Using this, we can easily obtain the fundamental group of a torus:

$$\pi_1(T^2) \simeq \pi_1(S^1 \times S^1) \simeq \pi_1(S^1) \oplus \pi_1(S^1) \simeq \mathbb{Z} \oplus \mathbb{Z}. \tag{2.4}$$

We have now only talked about the first homotopy group. Higher homotopy groups $\pi_n, n > 1$, are concerned with equivalence classes of higher dimensional loops, for instance $\pi_2(S^2) = \mathbb{Z}$, since spheres can wrap themselves around other spheres an integer number of times.

The homotopy groups of a manifold (or, more generally, a topological space), are examples of topological invariants, so they can be used to determine whether two manifolds are homeomorphic to each other or not.

2.2 Topology in physics

So what does all this have to do with condensed matter physics? A field in physics is a function $\phi(z)$ associating a physical quantity to each point z in space-time, or rather, to each point in the part of space-time relevant to the physical system we are dealing with. In a classical field theory, the values of the fields can be represented by numbers, while in a quantum field theory, the values are represented by quantum operators.

Mathematically, a quantum field can be viewed as a map

$$\phi : M \to T \tag{2.5}$$
$$z \mapsto \phi(z) \tag{2.6}$$

from a base manifold M to a target manifold T. This base manifold M will almost always be equivalent to S^d. This is because the microscopic

theory is usually defined on $\mathbb{R}^d$, which will be infinitely large in the thermodynamic limit. In order for us to have a finite action of the theory, the fields must be constant at infinity. If we then identify all boundary points to a point, the whole manifold becomes a sphere, and $M \simeq S^d$. The target manifold T contains the values that the fields take. In a quantum field theory, this is typically the symmetry group G of the fields, often $O(N)$, $U(N)$ or $Sp(N)$, divided by a subgroup H of G.

The simplest example of topology in physics is perhaps the well-known problem of a particle in a ring with a magnetic flux Φ going through it [29]. In that case, the field is a map

$$\phi : S^1 \to S^1 \tag{2.7}$$
$$\tau \mapsto \phi(\tau), \tag{2.8}$$

where $\tau \in [0, \beta]$ is imaginary time, and the base manifold is equivalent to S^1, because τ is periodic with $0 = \beta$. The target manifold is also S^1, because the field $\phi(\tau)$ is also periodic. There is a unique map from the value of $\phi(\tau)$ to the particle's position on the ring, but the opposite is not true. If, for instance, the particle goes around the ring twice when τ goes from 0 to β, every point on the ring is associated with two different values of $\phi(\tau)$, for two different values of τ, with the difference $\phi(\tau_1) - \phi(\tau_2) = 2\pi$.

The partition function of the system is

$$\mathcal{Z} = \int_{\phi(\beta)-\phi(0)=2\pi n} \mathcal{D}\phi e^{-\int \mathrm{d}\tau \left(\frac{1}{2}\dot{\phi}^2 - iA\dot{\phi}\right)}, \tag{2.9}$$

where $A = \Phi/\Phi_0$ is the vector potential of the magnetic field and $n \in \mathbb{Z}$. The number n is called the *winding number* and is equal to the number of times the particle goes around the ring as τ goes from 0 to β. We are thus integrating over all possible realisations of the field $\phi(\tau)$, with the boundary condition that the particle must have gone a whole number of times around the ring as τ goes from 0 to β. What makes this different from ordinary path integrals over field configurations is the term proportional to A in the Langrangian. The constraint $\phi(\beta) - \phi(0) = 2\pi n$ gives us

$$\int \mathrm{d}\tau(-iA\dot{\phi}) = -iA(\phi(\beta) - \phi(0)) = -iA2\pi n, \tag{2.10}$$

and so, we have a term in the Lagrangian proportional to the winding number, but independent of the field. We can thus write

$$\mathcal{Z} = \sum_n e^{2\pi i n A} \int_{\phi(\beta)-\phi(0)=2\pi n} \mathcal{D}\phi e^{-\int \mathrm{d}\tau \frac{1}{2}\dot{\phi}^2}. \tag{2.11}$$

We now have a theory which depends not only on the field, but also on the winding number. This is where the concept of homotopy comes in. The fields are maps from S^d onto a target space T, or put differently, ways of putting d-dimensional loops on T. They thus fulfil the definition of loops and we can thus define a homotopy in the same way as before, i.e. an equivalence class of all fields that can be continuously deformed into one another. In the case of the particle on a ring, all fields with the same winding number are homotopic, and the fundamental group of the target space is $\pi_1(S^1) = \mathbb{Z}$.

We define a *topological action*, S_{top} as a part of an action that depends only on the homotopy class of the field. This means that the topological action will not affect the equations of motion of a system, since these tell us how the action changes under small variations of the field configuration. In the case of the particle on a ring, the relevant homotopy group was $\mathbb{Z}$, so the different classes were defined by an integer (the winding number n). In these cases, the homotopy class is called the *topological charge* of the configuration. We had $S[\phi] = S_0[\phi] + S_{\text{top}}[\phi]$, where $S_0[\phi] = 1/2 \int \mathrm{d}\tau \dot{\phi}^2$ and $S_{\text{top}}[\phi] = 2\pi i n A$. More generally, in all cases where the relevant homotopy group is $\simeq \mathbb{Z}$, the topological action can be written on the form

$$S_{\text{top}}[\phi] = i\theta n, \tag{2.12}$$

where θ is called a *topological angle* and the factor $\exp(-S_{\text{top}}) = \exp(-i\theta n)$ weighing the different topological sectors in the partition function becomes a phase. A topological action like this is often referred to as a *θ-term*. In our example, the topological angle was

$$\theta = 2\pi A = 2\pi \frac{\Phi}{\Phi_0}. \tag{2.13}$$

We have only considered the simplest example here, but more complicated topological actions are indeed possible. Examples are found in the integer [6] and fractional [30] quantum Hall effects, and of course in the theory of topological insulators. The important thing to remember is that the action encodes a homotopy group of the target space of the fields in the theory. The homotopy group is a topological invariant, so in this sense the action decides what target spaces are homeomorphic. In the following, when switching to band theory, we will discuss whether a Hamiltonian is topologically equivalent to another. What we mean then,

is that we want to decide whether the actions of the two theories have topological parts that make the target spaces of their respective fields homeomorphic.

To summarise, certain properties of certain systems will remain unchanged under smooth deformations of the target manifold of the fields, i.e. under continuous changes of the Hamiltonians.

2.3 Topological band theory

So far, we have discussed topology in physics in terms of the quantum field theory underlying the theory. The easiest way to understand topological insulators is however to consider the band theory of the physical systems.

Most insulators are explained by band theory. They are then called band insulators and this explanation of the difference between insulators and metals is one of the most important aspects of the band theory. The eigenvalues $E_n(k)$ of the Bloch Hamiltonian $H(k)$ define the energy bands of the band structure. Both insulators and semiconductors have an energy band where all states are occupied (the valence band) and a band of higher energy where all states are empty (the conduction band). The difference between an insulator and a semiconductor is just the size of the band gap between the valence band and the conduction band. In an insulator, the gap is large enough so that in an ordinary situation, the electrons will never gain energy enough to move up to the conduction band. The gap in a semiconductor is smaller, making the jump to the conduction band for the electrons possible.

Topologically, these two states of matter are equivalent in the sense that the Hamiltonian, encoding the dispersion relation leading to the band structure, can be continuously deformed from one of the two to the other, without closing this gap.

As a first example of a topologically non-trivial state with a band gap, we consider the integer quantum Hall state [6]. When a two-dimensional electron system is exposed to a strong magnetic field, the electrons start to move in cyclotron orbits. Energetically, they will arrange themselves in so called Landau levels with certain energies. Their structure resembles that of a band structure, with gaps between the levels. A two dimensional band structure is a map from the crystal momentum $\mathbf{k}$ defined on a 2-torus T^2 to the Bloch Hamiltonian $H(\mathbf{k})$ with eigenvalues $E_m(\mathbf{k})$. Consider the case where the bands are occupied up to the level $m = N$, and an energy gap $E_{N+1}(\mathbf{k}) - E_N(\mathbf{k})$ is formed. We can classify these possible band structures by forming equivalence classes of Hamiltonians

that can be continuously deformed into one another without closing the gap. We can also characterise the Bloch Hamiltonians by the set of N occupied Bloch wavefunctions $\{u_m(\mathbf{k})\}$. This set defines the groundstate of the system. The groundstate is symmetric under $U(N)$ rotations among these occupied states, so the wavefunctions $\{u_m(\mathbf{k})\}$ form a $U(N)$ *fibre bundle* over the Brillouin zone torus. A fibre bundle is a base manifold, together with a map that associates another manifold to each point in the base manifold. In this case, the base manifold is the Brillouin zone and the manifold associated to each point in the Brillouin zone is the Hilbert space of the wavefunctions $\{u_m(\mathbf{k})\}$. These bundles are classified by the integers, and can be distinguished by their *first Chern class* [6],

$$n = \frac{1}{2\pi} \int \mathrm{d}^2\mathbf{k}\mathcal{F}, \tag{2.14}$$

related to the Bloch wavefunction through the Berry's curvature $\mathcal{F} = \nabla \times \mathcal{A}$, with the Berry's connection $\mathcal{A} = i\sum_{m=1}^{N} \langle u_m|\nabla_{\mathbf{k}}|u_m\rangle$. This Chern class is always an integer, and it can be interpreted as the Berry's phase that the valence band states acquire when they are transported around the outline of the Brillouin zone, so it bears a resemblance with the winding number that we discussed for the particle on a ring. The Chern number n is another example of a topological invariant, so it can not be changed through continuous deformations of the Hamiltonian.

The physical significance of the Chern number n is found in the Hall conductance of the system. When an electric field is applied to an integer quantum Hall state, the cyclotron orbits start to drift, which leads to a Hall current with the quantised Hall conductivity $\sigma_{xy} = ne^2/h$. Since the number n is robust against smooth variations of $H(\mathbf{k})$, the Hall conductivity is incredibly precise, a feature used both for the definition of electrical resistance and for the calculation of the fine structure constant.

Relating this to the band theory, the dispersion relations and thereby the band structure of the edge states can be changed by modifying the Hamiltonian near the edge. For instance, if we have a single edge state to start with, going in one direction, this crosses the Fermi energy at precisely one point. The Hamiltonian can now be smoothly varied so that the edge states will cross the Fermi energy three times instead, adding one right moving and one left moving mode. We see that this smooth variation of the Hamiltonian can change the number of right and left movers individually, but the difference between these numbers, $N_R - N_L$, is constant. Since the Hamiltonian was only smoothly varied, the new Hamiltonian is homeomorphic to the old one and thus, the Chern number n, being a topological invariant, cannot change. This is determined by the topological structure of the bulk states, and so the relation between

these two is called the *bulk-boundary correspondence* [8],

$$N_R - N_L = \Delta n. \tag{2.15}$$

At interfaces between gapped systems with different topological invariants there will be gapless conducting states. This is because a topological invariant will not change as long as the gap stays open. For instance, consider the edge of an integer quantum Hall system with $n = 1$, bordering to a topologically trivial insulator with $n = 0$. In changing the topological invariant n, the gap has to go to zero, and when it does, there will be low energy electronic states.

2.3.1 Topological insulators

The Chern number in eq. (2.14) is odd under time reversal, so in order to have a system like the integer quantum Hall one, time-reversal symmetry has to be broken (in this case explicitly by the strong magnetic field). It is however possible to use a spin-orbit interaction to obtain a time-reversal symmetric class of topologically nontrivial gapped systems. The antiunitary time-reversal operator T squares to $T^2 = -1$ for spin-1/2 particles, which leads to the quite simple, but very important *Kramers' theorem* [31]. It states that all eigenstates of a time-reversal invariant Hamiltonian commuting with T must be at least twofold degenerate. In systems without spin-orbit interaction, this is automatically fulfilled, since states with different spins are degenerate in the absence of a magnetic field (which would break T symmetry).

In the presence of SO interaction, however, the energy levels of different spin will be shifted. If there are electronic states inside the band gap, bound to the surface of the system (or the edge in the case of a 2D topological insulator), they have to be degenerate. This becomes interesting at the points in the Brillouin zone where $k = 0$ and $k = \pm\pi/a_0$, where a_0 is the lattice spacing, since these points transform to themselves under time reversal. Consider the states at the Γ point, $k = 0$. Kramers' theorem demands these to be degenerate, so the only possibility for a gap to open, is if the states are pairwise connected at $k = 0$. If there is only one state available for each spin, the opening of a gap would lead to non-degenerate edge states, which would violate Kramers' theorem. Fig. 2.2a shows a band configuration with a pair of gapless edge states. Every energy is fourfold degenerate, so we have two Kramers' pairs. This state can be transformed into the gapped configuration in fig. 2.2b without violating Kramers' theorem, since the states at $k = 0$ are still degenerate. The edge states can be further pushed into the bulk states, which would make the edge as insulating as the bulk.

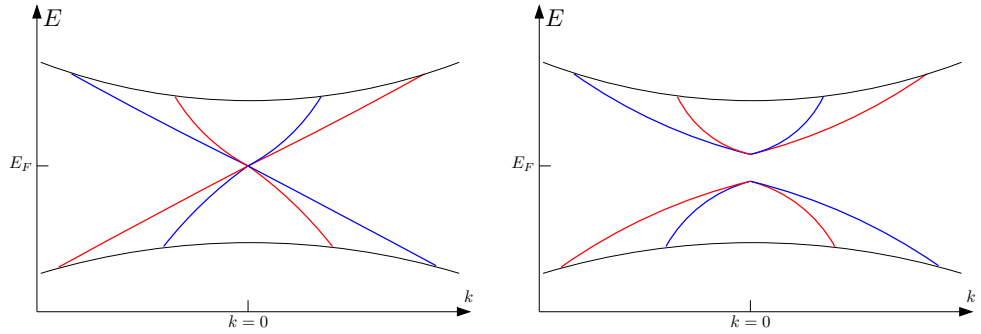

(a) (b)

Figure 2.2: A gapless (a) and a gapped (b) configuration of edge bands in the gap between the bulk bands, with two Kramers' pairs. Red and blue colours denote opposite spins.

Now, consider the configuration in fig. 2.3a. At all energies, the system is doubly degenerate, i.e. it has one Kramers' pair. This is also true at the Γ point $k = 0$, but in the configuration shown in fig. 2.3b the degeneracy has been lifted. In this case Kramers' theorem would be violated, which is impossible in a time-reversal invariant system.

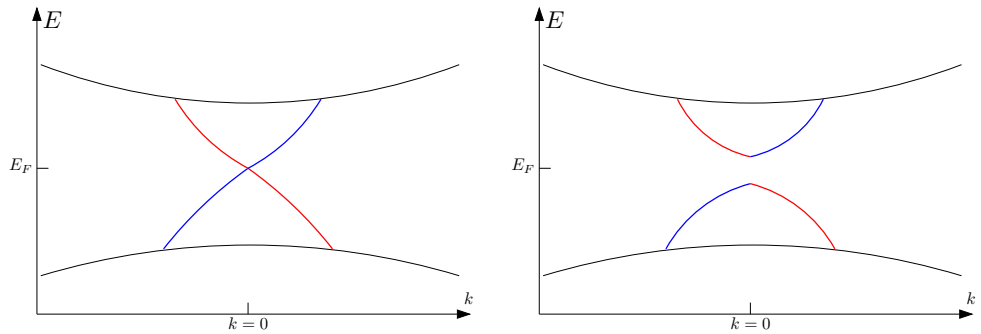

(a) (b)

Figure 2.3: A gapless (a) and a forbidden, gapped, (b) configuration with one Kramers' pair on the edge. Red and blue colours denote opposite spins.

Kramers' theorem thus allows the band structure to be continuously deformed into a gapped configuration if the Kramers' pairs form the

gap two by two. This means that we have two topologically distinct configurations, one with an even number of Kramers' pairs, where a gap can form, and one with an odd number of pairs, where one pair will always be left gapless. Which of these two alternatives that occurs depends on the topological class of the bulk structure. There is thus a $\mathbb{Z}_2$ topological invariant ν, defined modulo 2, which tells us if the system is a topologically trivial insulator or a topological insulator with conducting edge states.

Comparing with the integer quantum Hall case, the Chern number is $n = 0$ in these systems, but we now have a new topological invariant to consider, ν, with the values 0 or 1, corresponding to an even or an odd number of Kramers' pairs, respectively. We can now form a "bulk-boundary correspondence" for the Kramers' pairs,

$$N_K = \Delta\nu \mod 2, \tag{2.16}$$

where N_K is the number of Kramers' pairs intersecting the Fermi energy and $\Delta\nu$ is the change of the value of ν as the interface between two different materials is crossed.

So, just as for the integer quantum Hall effect, we can consider homeomorphisms between target spaces of the fields of the theory. This will be determined by the action, or the Hamiltonian. The fact that we have to change a topological invariant, in this case ν, in order to destroy the gapless edge modes, tells us that the gapless edge modes are robust against smooth deformations of the Hamiltonian.

The very simplicity of using band theory to explain the topological nature of topological insulators is both the primary advantage and the disadvantage of this. A more mathematical approach to the $\mathbb{Z}_2$ invariant ν is given for instance in ref. [10].

We have chosen to explain the topological insulators in terms of band theory, which has the advantage of being easy to comprehend. The disadvantages are both that we will not be able to treat interactions on the edge, and that the field theory provides more powerful tools when it comes to classification of topological invariants and in looking for candidates for being topological insulators. The field theory can be shown to be equivalent to the band theory in the non-interacting limit [32].

We again compare with the integer quantum Hall effect. Field theoretically, the Chern number n from (2.14) appears in the topological action of the system [33],

$$S_{\text{top}} = \frac{n}{4\pi} \int \mathrm{d}^2x \int \mathrm{d}t A_\mu \epsilon^{\mu\nu\tau} \partial_\nu A_\tau. \tag{2.17}$$

It can be shown that the Chern number can be expressed in terms of the

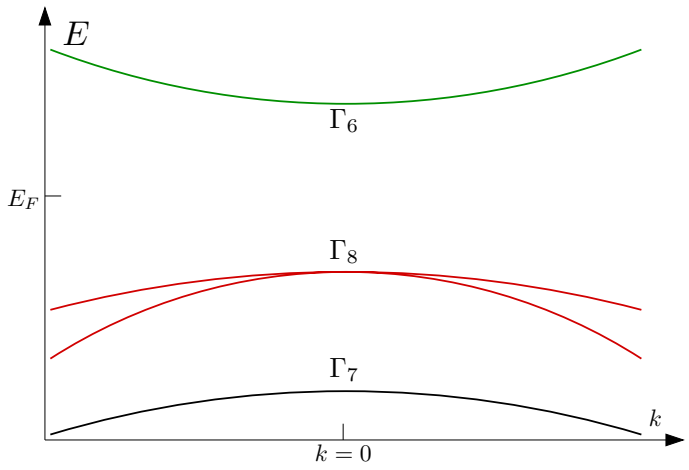

Figure 2.4: The band structure of CdTe near $k = 0$.

nonsingular Green's functions, so the field theory of this system constitutes a map from the three dimensional momentum space $\simeq S^3$ to the space of nonsingular Green's functions, belonging to the group $\mathrm{GL}(n, \mathbb{C})$ (the integer n is the number of relevant bands). The relevant homotopy group is therefore $\pi_3(\mathrm{GL}(n, \mathbb{C})) \simeq \mathbb{Z}$ [32].

In 2001, Zhang and Hu [34] generalised this time-reversal symmetry breaking theory in 2+1 dimensions to a similar theory in 4+1 dimensions, which turns out to be time-reversal symmetric. The theory of $(3 + 1)$-dimensional topological insulators was then formed from this via dimensional reduction, and from this, further dimensional reduction yields the $(2 + 1)$-dimensional topological insulators, or QSH insulators. Here, the characteristic $\mathbb{Z}_2$ topological invariant discussed previously arises directly from the field theory [35].

2.4 The quantum spin Hall effect in HgTe quantum wells

For a good review of the physics of the QSH effect in HgTe/CdTe quantum wells (QW:s), including the earliest experiments, see the article by König et al. [36]. We will here sketch only the basics.

The idea of using HgTe QW:s as QSH systems was presented by Bernevig, Hughes and Zhang in 2006 [37]. These authors were looking for a band structure of the type depicted in fig. 2.3a. As shown by Kane and Mele [10], graphene could be a candidate for this type of band struc-

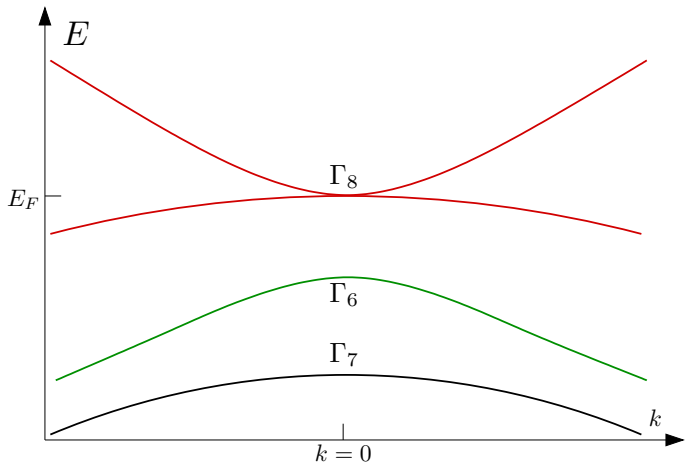

Figure 2.5: The inverted band structure of HgTe near $k = 0$.

ture and indeed, the degeneracy at the Dirac point gives the appropriate helical edge states, protected by time-reversal symmetry. The problem with graphene is that the carbon atoms are too light to produce a spin-orbit coupling strong enough to give a large enough energy gap for the bulk states.

Instead, Bernevig et al. started to look for a heavier material, with the same Kramer's degeneracy at $k = 0$, i.e. the Γ point in the Brillouin zone. Let us have a look at the energy bands near the Fermi level in two heavy semiconductor materials, namely CdTe and HgTe. In CdTe (as in GaAs), the conductance band is an s-type antibondning Γ_6 band. Its molecular orbitals are odd under parity. The valence band is a p-type binding Γ_8 band with with parity-even molecular orbitals. This band structure is sketched in fig. 2.4.

In HgTe on the other hand, the spin-orbit interaction is large enough to push the Γ_8 band above the Γ_6 band, thus shifting the valence and conductance bands one step, as shown in fig. 2.5. The importance of the inversion of the bands lies in the fact that the parity eigenvalues are shifted between the valence and conductance bands. In an interface between a material with normal and one with inverted bandstructure, the parity eigenvalue switches sign. One can then show that this will give rise to gapless states, exponentially confined to the interface, i.e. the surface of the material with the inverted bandstructure, in analogy with the discussion of the bulk-boundary correspondence around eq. (2.15).

This theory was tested experimentally by König et al. [11]. They used a HgTe quantum well with thickness d that was sandwiched between

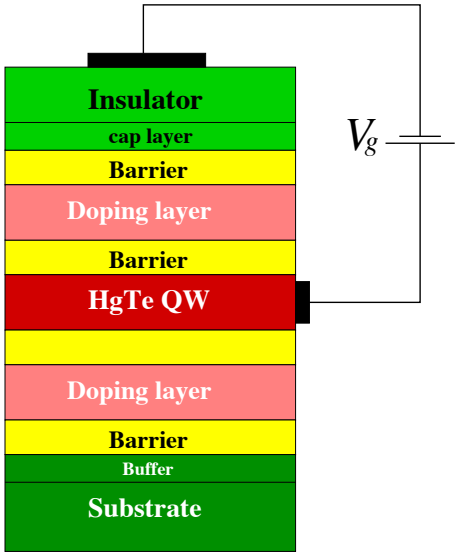

Figure 2.6: A simple sketch of a HgTe QW. For a more detailed figure, see ref. [36].

$Hg_{0.3}Cd_{0.7}Te$ layers (see figure 2.6). The idea was that the QW should behave more like HgTe, with the inverted band gap, for a thick HgTe layer and more like CdTe, with the normal band gap, when the HgTe is thinner. In ref. [36], the critical thickness, where the SO coupling of the QW material pushes the Γ_8 band above the Γ_6 band, was calculated to be $d_c = 6.3$ nm. In the experiment, the thickness of the HgTe layer was varied between $d = 5.5$ nm and $d = 12$ nm, so that the critical thickness d_c should be covered. The fundamental quantum of conductance is $G_0 = e^2/h$. Since the edges of a QSH system together carry two channels of dissipationless current, the Hall conductance should be twice this value, i.e. $\sigma_{xy} = 2e^2/h$. A four-terminal conductance measurement was performed to see if this was possible to detect.

Indeed, a quantised Landauer conductance of $2e^2/h$ was found as predicted for $d > d_c$, while the QW was shown to be an ordinary insulator for $d < d_c$. This predicted conductance was found in samples of size ~ 1 μm. Larger samples (~ 20 μm) also showed the behaviour of a conventional insulator for $d < d_c$ and a finite conductance for $d > d_c$, but with a lower, non-quantised, value.

Importantly, they also found that breaking time-reversal symmetry with even a small magnetic field destroyed the conductivity, again making the QW an ordinary insulator.

3

Tunnelling at a point contact

A very interesting problem is to understand what happens when two edges of a quantum spin Hall insulator are connected via a point contact, through which a tunnelling current may flow. We start by considering an unbiased point contact and use perturbative renormalisation group methods to investigate the conditions for electron tunnelling. We then consider the effect of connecting a battery to the bar, driving a spin-current through the contact. Using linear response theory, we investigate the temperature dependence of the conductivity, and also consider the effects of applying an alternating voltage over the quantum spin Hall sample. To set the stage, we will begin the chapter by a brief introduction to the theoretical tools that we use: bosonisation and the renormalisation group. Much of the exposition of this chapter follows ref. [27]. This work was published as Paper I, as a collaboration with Henrik Johannesson [23].

3.1 Introduction to bosonisation and the renormalisation group

All problems treated in this thesis will be approached primarily by different takes on bosonisation and renormalisation group (RG) methods. We will therefore start this chapter by a very brief introduction to these techniques, and then show their applications by applying them to the different research works presented in the thesis.

3.1.1 One dimensional field theory

In this chapter, and the following, we will almost invariably use a quantum field theory description of the physics. The concept of a quantum field was touched upon in chapter section 2.2, but we need to understand a little better how a quantum field theory works in condensed matter physics. For a nice introduction to quantum field theory in general, ref. [38] is recommended, while ref. [29] is specifically aimed at the use of quantum field theory in condensed matter physics. This thesis is exclusively concerned with one-dimensional physics, so the derivation of the field theory we will use will be specific to one dimension, even though most of the concepts apply also to higher dimensions.

For this introduction to condensed matter field theory, we start by introducing electron annihilation and creation operators $c(k)$ and $c^\dagger(k)$ respectively, which annihilate or create an electron with momentum k. Considering the low-energy theory just around the Fermi level, we can define an annihilation operator $a(k) = c(k_F + k)$ for an electron with momentum $k_F + k$, and similarly one $b(k) = c(k_F - k)$ for a hole with momentum $k_F - k$. These have positive momenta, meaning they move in a specific direction, which we may choose to call "right". Annihilation and creation operators for "left-moving" (negative k) electrons and holes are defined in the same way by changing $k_F + k \to -k_F - k$ and $k_F - k \to -k_F + k$.

Taking the theory to the continuum limit, i.e. considering the physics on length scales much larger than the lattice constant a_0, the low-energy physics can now be captured in continuum fields defined as

$$\frac{c(x)}{\sqrt{a_0}} = \psi_R(x)e^{ik_F x} + \psi_L(x)e^{-ik_F x} \tag{3.1}$$

in position space. The two fields $\psi_R(x)$ and $\psi_L(x)$ vary only slowly, while the fast fluctuations are expressed through the exponential factors. The indices R and L ("right" and "left") indicate whether the particle and holes described exist around the positive or negative Fermi point. The fields are fermionic and anticommute.

We also write down Fourier expansions of the continuum fields:

$$\psi_R(x) = \int_{k>0} \frac{\mathrm{d}k}{2\pi} \left(a(k)e^{ikx} + b(k)e^{-ikx}\right) \tag{3.2}$$

$$\psi_L(x) = \int_{k<0} \frac{\mathrm{d}k}{2\pi} \left(a(k)e^{ikx} + b(k)e^{-ikx}\right). \tag{3.3}$$

Sometimes a convenient way to treat the time-dependence of the field theory is to use complex coordinates z and $\bar{z}$ together with imaginary

time $\tau = it$. Then we may define $z = i(vt - x) = \tau - ix$ and $\bar{z} = i(vt + x) = \tau + ix$. The time dependence of the creation and annihilation operators can be added with phase factors $e^{-iv_f|k|t}$, so that the time-dependent fields take the form

$$\psi_R(z) = \int_{k>0} \frac{\mathrm{d}k}{2\pi} \left(a(k)e^{-kz} + b(k)e^{kz}\right) \tag{3.4}$$

$$\psi_L(\bar{z}) = \int_{k<0} \frac{\mathrm{d}k}{2\pi} \left(a(k)e^{k\bar{z}} + b(k)e^{-k\bar{z}}\right), \tag{3.5}$$

showing that ψ_R and ψ_L depend solely on z and $\bar{z}$, respectively. In the following, the time dependence of the fields will be used when needed. In terms of the continuum fields, the fermionic Hamiltonian without interaction then becomes the Dirac Hamiltonian in one dimension,

$$H = -iv_F \int \mathrm{d}x \left(\psi_R^\dagger(x)\partial_x\psi_R(x) - \psi_L^\dagger(x)\partial_x\psi_L(x)\right). \tag{3.6}$$

This Hamiltonian is spinless, because we didn't specify the spins of the electrons annihilated and created by the operators we started with. If we would have started with operators c_μ carrying spin indices $\mu =\uparrow$ or $\mu =\downarrow$, we would have arrived with the spinful Hamiltonian

$$H = -iv_F \int \mathrm{d}x \sum_{\mu=\uparrow,\downarrow} \left(\psi_{R,\mu}^\dagger(x)\partial_x\psi_{R,\mu}(x) - \psi_{L,\mu}^\dagger(x)\partial_x\psi_{L,\mu}(x)\right). \tag{3.7}$$

Of course, we would also like to be able to treat interactions. We will classify the different possible interactions into four different types, with the following Hamiltonians

$$\begin{aligned} H_1 = \int \mathrm{d}x \sum_{\mu=\uparrow,\downarrow} \Big(& v_F g_{1\perp} \psi_{R,\mu}^\dagger(x)\psi_{L\mu}(x)\psi_{L,-\mu}^\dagger(x)\psi_{R,-\mu}(x) + H.c. \\ & + v_F g_{1\parallel} \psi_{R\mu}^\dagger(x)\psi_{L\mu}(x)\psi_{L,\mu}^\dagger(x)\psi_{R,\mu}(x)\Big) \end{aligned} \tag{3.8}$$

$$H_2 = \int \mathrm{d}x \sum_{\mu=\uparrow,\downarrow} \left(v_F g_{2\parallel}\rho_{R,\mu}(x)\rho_{L,\mu}(x) + v_F g_{2\perp}\rho_{R,\mu}(x)\rho_{L,-\mu}(x)\right) \tag{3.9}$$

$$H_3 = \int \mathrm{d}x \sum_{\mu=\uparrow,\downarrow} \frac{v_F g_3}{2} \psi_{R,\mu}^\dagger(x)\psi_{R,-\mu}^\dagger(x)\psi_{L,\mu}(x)\psi_{L,-\mu}(x) + H.c. \tag{3.10}$$

$$H_4 = \int \mathrm{d}x \sum_{r=R,L} \sum_{\mu=\uparrow,\downarrow} \left(\frac{v_F g_{4\parallel}}{2}\rho_{r,\mu}(x)\rho_{r,\mu}(x) + \frac{v_F g_{4\perp}}{2}\rho_{r,\mu}(x)\rho_{r,-\mu}(x)\right), \tag{3.11}$$

where $\rho_{r\mu}(x) = \psi^{\dagger}_{r\mu}(x)\psi_{r\mu}(x)$ are the electron density fluctuation operators of the different fermion fields with $r = R, L; \mu = \uparrow, \downarrow$. They describe particle-hole excitations near the Fermi points and thus the fluctuations of the electron density of the system. The four different interaction types are backward scattering, with coupling constants $g_{1\parallel,\perp}$; dispersion scattering, with coupling constants $g_{2\parallel,\perp}$; Umklapp, with coupling constant g_3 and forward scattering, with coupling constants $g_{4\parallel,\perp}$. The diagrams for the interactions are shown in Fig. 3.1. This classification is often referred to as "g-ology" [39].

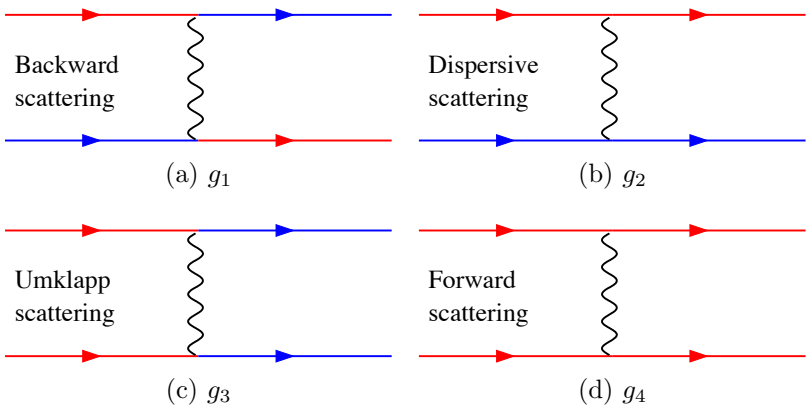

Figure 3.1: The low-energy "g-ology" scattering processes. Red and blue colours denote opposite momenta.

Note that Umklapp scattering needs to be accounted for only when the one-dimensional conduction band is half-filled, i.e. when it carries one electron per lattice site (Umklapp scattering at other commensurate fillings, such as quarter-filling, is also possible, but requires the transition of more than two particles from one of the Fermi points to the other, and is therefore a higher-order, less relevant process than the ones we consider here). In a semiconductor quantum well, such as the HgTe well which have been found to support a quantum spin Hall state, the filling of the edge bands is always far below half-filling, and hence Umklapp processes can be neglected [40]. From now on, we thus only consider the g_1, g_2 and g_3 scatterings.

3.1.2 Bosonisation

The idea of bosonisation is to express the fermionic fields of a theory in terms of bosonic fields. It is a very powerful tool in one-dimensional physics, allowing us to rewrite a fermionic theory with interactions as

a non-interacting bosonic theory [40, 41]. We use the notation $\phi_{r\mu}$ for the bosonic fields corresponding to the fermionic fields $\psi_{r\mu}$. Since we want to arrive at the non-interacting bosonic theory, we write down its Hamiltonian,

$$H_0 = \frac{v_F}{2}\int \mathrm{d}x \left(\Pi^2 + (\partial_x\varphi)^2\right), \tag{3.12}$$

which is valid for any massless bosonic field φ. The conjugate momentum to φ is $\Pi = \partial_t\varphi/v_F$, and the two conjugate fields obey the canonical commutation relations $[\varphi(x), \Pi(x')] = i\delta(x-x')$ and $[\varphi(x), \varphi(x')] = [\Pi(x), \Pi(x')] = 0$. From this, a dual boson θ is also defined as $\partial_x\theta \equiv -\Pi = -\partial_t\varphi/v_F$. It will be useful to define $\varphi = \phi_R + \phi_L$, which will have the conjugate field $\theta = \phi_R - \phi_L$.

Without going through the derivation, we simply state the transformation rules for going from the fermionic fields $\psi_{r\mu}$ to bosonic fields $\phi_{r\mu}$

$$\psi_{R\mu}(z) = \eta_{R\mu}\frac{1}{\sqrt{2\pi a_0}}e^{-2i\sqrt{\pi}\phi_{R\mu}(z)} \tag{3.13}$$

$$\psi_{L\mu}(z) = \eta_{L\mu}\frac{1}{\sqrt{2\pi a_0}}e^{2i\sqrt{\pi}\phi_{L\mu}(z)}, \tag{3.14}$$

where $\eta_{L/R\mu}$ are Klein factors, taking care of the fermionic anticommutation rules. They obey the Clifford algebra $\{\eta_{r\mu}, \eta_{s\nu}\} = 2\delta_{\mu\nu}\delta_{rs}$. A pedagogic derivation of eqs.(3.13) and (3.14) can be found in ref. [40].

We now want to use the bosonisation formulas, eqs. (3.13) and (3.14), to bosonise the interactions in eqs.(3.8) − (3.10). For that, we need to write down the bosonisation formulas for the density fluctuations $\rho_{r\mu}$. Naively employing the bosonisation rules in eqs.(3.13) and (3.14) on $\rho_{r\mu}$ would result in a constant, since the two constituent fields are defined in the same point, so we need to be slightly more clever. First, we use the mode expansion of the fermion fields, eqs. (3.4) and (3.5), to calculate the expectation value

$$\begin{aligned}\left\langle \psi_R^\dagger(z)\psi_R(z')\right\rangle &= \int_{k>0}\frac{\mathrm{d}k}{2\pi}\int_{k'>0}\frac{\mathrm{d}k'}{2\pi}\langle 0|a(k)b^\dagger(k')|0\rangle e^{-kz+k'z'} \\ &= \int_{k>0}\frac{\mathrm{d}k}{2\pi a_0}e^{-k(z-z')} = \frac{1}{2\pi}\frac{1}{z-z'}.\end{aligned} \tag{3.15}$$

Time ordering is here ensured by choosing $\tau > \tau'$. In order to have a well-defined theory, we need to normal order the density fluctuation operators, and for that we use what is often referred to as *point-splitting*, i.e.

$$\rho(z) \equiv \lim_{\epsilon\to 0}\left(\psi^\dagger(z+\epsilon)\psi(z) - \left\langle\psi^\dagger(z+\epsilon)\psi(z)\right\rangle\right), \tag{3.16}$$

where $z+\epsilon$ has a slightly larger τ component than z. This is again to ensure that time-ordering is done correctly. With eq. (3.15),

$$\left\langle\psi^\dagger(z+\epsilon)\psi(z)\right\rangle = \frac{1}{2\pi\epsilon} \tag{3.17}$$

and hence,

$$\begin{aligned}
\rho_R(z) &= \lim_{\epsilon\to 0}\left(\psi_R^\dagger(z+\epsilon)\psi_R(z) - \frac{1}{2\pi a_0\epsilon}\right) \\
&= \frac{1}{2\pi}\lim_{\epsilon\to 0}\left(e^{2i\sqrt{\pi}\phi_R(z+\epsilon)}e^{-2i\sqrt{\pi}\phi_R(z)} - \frac{1}{\epsilon}\right) \\
&= \frac{1}{2\pi}\lim_{\epsilon\to 0}\left(e^{2i\sqrt{\pi}(\phi_R(z+\epsilon)-\phi_R(z))}e^{4\pi\langle\phi_R(z+\epsilon)\phi(z)\rangle} - \frac{1}{\epsilon}\right) \\
&= \frac{1}{2\pi}\lim_{\epsilon\to 0}\left(e^{2i\sqrt{\pi}\epsilon\partial_z\phi_R(z)}e^{-4\pi\frac{1}{4\pi}\ln\epsilon} - \frac{1}{\epsilon}\right) \\
&= \frac{1}{2\pi}\lim_{\epsilon\to 0}\frac{1}{\epsilon}2i\sqrt{\pi}\epsilon\partial_z\phi_R(z) = \frac{i}{\sqrt{\pi}}\partial_z\phi_R(z),
\end{aligned} \tag{3.18}$$

where we have used the relation $e^{ia\phi(z)}e^{ib\phi(z')} = e^{ia\phi(z)+ib\phi(z')}e^{-ab\langle\phi(z)\phi(z')\rangle}$, which is valid for normal ordered exponentials, together with the bosonic Green's function $\langle\phi(z)\phi(z')\rangle = -\ln(z-z')/(4\pi)$. Similarly,

$$\rho_L(\bar{z}) = -\frac{i}{\sqrt{\pi}}\partial_{\bar{z}}\phi_L(\bar{z}). \tag{3.19}$$

The free fermionic Hamiltonian of eq. (3.6) can with these rules be shown to bosonise into the free bosonic Hamiltonian of eq. (3.12). Defining the charge and spin fields

$$\phi_\rho \equiv \frac{1}{\sqrt{2}}(\varphi_\uparrow + \varphi_\downarrow) \tag{3.20}$$

$$\theta_\rho \equiv \frac{1}{\sqrt{2}}(\theta_\uparrow + \theta_\downarrow) \tag{3.21}$$

$$\phi_\sigma \equiv \frac{1}{\sqrt{2}}(\varphi_\uparrow - \varphi_\downarrow) \tag{3.22}$$

$$\theta_\sigma \equiv \frac{1}{\sqrt{2}}(\theta_\uparrow - \theta_\downarrow), \tag{3.23}$$

the spinful Dirac Hamiltonian, eq. (3.7), can be written

$$H_0 = \frac{v_F}{2}\int \mathrm{d}x \left(\Pi_\rho^2 + (\partial_x\phi_\rho)^2 + \Pi_\sigma^2 + (\partial_x\phi_\sigma)^2\right)^2, \tag{3.24}$$

where now $\Pi_\rho = \partial_t\phi_\rho/v_F$ and $\Pi_\sigma = \partial_t\phi_\sigma/v_F$.

We are now ready to bosonise the g-ology interactions H_1, H_2 and H_4 from eqs. (3.8), (3.9) and (3.11). Starting with the backscattering Hamiltonian H_1, we treat the spin-parallel and spin-perpendicular backscatterings independently. Using the bosonisation rules of eqns. (3.13)-(3.14),

$$\begin{aligned}
H_{1\perp} &= \int \mathrm{d}x \sum_{\mu=\uparrow,\downarrow} v_F g_{1\perp} \psi^\dagger_{R\mu}(x)\psi_{L\mu}(x)\psi^\dagger_{L,-\mu}(x)\psi_{R,-\mu}(x) \\
&= \int \mathrm{d}x \sum_{\mu=\uparrow,\downarrow} v_F g_{1\perp} \psi^\dagger_{R\mu}(x)\psi_{L\mu}(x)\psi^\dagger_{L,-\mu}(x)\psi_{R,-\mu}(x) \\
&= \int \mathrm{d}x \sum_{\mu=\uparrow,\downarrow} \frac{v_F g_{1\perp}}{(2\pi a_0)^2} e^{2i\sqrt{\pi}(\phi_{R\mu}(x)+\phi_{L\mu}(x)-\phi_{R,-\mu}(x)-\phi_{L,-\mu}(x))} \\
&= \int \mathrm{d}x \frac{v_F g_{1\perp}}{(2\pi a_0)^2} \left(e^{2i\sqrt{2\pi}\phi_\mu(x)} + e^{-2i\sqrt{2\pi}\phi_\mu(x)}\right) \\
&= \int \mathrm{d}x \frac{2v_F g_{1\perp}}{(2\pi a_0)^2} \cos(2\sqrt{2\pi}\phi_\mu(x)).
\end{aligned} \tag{3.25}$$

This term is a so called *sine-Gordon* term (a pun on the related "Klein-Gordon" equation [42]), and it has been discussed extensively in the literature. Sine-Gordon terms often appear in bosonised theories, and the study of the flow of their coupling constants during renormalisation is crucial for determining physical properties.

The remainder of H_1 (eq. (3.8)), together with H_2 and H_4 (eq. (3.9) and eq. (3.11), respectively), will be a part of a free bosonic theory. The spin-parallel part of H_1 is

$$\begin{aligned}
H_{1\parallel} &= \int \mathrm{d}x \sum_{\mu=\uparrow,\downarrow} v_F g_{1\parallel} \psi^\dagger_{R\mu}(x)\psi_{L\mu}(x)\psi^\dagger_{L,\mu}(x)\psi_{R,\mu}(x) \\
&= \int \mathrm{d}x \sum_{\mu=\uparrow,\downarrow} -v_F g_{1\parallel} \psi^\dagger_{R\mu}(x)\psi_{R\mu}(x)\psi^\dagger_{L,\mu}(x)\psi_{L,\mu}(x) \\
&= \int \mathrm{d}x \sum_{\mu=\uparrow,\downarrow} -v_F g_{1\parallel} \rho_{R,\mu}(x)\rho_{L,\mu}(x)
\end{aligned} \tag{3.26}$$

and we see that it is equivalent to the $g_{2\parallel}$ term of eq. (3.9). We may thus account for $g_{1\parallel}$ by just changing $g_{2\parallel} \to g_{2\parallel} - g_{1\parallel}$. If we now introduce spin- and charge-separated versions of the coupling constants according to

$$g_\rho = g_{1\parallel} - g_{2\parallel} - g_{2\perp} \tag{3.27}$$
$$g_\sigma = g_{1\parallel} - g_{2\parallel} + g_{2\perp} \tag{3.28}$$
$$g_{4\rho} = g_{4\parallel} + g_{4\perp} \tag{3.29}$$
$$g_{4\sigma} = g_{4\parallel} - g_{4\perp}, \tag{3.30}$$

the bosonised versions of the g-ology Hamiltonians can, after some easy but rather lengthy algebra, be written

$$H_{1\parallel+2} = \frac{v_F}{4\pi^2} \int \mathrm{d}x \left(g_\rho \left[(\partial_x \phi_\rho)^2 + (\partial_x \theta_\rho)^2 \right] + g_\sigma \left[(\partial_x \phi_\sigma)^2 + (\partial_x \theta_\sigma)^2 \right] \right) \tag{3.31}$$

$$H_4 = \frac{v_F}{4\pi^2} \int \mathrm{d}x \left(g_{4\rho} \left[(\partial_x \phi_\rho)^2 - (\partial_x \theta_\rho)^2 \right] + g_{4\sigma} \left[(\partial_x \phi_\sigma)^2 - (\partial_x \theta_\sigma)^2 \right] \right). \tag{3.32}$$

We have now shown that the full Hamiltonian $H_0 + H_{1\parallel+2} + H_4$ can be separated into a spin and a charge part, H_ρ and H_σ, respectively. If we also introduce

$$K_\lambda = \sqrt{\frac{\pi - g_\lambda + g_{4\lambda}}{\pi + g_\lambda + g_{4\lambda}}} \tag{3.33}$$
$$v_\lambda = v_F \sqrt{\left(1 + \frac{g_{4\lambda}}{\pi}\right)^2 - \left(\frac{g_\lambda}{\pi}\right)^2}, \tag{3.34}$$

the interacting Hamiltonian (with the backscattering term $H_{1\perp}$ subtracted) can be written as $\sum_{\lambda=\sigma,\rho} H_\mu$ with

$$H_\lambda = \frac{v_\lambda}{2} \int \mathrm{d}x \left(K_\lambda \Pi_\lambda^2 + \frac{1}{K_\lambda} (\partial_x \phi_\lambda)^2 \right). \tag{3.35}$$

The interactions are thus accounted for in the definitions of the parameters v_λ, which we will refer to as the *renormalised velocity*, and K_λ, the *Luttinger liquid parameter*, with $\lambda = \rho$ and $\lambda = \sigma$ in the charge and spin sectors of the theory, respectively. For repulsive electron-electron interactions, $K_\rho < 1$ and the strength of the interactions is encoded in the magnitude of K_ρ. A non-interacting theory has $K_\rho = 1$ and the stronger

the interaction the lower K is. As for the K_σ parameter, spin-rotational invariance of the electron-electron interaction requires that $K_\sigma = 1$. The fact that eq. (3.27) implies a value of $K_\sigma \neq 1$ is an artifact of the particular version of bosonisation we use (Abelian bosonisation, to be contrasted to non-Abelian bosonisation, see ref. [40]).

Comparing eq. (3.12) and eq. (3.35), we see that H_λ is not yet written on canonical form. This can be fixed by defining $\phi'_\lambda \equiv \phi_\lambda/\sqrt{K_\lambda}$ and $\Pi'_\lambda \equiv \sqrt{K_\lambda}\Pi_\lambda$. Then

$$H_\lambda = \frac{v_\lambda}{2}\int \mathrm{d}x \left((\Pi'_\lambda)^2 + (\partial_x \phi'_\lambda)^2\right), \tag{3.36}$$

which has the same form as eq. (3.12).

Other aspects of bosonisation will be introduced further on.

3.1.3 Renormalisation

Quantum field theory in its early days was notorious for producing divergent integrals in the high-energy limit where it was used. This was considered a serious problem for a long time. Whereas the infinities in quantum electro dynamics (QED), the quantum field theory describing the electromagnetic field, were tamed by Feynman, Schwinger, and Tomonaga already in the 1940s, it was not until Ken Wilson's work on the renormalisation group in the early 1970s that a conceptually satisfactory account of the very meaning of regularisation and renormalisation was presented [43]. We will return to Wilson and the renormalisation group below. If we regard quantum field theory as a low-energy effective theory valid up to a certain momentum (or energy) scale Λ, the encountered infinities are merely a sign that we are trying to use the theory in a realm where it is not valid.

There is also an associated cutoff in space, below which a quantum field theory formulation looses its meaning. In condensed matter physics this cutoff is given by the lattice spacing a_0 that defines the characteristic length of the underlying crystal lattice. It makes no sense to use a continuum theory at this length scale. The high momentum cutoff Λ is then naturally defined as the inverse of the lattice spacing (or $\Lambda = v_F/a_0$ if we want a high-energy cutoff).

Since we are interested in the low-energy physics of excitations close to the Fermi level, it is important to understand how the physics change if we integrate out, or average over, the degrees of freedom that belong to higher energy physics. The way to do it is to start by integrating over all momenta between Λ and a slightly lower momentum Λ/b, where $b > 1$, so that Λ/b becomes the new high-momentum cutoff for the effective

low-energy theory. If this theory is similar to the original one, apart from the new cutoff and, importantly, a new set of coupling constants, it is a sign that this way of focusing on the low-energy theory makes sense. The new set of coupling constants is referred to as *renormalised* coupling constants. By iterating this procedure, successively integrating over larger and larger momentum shells between Λ/b and Λ increasing b, the coupling constants will change, or *flow*, from their original values, until the cutoff Λ/b is comparable to the energy scales of the physics we are interested in. In this chapter, the coupling constant we are interested in is a tunnelling amplitude, to be defined below and denoted u. When b grows large, u will approach a certain effective value in the low-energy theory. If $u \to \infty$, the coupling is said to be *relevant*, meaning in this case that tunnelling is certain to happen. If on the other hand $u \to 0$ under renormalisation, the coupling is *irrelevant*, and we will have no tunnelling.

The theory of these rescaling flows, or *renormalisation group flows* as they are known, was developed primarily by Kenneth Wilson in the 1970s, a work for which he was awarded the Nobel Prize in physics in 1982 [43]. Before moving on, a few words on the term "renormalisation group" (RG) is in place. Particle physics in the 1960s was to a large extent concerned with understanding physics in terms of symmetries and group structures of these. The sequence of renormalisation transformations was viewed as constituting a semi-group, where the mapping between the actions before and after renormalisation made up the group elements. The iteration of the mappings was thought to be the group multiplication, which indeed is associative. There is a unit element (not integrating out anything), but there is no inverse, since the RG procedure is irreversible. In that sense, one can talk about a semi-group. This view is however completely useless, and there is no connection with the use of groups for instance in organising elementary particles according to how they transform under symmetries [29].

The practical use of RG will be demonstrated in this chapter, by going through the RG analysis of the coupling constant for the tunnelling operator in the problem of point-contact tunnelling on a QSH edge. Concepts and techniques important for the RG analysis will be introduced as we go along.

3.2 Model

The system we are interested in consists of a QSH bar connected to a battery with left and right contacts, as in fig. 3.2. The point contact is

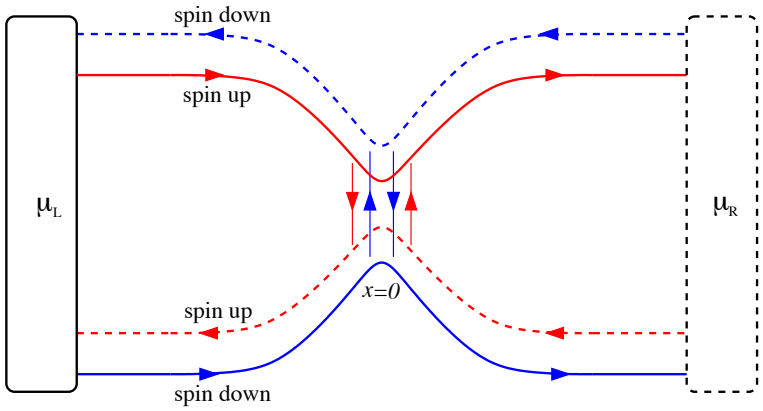

Figure 3.2: The point contact. The full (dashed) lines represent helical edge states in equilibrium with the left (right) contact.

formed by applying a gate voltage perpendicular to the edges, allowing the electrons to tunnel between the edges. The right-moving electrons are in equilibrium with the left reservoir, so that their Fermi energy is the same as the chemical potential μ_L of that reservoir. In the same way, the left-movers are in equilibrium with the right reservoir, with chemical potential μ_R. Turning on the battery means that a voltage, chosen to be $V \equiv (\mu_L - \mu_R)/e$, will drive a current from the left to the right end of the bar. We will investigate the possibility of tunnelling when $V = 0$ and the conductivity associated with the tunnelling when $V \neq 0$. In fig. 3.2, the right-movers of the upper edge have their spin pointing "up", while on the lower edge, the right-movers have spin "down". Since the point contact also allows the electrons to travel between the edges, and there is a potential difference between electrons with the same spin on the different edges, right-movers from the lower edge and from the upper edge will also tunnel to the opposite edge, where they become left-movers. We here assume that the spin is conserved in the tunnelling process, and since the right-movers on the opposite edges come with opposite spin and an equal amount of electrons tunnel from both edges, a spin current, but no charge current, will flow between the edges through the tunnelling junction. One may also consider possible spin-flip processes during the tunnelling, as was done by Dolcini in ref. [44], where the use of tunnelling between QSH edges as quantum interferometers was studied.

As a preamble, we must first define our Hamiltonian and then bosonise it. This is the topic of the next section.

3.2.1 Hamiltonian formulation and bosonisation

Our Hamiltonian will consist of a free part, representing the kinetic energy of the system, plus one term for each allowed interaction. We will also include a tunnelling Hamiltonian, to model the tunnelling through the point contact. The time-reversal symmetry of the QSH system makes backscattering impossible and we will also have no Umklapp scattering, assuming the system to be away from half-filling.

When writing down our theory, we will use a one-dimensional low-energy field theory, as discussed in section 3.1.1, and write the electron fields as

$$\Psi_\sigma(x) = \psi_{R\sigma} e^{ik_F x} + \psi_{L\sigma} e^{-ik_F x}. \tag{3.37}$$

Having the experimentally realised HgTe QW in mind, the spins are "up" and "down", quantised along the growth direction $\hat{z}$ of the quantum well (even though, as we have pointed out earlier, the two "spin" indices would in a real system denote the two Kramers' partners). Moreover, L and R denote "left" and "right" respectively, meaning left and right as seen from the point contact. This means that a "right" electron moves clockwise on the upper edge and vice versa. Here, the slowly varying fields $\psi_{\alpha\sigma}(x)$ annihilate an electron-hole pair just above/below the Fermi level at x moving in the $\alpha = L$ or R direction with spin $\sigma = \uparrow$ or $\downarrow$. The fast variations are encoded in the $e^{\pm ik_F x}$ factors.

In writing down the Hamiltonian, there are a only two allowed scattering processes that need to be accounted for. The system is one-dimensional and the energies of the particles are assumed to be close to the Fermi energy, so the processes are specified by the direction(s) and the spin(s) of the particles involved. This already limits the number of possible interactions to a handful, but the presence of time-reversal symmetry leaves us with two interaction processes only. These are forward and dispersive scattering (see figs. 3.1d and 3.1b, respectively).

In our case, we also need to model the tunnelling. We do this by introducing a tunnelling term in the Hamiltonian,

$$\mathcal{H}_t = u\left(\psi^\dagger_{L\uparrow}\psi_{R\uparrow} + \psi^\dagger_{R\uparrow}\psi_{L\uparrow} + \psi^\dagger_{R\downarrow}\psi_{L\downarrow} + \psi^\dagger_{L\downarrow}\psi_{R\downarrow}\right), \tag{3.38}$$

where u is the strength of the tunnelling. The idea is to use RG analysis, to see whether the coupling constant u is a relevant or an irrelevant coupling. The high-momentum cutoff will be $\Lambda = v_F/\kappa$, and in our case, the short-distance cutoff κ, where the continuum theory breaks down, is the penetration depth of the edge states into the QW.

The allowed parts of the Hamiltonian are thus the free part, $\mathcal{H}_0$, the forward-scattering part, $\mathcal{H}_4$, the dispersive scattering part, $\mathcal{H}_2$ and the

tunnelling part, $\mathcal{H}_t$. The fermionic operators belonging to the upper edge of the system are $\psi_{R\uparrow}$ and $\psi_{L\downarrow}$ and the ones living on the lower edge are $\psi_{L\uparrow}$ and $\psi_{R\downarrow}$. The four parts of the Hamiltonian are then:

$$\mathcal{H}_0 = -iv_F \left(\psi^\dagger_{R\uparrow}\partial_x\psi_{R\uparrow} - \psi^\dagger_{L\downarrow}\partial_x\psi_{L\downarrow} + \psi^\dagger_{R\downarrow}\partial_x\psi_{R\downarrow} - \psi^\dagger_{L\uparrow}\partial_x\psi_{L\uparrow} \right) \tag{3.39}$$

$$\mathcal{H}_2 = g_2 \left(\psi^\dagger_{R\uparrow}\psi_{R\uparrow}\psi^\dagger_{L\downarrow}\psi_{L\downarrow} + \psi^\dagger_{L\uparrow}\psi_{L\uparrow}\psi^\dagger_{R\downarrow}\psi_{R\downarrow} \right) \tag{3.40}$$

$$\mathcal{H}_4 = g_4 \sum_{\substack{\alpha=R,L \\ \sigma=\uparrow,\downarrow}} \psi^\dagger_{\alpha\sigma}\psi_{\alpha\sigma}\psi^\dagger_{\alpha\sigma}\psi_{\alpha\sigma} \tag{3.41}$$

$$\mathcal{H}_t = u \left(\psi^\dagger_{L\uparrow}\psi_{R\uparrow} + \psi^\dagger_{R\uparrow}\psi_{L\uparrow} + \psi^\dagger_{R\downarrow}\psi_{L\downarrow} + \psi^\dagger_{L\downarrow}\psi_{R\downarrow} \right), \tag{3.42}$$

The next step is to bosonise the different parts of the Hamiltonian. We obtain for $\mathcal{H}_0$, using eq. (3.14) and eq. (3.13),

$$\mathcal{H}_0 = v_F \left[(\partial_x\phi_{R\uparrow})^2 + (\partial_x\phi_{L\uparrow})^2 + (\partial_x\phi_{R\downarrow})^2 + (\partial_x\phi_{L\downarrow})^2 \right], \tag{3.43}$$

while the bosonised versions of $\mathcal{H}_2$, $\mathcal{H}_4$ and $\mathcal{H}_t$ become:

$$\mathcal{H}_2 = -\frac{g_2}{2\pi} \left[(\partial_x\phi_{R\uparrow})^2 + (\partial_x\phi_{L\uparrow})^2 + (\partial_x\phi_{R\downarrow})^2 + (\partial_x\phi_{L\downarrow})^2 \right] \tag{3.44}$$

$$\mathcal{H}_4 = \frac{g_4}{\pi} (\partial_x\phi_{R\uparrow}\partial_x\phi_{L\downarrow} + \partial_x\phi_{R\downarrow}\partial_x\phi_{L\uparrow}) \tag{3.45}$$

$$\mathcal{H}_t = \frac{2u}{\pi} \Big(\sin[\sqrt{\pi}(\phi_{L\uparrow} + \phi_{R\uparrow} + \phi_{L\downarrow} + \phi_{R\downarrow})] \tag{3.46}$$

$$\times \cos[\sqrt{\pi}(\phi_{L\uparrow} + \phi_{R\uparrow} - \phi_{L\downarrow} - \phi_{R\downarrow})] \Big). \tag{3.47}$$

In order to write $\mathcal{H}_0 + \mathcal{H}_2 + \mathcal{H}_4$ on the form of a free Hamiltonian, we introduce the fields:

$$\phi_1 = \phi_{R\uparrow} + \phi_{L\downarrow} \qquad \theta_1 = \phi_{R\uparrow} - \phi_{L\downarrow} \tag{3.48}$$

$$\phi_2 = \phi_{L\uparrow} + \phi_{R\downarrow} \qquad \theta_2 = \phi_{L\uparrow} - \phi_{R\downarrow}, \tag{3.49}$$

so that the indices 1 and 2 now denote the upper and the lower edge of the system, respectively. Expressed in these fields, the four parts of the Hamiltonian can be written

$$\mathcal{H}_0 + \mathcal{H}_2 + \mathcal{H}_4 = \frac{v}{2} \left(\frac{1}{K} \left[(\partial_x\phi_1)^2) + (\partial_x\phi_2)^2 \right] + K \left[(\partial_x\theta_1)^2 + (\partial_x\theta_2)^2 \right] \right) \tag{3.50}$$

$$\mathcal{H}_t = \frac{2u}{\pi} \sin[\sqrt{\pi}(\phi_1 + \phi_2)] \cos[\sqrt{\pi}(\theta_1 + \theta_2)], \tag{3.51}$$

where we have introduced

$$v = \sqrt{\left(v_F + \frac{g_4}{\pi}\right)^2 - \left(\frac{g_2}{2\pi}\right)^2} \tag{3.52}$$

and

$$K = \sqrt{\frac{2\pi v_F + 2g_4 - g_2}{2\pi v_F + 2g_4 + g_2}}. \tag{3.53}$$

As expected, the bosonised Hamiltonian looks like a free Hamiltonian, apart from the K and K^{-1} factors, the Luttinger liquid parameter for a spinless theory and its inverse. (A mix-up between the parameters caused a different parametrisation of v and K in Paper I. This has no effect on the final results, though.)

3.2.2 Lagrangian formulation

We now set the stage for the RG analysis by rewriting the Hamiltonian density as a Lagrangian density. We will use the notation $\mathcal{L}_0$ for the part of the Lagrangian that comes from $\mathcal{H}_0 + \mathcal{H}_4 + \mathcal{H}_2$, i.e. $\mathcal{L}_0 = \sum_i \Pi_i \partial_t \phi_i - (\mathcal{H}_0 + \mathcal{H}_4 + \mathcal{H}_2)$. Also, we write $\mathcal{L}_t = -\mathcal{H}_t$.

In order to re-express eq. (3.50) as a Lagrangian, we put it in an explicitly canonical form with the aid of the fields $\phi_i' = \frac{1}{\sqrt{K}}\phi_i$ and $\theta_i' = \sqrt{K}\theta_i$, so that

$$\mathcal{H}_0 + \mathcal{H}_2 + \mathcal{H}_4 = \frac{v}{2}\left[(\partial_x\phi_1')^2 + (\partial_x\phi_2')^2 + (\partial_x\theta_1')^2 + (\partial_x\theta_2')^2\right]. \tag{3.54}$$

Using the relations

$$\partial_x\theta_i' = -\frac{1}{v}\partial_t\phi_i' \tag{3.55}$$

$$\partial_x\phi_i' = -\frac{1}{v}\partial_t\theta_i', \tag{3.56}$$

which are valid for a canonical theory, we can write the Hamiltonian expressed exclusively in the ϕ'- or θ'-fields:

$$\begin{aligned}\mathcal{H}_0 + \mathcal{H}_4 &= \frac{v}{2}\left(\left[(\partial_x\phi_1')^2 + (\partial_x\phi_2')^2\right] + \frac{1}{v^2}\left[(\partial_t\phi_1')^2 + (\partial_t\phi_2')^2\right]\right) \\ &= \frac{v}{2}\left(\frac{1}{v^2}\left[(\partial_t\theta_1')^2 + (\partial_t\theta_2')^2\right] + \left[(\partial_x\theta_1')^2 + (\partial_x\theta_2')^2\right]\right).\end{aligned} \tag{3.57}$$

This makes it possible for us to write the Lagrangian in the ϕ'-fields:

$$\begin{aligned}\mathcal{L}_0 &= \sum_i \Pi_i \partial_t \phi_i' - (\mathcal{H}_0 + \mathcal{H}_{fw}) \\ &= \frac{1}{2}\left(\frac{1}{v}\left[(\partial_t\phi_1')^2 + (\partial_t\phi_2')^2\right] - v\left[(\partial_x\phi_1')^2 + (\partial_x\phi_2')^2\right]\right) \\ &= \frac{1}{2}\left(\frac{1}{vK}\left[(\partial_t\phi_1)^2 + (\partial_t\phi_2)^2\right] - \frac{v}{K}\left[(\partial_x\phi_1)^2 + (\partial_x\phi_2)^2\right]\right),\end{aligned} \tag{3.58}$$

where the canonical momentum is $\Pi = \frac{\partial \mathcal{L}_0}{\partial \dot{\phi}_i'} = \frac{1}{v}\dot{\phi}_i'$. We may also, equivalently, use the θ'-fields:

$$\begin{aligned}\mathcal{L}_0 &= \sum_i \Pi_i \partial_t \theta_i' - (\mathcal{H}_0 + \mathcal{H}_{fw}) \\ &= \frac{1}{2}\left(\frac{1}{v}\left[(\partial_t\theta_1')^2 + (\partial_t\theta_2')^2\right] - v\left[(\partial_x\theta_1')^2 + (\partial_x\theta_2')^2\right]\right) \\ &= \frac{1}{2}\left(\frac{K}{v}\left[(\partial_t\theta_1)^2 + (\partial_t\theta_2)^2\right] - vK\left[(\partial_x\theta_1)^2 + (\partial_x\theta_2)^2\right]\right),\end{aligned} \tag{3.59}$$

Putting these two expressions together gives us a "free" Lagrangian consisting of four different fields:

$$\begin{aligned}\mathcal{L}_0 = \frac{1}{4}\Bigg(&\frac{1}{vK}\left[(\partial_t\phi_1)^2 + (\partial_t\phi_2)^2\right] - \frac{v}{K}\left[(\partial_x\phi_1)^2 + (\partial_x\phi_2)^2\right] \\ &+ \frac{K}{v}\left[(\partial_t\theta_1)^2 + (\partial_t\theta_2)^2\right] - vK\left[(\partial_x\theta_1)^2 + (\partial_x\theta_2)^2\right]\Bigg).\end{aligned} \tag{3.60}$$

The total Lagrangian is now $\mathcal{L} = \mathcal{L}_0 + \mathcal{L}_t$. Written in imaginary time $\tau = it$, the two parts of the Lagrangian are:

$$\begin{aligned}\mathcal{L}_0 &= -\frac{1}{4}\sum_{i=1}^{2}\left(\frac{1}{vK}(\partial_\tau\phi_i)^2 + \frac{K}{v}(\partial_\tau\theta_i)^2 + \frac{v}{K}(\partial_x\phi_i)^2 + vK(\partial_x\theta_i)^2\right) \\ &= -\frac{1}{4}\sum_{i=1}^{2}\left(v(\partial_x\phi_i') + v^{-1}(\partial_\tau\phi_i') + v(\partial_x\theta_i') + v^{-1}(\partial_\tau\theta_i')\right)\end{aligned} \tag{3.61}$$

$$\mathcal{L}_t = -\frac{2u}{\pi}\sin\left[\sqrt{\pi}\left(\phi_1(0,\tau) + \phi_2(0,\tau)\right)\right]\cos\left[\sqrt{\pi}\left(\theta_1(0,\tau) + \theta_2(0,\tau)\right)\right] \tag{3.62}$$

$$= \frac{2u}{\pi}\sin\left[\sqrt{\pi K}\left(\phi_1'(0,\tau) + \phi_2'(0,\tau)\right)\right]\cos\left[\sqrt{\frac{\pi}{K}}\left(\theta_1'(0,\tau) + \theta_2'(0,\tau)\right)\right]. \tag{3.63}$$

3.2.3 Local partition function

Before we start extracting the scaling equations for the system, we want to write the partition function in a local form, i.e. expressed in space-independent fields describing the system at the point contact, where $x = 0$. Inspired by [45] and [46], we do this by integrating over the fields everywhere except at $x = 0$. This is quite easily done because the only part of the Lagrangian that is not Gaussian in the fields is $\mathcal{L}_t$, which precisely describes the system at the point contact.

The partition function is

$$\mathcal{Z} = \int \mathcal{D}\phi_1 \mathcal{D}\phi_2 \mathcal{D}\theta_1 \mathcal{D}\theta_2 \exp(-S[\phi_1, \phi_2, \theta_1, \theta_2]), \tag{3.64}$$

with the action

$$\begin{aligned} S &= -\int_0^\beta \mathrm{d}\tau \int_{-L/2}^{L/2} \mathrm{d}x \mathcal{L} \\ &= \int \mathrm{d}x \mathrm{d}\tau \Bigg\{ \frac{1}{4} \sum_{i=1}^{2} \left(v(\partial_x \phi_i') + v^{-1}(\partial_\tau \phi_i') + v(\partial_x \theta_i') + v^{-1}(\partial_\tau \theta_i') \right) \\ &+ \frac{2u}{\pi} \sin\left[\sqrt{\pi K} \left(\phi_1'(0,\tau) + \phi_2'(0,\tau) \right) \right] \cos\left[\sqrt{\frac{\pi}{K}} \left(\theta_1'(0,\tau) + \theta_2'(0,\tau) \right) \right] \Bigg\}. \end{aligned} \tag{3.65}$$

We rewrite $\mathcal{Z}$ as:

$$\begin{aligned} \mathcal{Z} = \int & \mathcal{D}\phi_1 \mathcal{D}\phi_2 \mathcal{D}\theta_1 \mathcal{D}\theta_2 \mathcal{D}\tilde{\phi}_1 \mathcal{D}\tilde{\phi}_2 \mathcal{D}\tilde{\theta}_1 \mathcal{D}\tilde{\theta}2 \\ & \times e^{-S} \prod_\tau \Big[\delta\left(\tilde{\phi}_1(\tau) - \phi_1(0,\tau) \right) \delta\left(\tilde{\phi}_2(\tau) - \phi_2(0,\tau) \right) \\ & \times \delta\left(\tilde{\theta}_1(\tau) - \theta_1(0,\tau) \right) \delta\left(\tilde{\theta}_2(\tau) - \theta_2(0,\tau) \right) \Big] \\ & = \int \mathcal{D}\phi_1 \ldots \mathcal{D}\tilde{\theta}_2 \mathcal{D}k_{\phi_1} \ldots \mathcal{D}k_{\theta_2} \exp\Bigg[-S \\ & + i \int \mathrm{d}\tau \Big[k_{\phi_1}(\tau) \left(\tilde{\phi}_1 - \phi_1(0,\tau) \right) + \ldots + k_{\theta_2}(\tau) \left(\tilde{\theta}_2 - \theta_2(0,\tau) \right) \Big] \Bigg], \end{aligned} \tag{3.66}$$

where the relation $\delta(\tilde{\phi}_1(\tau) - \phi_1(0,\tau)) = \frac{1}{2\pi} \int \mathrm{d}k_{\phi_1}(\tau) \exp(ik(\tilde{\phi} - \phi(0,\tau)))$ has been used. The action in eq. (3.65) contains

$$I = \int \mathrm{d}x\mathrm{d}\tau \left(v(\partial_x \varphi_i)^2 + v^{-1}(\partial_\tau \varphi_i)^2 \right) \tag{3.67}$$

for both $\varphi = \phi'$ and $\varphi = \theta'$. This integral can be rewritten in terms of Fourier sums as

$$\begin{aligned}
I = &\int \mathrm{d}x\mathrm{d}\tau \\
&\times \Bigg(v(\beta L)^{-1} \sum_{q,\omega_n} iq\varphi_{q,\omega_n} e^{i(qx-\omega_n\tau)} (\beta L)^{-1} \sum_{q',\omega_n'} (-iq'\varphi^*_{q',\omega_n'}) e^{-i(q'x-\omega_n'\tau)} \\
&\quad + v^{-1}(\beta L)^{-1} \sum_{q,\omega_n} (-i\omega_n \varphi_{q,\omega_n}) e^{i(qx-\omega_n\tau)} (\beta L)^{-1} \sum_{q',\omega_n'} i\omega_n' \varphi^*_{q',\omega_n'} e^{-i(q'x-\omega_n'\tau)} \Bigg) \\
&= \int \mathrm{d}x\mathrm{d}\tau \frac{1}{(\beta L)^2} \sum_{q,q',\omega_n,\omega_n'} \Big(vqq' \varphi_{q,\omega_n} \varphi^*_{q',\omega_n'} e^{i(q-q')x} e^{i(\omega_n-\omega_n')\tau} \\
&\qquad + v^{-1}\omega_n\omega_n' \varphi_{q,\omega_n} \varphi^*_{q',\omega_n'} e^{i(q-q')x} e^{i(\omega_n-\omega_n')\tau} \Big) \\
&= \frac{1}{\beta L} \sum_{q,q',\omega_n,\omega_n'} (vqq' + v^{-1}\omega_n\omega_n') \varphi_{q,\omega_n} \varphi^*_{q',\omega_n'} \delta_{q,q'} \delta_{\omega_n,\omega_n'} \\
&= \frac{1}{\beta L} \sum_{q,\omega_n} (vq^2 + v^{-1}\omega_n^2) |\varphi|^2.
\end{aligned} \tag{3.68}$$

We use this for both $\varphi = \phi_i'$ and $\varphi = \theta_i'$. Also, in the same manner,

$$i \int \mathrm{d}\tau k\tilde{\phi}(\tau) = i \int \mathrm{d}\tau \beta^{-1} \sum_{\omega_n,\omega_n'} k(\omega_n) \tilde{\phi}\omega_n' e^{i(\omega_n+\omega_n')\tau} = \frac{i}{\beta} \sum_{\omega_n} k\omega_n \tilde{\phi}_{-\omega_n} \tag{3.69}$$

and

$$\begin{aligned}
-i \int \mathrm{d}\tau k\phi(0,\tau) &= -i \int \mathrm{d}\tau \beta^{-1} \sum_{\omega_n} k(\omega_n) e^{-i\omega_n\tau} (\beta L)^{-1} \sum_{q,\omega_n'} \phi_{q,\omega_n'} e^{i(qx-\omega_n'\tau)} \\
&= -i \int \mathrm{d}\tau \frac{1}{\beta^2 L} \sum_{q,\omega_n,\omega_n'} k(\omega_n) \phi_{q,\omega_n'} e^{-i(\omega_n+\omega_n')\tau} e^{iqx} \\
&= -\frac{i}{\beta L} \sum_{q,\omega_n} k(-\omega_n) \phi_{q,\omega_n},
\end{aligned} \tag{3.70}$$

where in the last expression we have used that $\exp[iqx] = 1$ when $x = 0$. The partition function can now be rewritten as

$$\begin{aligned}\mathcal{Z} = &\int \mathcal{D}\phi_1 \ldots \mathcal{D}\tilde{\theta}_2 \mathcal{D}k_{\phi_1} \ldots \mathcal{D}k_{\theta_2} \\ &\times \exp \sum_{i=1}^{2} \Bigg[-\frac{1}{4}\frac{1}{\beta L} \sum_{q,\omega_n} \Bigg\{ \left(\frac{1}{vK}\omega_n^2 + \frac{v}{K}q^2 \right) |\phi_i|^2 + \left(\frac{K}{v}\omega_n^2 + Kvq^2 \right) |\theta_i|^2 \\ &\qquad - 4ik_{\phi_i}(-\omega_n)\phi_i(q,\omega_n) - 4ik_{\theta_i}(-\omega_n)\theta_i(q,\omega_n) \Bigg\} \\ &\qquad + \frac{i}{\beta} \sum_{\omega_n} \left(k_{\phi_i}(\omega_n)\tilde{\phi}_i(-\omega_n) + k_{\theta_i}(\omega_n)\tilde{\theta}_i(-\omega_n) \right) \\ &\qquad - \int \mathrm{d}x \mathrm{d}\tau \mathcal{L}_t \left[\tilde{\phi}_i, \tilde{\theta}_i \right] \Bigg]. \end{aligned} \tag{3.71}$$

We are now ready to perform the Gaussian integrations, first over ϕ_1, ϕ_2, θ_1 and θ_2:

$$\begin{aligned}\mathcal{Z} \propto &\int \mathcal{D}\tilde{\phi}_1 \mathcal{D}\tilde{\phi}_2 \mathcal{D}\tilde{\theta}_1 \mathcal{D}\tilde{\theta}_2 \mathcal{D}k_{\phi_1} \mathcal{D}k_{\phi_2} \mathcal{D}k_{\theta_1} \mathcal{D}k_{\theta_2} \\ &\exp \sum_{i=1}^{2} \Bigg[-\frac{1}{\beta L} \sum_{q,\omega_n} \Bigg\{ k_{\phi_i}(-\omega_n) \left(\frac{1}{vK}\omega_n^2 + \frac{v}{K}q^2 \right)^{-1} k_{\phi_i}(\omega_n) \\ &k_{\theta_i}(-\omega_n) \left(\frac{K}{v}\omega_n^2 + Kvq^2 \right)^{-1} k_{\theta_i}(\omega_n) \Bigg\} \\ &+ \frac{i}{\beta} \sum_{\omega_n} \left(k_{\phi_i}(\omega_n)\tilde{\phi}_i(-\omega_n) + k_{\theta_i}(\omega_n)\tilde{\theta}_i(-\omega_n) \right) - \int \mathrm{d}x \mathrm{d}\tau \mathcal{L}_t \left[\tilde{\phi}_i, \tilde{\theta}_i \right] \Bigg]. \end{aligned} \tag{3.72}$$

Taking the q-sums to the continuum limit and performing the resulting integrals,

$$
\begin{aligned}
\mathcal{Z} \propto & \int \mathcal{D}\tilde{\phi}_1 \mathcal{D}\tilde{\phi}_2 \mathcal{D}\tilde{\theta}_1 \mathcal{D}\tilde{\theta}_2 \mathcal{D}k_{\phi_1} \mathcal{D}k_{\phi_2} \mathcal{D}k_{\theta_1} \mathcal{D}k_{\theta_2} \\
& \exp \sum_{i=1}^{2} \Bigg[- \frac{1}{\beta} \sum_{\omega_n} \Bigg\{ k_{\phi_i}(-\omega_n) k_{\phi_i}(\omega_n) K \int \frac{\mathrm{d}q}{2\pi} \left(\frac{1}{v} \omega_n^2 + v q^2 \right)^{-1} \\
& + k_{\theta_i}(-\omega_n) k_{\theta_i}(\omega_n) \frac{1}{K} \int \frac{\mathrm{d}q}{2\pi} \left(\frac{1}{v} \omega_n^2 + v q^2 \right)^{-1} \Bigg\} \\
& + \frac{i}{\beta} \sum_{\omega_n} \Big(k_{\phi_i}(\omega_n) \tilde{\phi}_i(-\omega_n) + k_{\theta_i}(\omega_n) \tilde{\theta}_i(-\omega_n) \Big) - \int \mathrm{d}x \mathrm{d}\tau \mathcal{L}_t \left[\tilde{\phi}_i, \tilde{\theta}_i \right] \Bigg] \\
= & \int \mathcal{D}\tilde{\phi}_1 \mathcal{D}\tilde{\phi}_2 \mathcal{D}\tilde{\theta}_1 \mathcal{D}\tilde{\theta}_2 \mathcal{D}k_{\phi_1} \mathcal{D}k_{\phi_2} \mathcal{D}k_{\theta_1} \mathcal{D}k_{\theta_2} \\
& \exp \sum_{i=1}^{2} \Bigg[- \frac{1}{\beta} \sum_{\omega_n} \Bigg\{ k_{\phi_i}(-\omega_n) k_{\phi_i}(\omega_n) K \left(\frac{\pi}{2\pi|\omega_n|} \right) \\
& + k_{\theta_i}(-\omega_n) k_{\theta_i}(\omega_n) \frac{1}{K} \left(\frac{\pi}{2\pi|\omega_n|} \right) \Bigg\} \\
& + \frac{i}{\beta} \sum_{\omega_n} \Big(k_{\phi_i}(\omega_n) \tilde{\phi}_i(-\omega_n) + k_{\theta_i}(\omega_n) \tilde{\theta}_i(-\omega_n) \Big) - \int \mathrm{d}x \mathrm{d}\tau \mathcal{L}_t \left[\tilde{\phi}_i, \tilde{\theta}_i \right] \Bigg].
\end{aligned}
\tag{3.73}
$$

Finally, we perform the Gaussian integrals over k_{ϕ_1}, k_{ϕ_2}, k_{θ_1} and k_{θ_2}:

$$
\begin{aligned}
\mathcal{Z} \propto \int \mathcal{D}\tilde{\phi}_1 \mathcal{D}\tilde{\phi}_2 \mathcal{D}\tilde{\theta}_1 \mathcal{D}\tilde{\theta}_2 \exp \sum_i \Bigg[& - \frac{1}{2\beta} \sum_{\omega_n} \left(\frac{|\omega_n|}{K} |\tilde{\phi}_i|^2 + K |\omega_n| |\tilde{\theta}_i|^2 \right) \\
& - \int \mathrm{d}x \mathrm{d}\tau \mathcal{L}_t \left[\tilde{\phi}_i, \tilde{\theta}_i \right] \Bigg].
\end{aligned}
\tag{3.74}
$$

In the continuum limit of ω_n, this is

$$
\begin{aligned}
\mathcal{Z} \propto & \int \mathcal{D}\tilde{\phi}_1 \mathcal{D}\tilde{\phi}_2 \mathcal{D}\tilde{\theta}_1 \mathcal{D}\tilde{\theta}_2 \\
& \times \exp \sum_i \Bigg[- \int_{-\Lambda}^{\Lambda} \frac{\mathrm{d}\omega}{2\pi} |\omega| \left(\frac{1}{2K} |\tilde{\phi}_i(\omega)|^2 + \frac{K}{2} |\tilde{\theta}_i(\omega)|^2 \right) \\
& - \int \mathrm{d}x \mathrm{d}\tau \mathcal{L}_t \left[\tilde{\phi}_i, \tilde{\theta}_i \right] \Bigg].
\end{aligned}
\tag{3.75}
$$

In the time domain, this can be written as

$$\mathcal{Z} \propto \int \mathcal{D}\tilde{\phi}_1 \mathcal{D}\tilde{\phi}_2 \mathcal{D}\tilde{\theta}_1 \mathcal{D}\tilde{\theta}_2 \times \exp \sum_i \left[- \int_0^\beta \int_{-\infty}^\infty \mathrm{d}t\mathrm{d}t' \left(\frac{1}{2K} \frac{\phi(t)\phi(t')}{\pi t} + \frac{K}{2} \frac{\theta(t)\theta(t')}{\pi t} \right) - \int \mathrm{d}x \mathrm{d}\tau \mathcal{L}_t \left[\tilde{\phi}_i, \tilde{\theta}_i \right] \right]. \quad (3.76)$$

3.3 RG analysis

The partition function is now written in a form appropriate for the RG analysis. The coupling constant u that enters the tunnelling Lagrangian $\mathcal{L}_t$ is treated as a perturbation to the theory, and we will start with extracting the scaling equations to first order in u. This is done by integrating out a larger and larger portion of the high-energy part of the theory. This will yield a set of differential equations for the flow of the different variables with the renormalisation parameter, and these will in turn tell us what happens with u in the low-energy limit. After that, we perform the renormalisation to order u^2. As we will see, this will yield some new terms different from the tunnelling term, so we will have to analyse these as well.

3.3.1 First order scaling equation

We now focus on the tunnelling part of the action, $S_t = -\int \mathrm{d}x\mathrm{d}\tau \mathcal{L}_t \left[\tilde{\phi}_i, \tilde{\theta}_i \right]$. From now on, we will skip the tilde on the fields, assuming all the fields are x-independent, living at the point $x = 0$. The idea is to divide the fields into a slow and a fast part, i.e. $\phi(\tau) = \phi_s(\tau) + \phi_f(\tau)$ with

$$\phi_s(\tau) = \sum_{|\omega_n|<\Lambda/b} e^{-i\omega_n\tau}\phi_{\omega_n} = \int_{-\Lambda/b}^{\Lambda/b} \frac{\mathrm{d}\omega}{2\pi} e^{-i\omega\tau}\phi(\omega) \quad (3.77)$$

$$\phi_f(\tau) = \sum_{\Lambda/b<|\omega_n|<\Lambda} e^{-i\omega_n\tau}\phi_{\omega_n} = \int_{\Lambda/b<|\omega_n|<\Lambda} \frac{\mathrm{d}\omega}{2\pi} e^{-i\omega\tau}\phi(\omega). \quad (3.78)$$

We want to find an expression for the effective action, S_{eff}, of the slow fields. It is:

$$e^{-S_{\mathit{eff}}[\phi_s]} = e^{-S_s[\phi_s]} \left\langle e^{-S_t[\phi_s,\phi_f]} \right\rangle_f, \quad (3.79)$$

where $\langle A\rangle_f = \int \mathcal{D}\phi_f e^{-S_f[\phi_f]} A$. Since

$$S_t = -\frac{2u}{\pi}\int \mathrm{d}\tau \sin\left[\sqrt{\pi}\left(\phi_1(0,\tau)+\phi_2(0,\tau)\right)\right]\cos\left[\sqrt{\pi}\left(\theta_1(0,\tau)+\theta_2(0,\tau)\right)\right], \tag{3.80}$$

we can write $e^{-S_t} = 1 - S_t + \ldots$ and make the observation that the approximation $\left\langle e^{-S_t}\right\rangle_f \approx e^{-\langle S_t\rangle_f}$ holds to first order in u. Thus, $e^{-S_{eff}} \approx e^{-S_s[\phi_s]} e^{-\left\langle S_t[\phi_s,\phi_f]\right\rangle_f}$. We will do the first order calculation here and the second order in the next section. The average is

$$\begin{aligned}\langle S_t\rangle_f = \frac{2u}{\pi}\int \mathcal{D}\phi_{1f}\mathcal{D}\phi_{2f}\mathcal{D}\theta_{1f}\mathcal{D}\theta_{2f} e^{-S_f[\phi_{1f},\phi_{2f},\theta_{1f},\theta_{2f}]} \\ \times \int \mathrm{d}\tau \sin\left[\sqrt{\pi}\left(\phi_1(\tau)+\phi_2(\tau)\right)\right]\cos\left[\sqrt{\pi}\left(\theta_1(\tau)+\theta_2(\tau)\right)\right].\end{aligned} \tag{3.81}$$

Using

$$\begin{aligned}\sin\left[\sqrt{\pi}(\phi_1+\phi_2)\right] &= \frac{1}{2i}\left(e^{i\sqrt{\pi}(\phi_{1s}+\phi_{2s})} e^{i\sqrt{\pi}(\phi_{1f}+\phi_{2f})} - \text{H.c.}\right) \\ &= \frac{1}{2i}\left(e^{i\sqrt{\pi}(\phi_{1s}+\phi_{2s})} e^{i\sqrt{\pi}\left(\int_f \frac{\mathrm{d}\omega}{2\pi} e^{i\omega\tau}(\phi_1(\omega)+\phi_2(\omega))\right)} - \text{H.c.}\right),\end{aligned} \tag{3.82}$$

and similarly for the θ fields, we can perform two Gaussian integrations of eq. (3.81), first over the ϕ fields and then over the θ fields. Here, "H.c." denotes Hermitian conjugate. Using the notation $\int_f \equiv \int_{\Lambda/b<|\omega|<\Lambda}$ for the integrals over the fast fields, we obtain

$$
\begin{aligned}
\langle S_t\rangle_f &= \frac{u}{i\pi}\Bigg(\int \mathrm{d}\tau e^{i\sqrt{\pi}(\phi_{1s}+\phi_{2s})}\int \mathcal{D}\phi_{1f}\ldots\mathcal{D}\theta_{2f}\cos\left[\sqrt{\pi}(\theta_1+\theta_2)\right]\\
&\quad\times\exp\left[\int_f\frac{\mathrm{d}\omega}{2\pi}\sum_i\left(i\sqrt{\pi}e^{i\omega\tau}\phi_{if}(\omega)-\frac{1}{2K}|\omega||\phi_{if}|^2\right)\right]-\text{H.c.}\Bigg)\\
&= \frac{u}{i\pi}\Bigg(\int \mathrm{d}\tau e^{i\sqrt{\pi}(\phi_{1s}+\phi_{2s})}\int \mathcal{D}\theta_{1f}\mathcal{D}\theta_{2f}\cos\left[\sqrt{\pi}(\theta_1+\theta_2)\right]\\
&\quad\times\exp\left[\int_f\frac{\mathrm{d}\omega}{2\pi}\left(-\frac{\pi}{2}\left(\frac{|\omega|}{K}\right)^{-1}-\frac{\pi}{2}\left(\frac{|\omega|}{K}\right)^{-1}\right)\right]-\text{H.c.}\Bigg)\\
&= \frac{2u}{\pi}\Bigg(\int \mathrm{d}\tau\sin\left[\sqrt{\pi}(\phi_{1s}+\phi_{2s})\right]e^{-\int_f\mathrm{d}\omega\frac{K}{2|\omega|}}\\
&\quad\times\int\mathcal{D}\theta_{1f}\mathcal{D}\theta_{2f}\cos\left[\sqrt{\pi}(\theta_1+\theta_2)\right]\Bigg)\\
&= \frac{u}{\pi}\Bigg(\int \mathrm{d}\tau\sin\left[\sqrt{\pi}(\phi_{1s}+\phi_{2s})\right]e^{-\int_f\mathrm{d}\omega\frac{K}{2|\omega|}}e^{i\sqrt{\pi}(\theta_{1s}+\theta_{2s})}\int\mathcal{D}\theta_{1f}\mathcal{D}\theta_{2f}\\
&\quad\times\exp\left[\int_f\frac{\mathrm{d}\omega}{2\pi}\sum_i\left(i\sqrt{\pi}e^{i\omega\tau}\theta_{if}(\omega)-\frac{K}{2}|\omega||\theta_{if}|^2\right)\right]+\text{H.c.}\Bigg)\\
&= \frac{2u}{\pi}\left(\int \mathrm{d}\tau\sin\left[\sqrt{\pi}(\phi_{1s}+\phi_{2s})\right]\cos\left[\sqrt{\pi}(\theta_{1s}+\theta_{2s})\right]e^{-\left(\frac{K}{2}+\frac{1}{2K}\right)\int_f\frac{\mathrm{d}\omega}{|\omega|}}\right).
\end{aligned}
\tag{3.83}
$$

Now, the integral

$$
\int_f\frac{\mathrm{d}\omega}{|\omega|}\equiv\int_{\Lambda/b<|\omega|<\Lambda}\frac{\mathrm{d}\omega}{|\omega|}=\int_{\Lambda/b}^{\Lambda}\frac{\mathrm{d}\omega}{\omega}=\ln b, \tag{3.84}
$$

so that

$$
e^{-\frac{1}{2}\left(K+\frac{1}{K}\right)\int_f\frac{\mathrm{d}\omega}{|\omega|}}=e^{-\frac{\ln b}{2}\left(K+\frac{1}{K}\right)}=b^{-\frac{1}{2}\left(K+\frac{1}{K}\right)}. \tag{3.85}
$$

We can now write the exponential of the effective action as

$$
e^{-S_{\mathit{eff}}}\approx\exp\left[-S_s[\phi_{1s},\phi_{2s},\theta_{1s},\theta_{2s}]-b^{-\frac{1}{2}\left(K+\frac{1}{K}\right)}S_t[\phi_{1s},\phi_{2s},\theta_{1s},\theta_{2s}]\right], \tag{3.86}
$$

i.e. our effective action is the same as the one we started from, apart from two crucial differences: firstly, the cutoff momentum Λ has been rescaled to Λ/b, so that the fields can only fluctuate on energy scales $|\omega|<\Lambda/b$,

and secondly, the coupling constant of the tunnelling has been rescaled from u to $b^{\frac{1}{2}\left(K+\frac{1}{K}\right)}u$. In order to complete the RG program and obtain the scaling equations, we want to compare the model before and after the integration over the fast fields. For this, we rescale τ and ω so that the fields fluctuate over the same energy/time scale in both of the actions. Since the ω-integrations before and after the fast-field integration are taken over $|\omega| < \Lambda$ and $|\omega| < \Lambda/b$ respectively, the rescaling is simply $\omega \to \omega' = b\omega$ and, consequently, $\tau \to \tau' = \tau/b$. We choose the rescaled fields to be $\phi'(\tau') = \phi_s(\tau)$, and from eq. (3.77), we see that this implies $\phi'(\omega') = \phi(\omega)/b$ (and, of course, $\theta'(\tau') = \theta(\tau) \Rightarrow \theta'(\omega') = \theta(\omega)/b$).

Putting this together, the rescaled effective action is

$$\begin{aligned} S_{\mathit{eff}}[\phi_{1s}, \phi_{2s}, \theta_{1s}, \theta_{2s}] &= S'[\phi'_1, \phi'_2, \theta'_1, \theta'_2] \\ &= \sum_i \int_{-\Lambda}^{\Lambda} \frac{\mathrm{d}\omega'}{2\pi} |\omega'| \left(\frac{1}{2K} |\phi'_i(\omega')|^2 + \frac{K}{2} |\theta'_i(\omega')|^2 \right) \\ &+ b^{-\frac{1}{2}\left(K+\frac{1}{K}\right)} \frac{u}{2\pi} \int b \mathrm{d}\tau' \sin\left[\sqrt{\pi}\left(\phi'_1(\tau') + \phi'_2(\tau')\right)\right] \\ &\times \cos\left[\sqrt{\pi}\left(\theta'_1(\tau') + \theta'_2(\tau')\right)\right] \end{aligned} \tag{3.87}$$

and from this, we see that the effect of "lowering the cutoff", i.e. looking at the theory with slower fluctuating fields, is the rescaling of the tunnelling coupling constant with $u \to u' = ub^{1-\frac{1}{2}\left(K+\frac{1}{K}\right)}$. We can now obtain the scaling equation to first order in u:

$$\frac{\mathrm{d}u'}{\mathrm{d}\ln b} = u' \left(1 - \frac{1}{2}\left(K + \frac{1}{K}\right)\right). \tag{3.88}$$

This tells us that the coupling constant u will be renormalised to zero when $K + 1/K < 2$ and to infinity when $K + 1/K > 2$. However, regardless of the value of $K = \sqrt{\frac{v_F - g/\pi}{v_F + g/\pi}}$, it will always be true that $K + 1/K \geq 2$ (see fig. 3.3), with equality only for $K = 1 \Leftrightarrow g = 0$. This means that the renormalisation flow will be towards $u = 0$, i.e. u is irrelevant under renormalisation.

3.3.2 Second order scaling equations

We will now perform the renormalisation to second order in u. The first order analysis showed no relevance of the tunnelling parameter u. As we will see, the second order analysis will yield RG equations also for new terms proportional to u^2, that may make the tunnelling relevant.

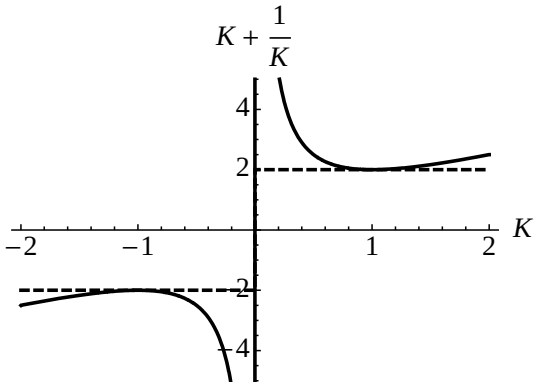

Figure 3.3: $K + \frac{1}{K}$

The full calculation in all its details is rather lengthy, but the interested reader can find all of it in my licentiate thesis, ref. [27].

If we expand the averaged exponential in eq. (3.79), we get

$$e^{-S_{\mathit{eff}}[\phi_s]} = e^{-S_s[\phi_s]} \left\langle e^{-S_t[\phi_s,\phi_f]} \right\rangle_f = e^{-S_s[\phi_s]} e^{\langle S_t\rangle_f - \frac{1}{2}\left(\left\langle S_t^2\right\rangle_f - \langle S_t\rangle_f^2\right)+\cdots}, \quad (3.89)$$

so in order to obtain the effective action to second order in u, we need to calculate both $\langle S_t\rangle_f$,$\langle S_t^2\rangle_f$ and $\langle S_t\rangle_f^2$. We start with $\langle S_t^2\rangle_f$.

$$\begin{aligned}\left\langle S_t^2\right\rangle_f = \frac{4u^2}{\pi^2} \int \mathcal{D}\phi_{f1} \ldots \mathcal{D}\theta_{f2} e^{-S_f[\phi_{f1},\ldots,\theta_{2f}]} \\ \times \int \mathrm{d}\tau \mathrm{d}\tau' \sin\left[\sqrt{\pi}(\phi_1+\phi_2)\right] \cos\left[\sqrt{\pi}(\theta_1+\theta_2)\right] \\ \times \sin\left[\sqrt{\pi}(\phi_1'+\phi_2')\right] \cos\left[\sqrt{\pi}(\theta_1'+\theta_2')\right], \quad (3.90)\end{aligned}$$

where $\phi_1 = \phi_1(\tau)$, $\phi_1' = \phi_1(\tau')$ and similarly for the other fields. This is calculated in ref. [27], and the result is

$$\begin{aligned}\left\langle S_t^2\right\rangle_f = \frac{u^2}{2\pi^2} \int \mathrm{d}\tau \mathrm{d}\tau' \\ \times\Big(\cos\left[\sqrt{\pi}(\phi_s^+ + \theta_s^+)\right] e^{-\frac{\pi}{2}\left\langle(\phi_f^+ + \theta_f^+)^2\right\rangle_f} + \cos\left[\sqrt{\pi}(\phi_s^+ - \theta_s^+)\right] e^{-\frac{\pi}{2}\left\langle(\phi_f^+ - \theta_f^+)^2\right\rangle_f} \\ + \cos\left[\sqrt{\pi}(\phi_s^+ + \theta_s^-)\right] e^{-\frac{\pi}{2}\left\langle(\phi_f^+ + \theta_f^-)^2\right\rangle_f} + \cos\left[\sqrt{\pi}(\phi_s^+ - \theta_s^-)\right] e^{-\frac{\pi}{2}\left\langle(\phi_f^+ - \theta_f^-)^2\right\rangle_f} \\ - \cos\left[\sqrt{\pi}(\phi_s^- + \theta_s^+)\right] e^{-\frac{\pi}{2}\left\langle(\phi_f^- + \theta_f^+)^2\right\rangle_f} - \cos\left[\sqrt{\pi}(\phi_s^- - \theta_s^+)\right] e^{-\frac{\pi}{2}\left\langle(\phi_f^- - \theta_f^+)^2\right\rangle_f} \\ - \cos\left[\sqrt{\pi}(\phi_s^- + \theta_s^-)\right] e^{-\frac{\pi}{2}\left\langle(\phi_f^- + \theta_f^-)^2\right\rangle_f} - \cos\left[\sqrt{\pi}(\phi_s^- - \theta_s^-)\right] e^{-\frac{\pi}{2}\left\langle(\phi_f^- - \theta_f^-)^2\right\rangle_f}\Big), \\ (3.91)\end{aligned}$$

where we have defined $\phi^+_{s/f} \equiv \phi_{1s/f} + \phi_{2s/f} + \phi'_{1s/f} + \phi'_{2s/f}$, $\phi^-_{s/f} \equiv \phi_{1s/f} + \phi_{2s/f} - \phi'_{1s/f} - \phi'_{2s/f}$, $\theta^+_{s/f} \equiv \theta_{1s/f} + \theta_{2s/f} + \theta'_{1s/f} + \theta'_{2s/f}$ and $\theta^-_{s/f} \equiv \theta_{1s/f} + \theta_{2s/f} - \theta'_{1s/f} - \theta'_{2s/f}$. Using

$$\langle S_t \rangle_f = \frac{2u}{\pi} \int \mathrm{d}\tau \left\langle \sin\left[\sqrt{\pi}(\phi_1 + \phi_2)\right] \cos\left[\sqrt{\pi}(\theta_1 + \theta_2)\right] \right\rangle_f , \tag{3.92}$$

the result for $\langle S_t \rangle_f^2$ is

$$\begin{aligned}
\langle S_t \rangle_f^2 = \frac{u^2}{2\pi^2} \int \mathrm{d}\tau \mathrm{d}\tau' \\
\times \Big(\left[\cos\left[\sqrt{\pi}(\phi_s^- + \theta_s^-)\right] - \cos\left[\sqrt{\pi}(\phi_s^+ + \theta_s^+)\right]\right] e^{-\frac{\pi}{2}\left(<a>_f + <a'>_f\right)} \\
+ \left[\cos\left[\sqrt{\pi}(\phi_s^- + \theta_s^+)\right] - \cos\left[\sqrt{\pi}(\phi_s^+ + \theta_s^-)\right]\right] e^{-\frac{\pi}{2}\left(<a>_f + <b'>_f\right)} \\
+ \left[\cos\left[\sqrt{\pi}(\phi_s^- - \theta_s^+)\right] - \cos\left[\sqrt{\pi}(\phi_s^+ - \theta_s^-)\right]\right] e^{-\frac{\pi}{2}\left(<b>_f + <a'>_f\right)} \\
+ \left[\cos\left[\sqrt{\pi}(\phi_s^- - \theta_s^-)\right] - \cos\left[\sqrt{\pi}(\phi_s^+ - \theta_s^+)\right]\right] e^{-\frac{\pi}{2}\left(<b>_f + <b'>_f\right)} \Big).,
\end{aligned} \tag{3.93}$$

where $a \equiv (\phi 1 f + \phi_{2f} + \theta_{1f} + \theta_{2f})$ and $b \equiv (\phi 1 f + \phi_{2f} - \theta_{1f} - \theta_{2f})$. Thus,

$$\begin{aligned}
\left\langle S_t^2 \right\rangle_f - \langle S_t \rangle_f^2 = \frac{u^2}{2\pi^2} \int \mathrm{d}\tau \mathrm{d}\tau' \\
\times \Bigg[\cos(\phi_s^+ + \theta_s^+) \left(-e^{-\frac{\pi}{2}\left\langle (\phi_f^+ + \theta_f^+)^2 \right\rangle_f} + e^{\frac{\pi}{2}\left(\langle a \rangle_f + \langle a' \rangle_f\right)} \right) \\
+ \cos(\phi_s^+ - \theta_s^+) \left(-e^{-\frac{\pi}{2}\left\langle (\phi_f^+ - \theta_f^+)^2 \right\rangle_f} + e^{\frac{\pi}{2}\left(\langle b \rangle_f + \langle b' \rangle_f\right)} \right) \\
+ \cos(\phi_s^+ + \theta_s^-) \left(-e^{-\frac{\pi}{2}\left\langle (\phi_f^+ + \theta_f^-)^2 \right\rangle_f} + e^{\frac{\pi}{2}\left(\langle a \rangle_f + \langle b' \rangle_f\right)} \right) \\
+ \cos(\phi_s^+ - \theta_s^-) \left(-e^{-\frac{\pi}{2}\left\langle (\phi_f^+ - \theta_f^-)^2 \right\rangle_f} + e^{\frac{\pi}{2}\left(\langle b \rangle_f + \langle a' \rangle_f\right)} \right) \\
+ \cos(\phi_s^- + \theta_s^+) \left(-e^{-\frac{\pi}{2}\left\langle (\phi_f^- + \theta_f^+)^2 \right\rangle_f} + e^{\frac{\pi}{2}\left(\langle a \rangle_f + \langle b' \rangle_f\right)} \right) \\
+ \cos(\phi_s^- - \theta_s^+) \left(-e^{-\frac{\pi}{2}\left\langle (\phi_f^- - \theta_f^+)^2 \right\rangle_f} + e^{\frac{\pi}{2}\left(\langle b \rangle_f + \langle a' \rangle_f\right)} \right) \\
+ \cos(\phi_s^- + \theta_s^-) \left(-e^{-\frac{\pi}{2}\left\langle (\phi_f^- + \theta_f^-)^2 \right\rangle_f} + e^{\frac{\pi}{2}\left(\langle a \rangle_f + \langle a' \rangle_f\right)} \right) \\
+ \cos(\phi_s^- - \theta_s^-) \left(-e^{-\frac{\pi}{2}\left\langle (\phi_f^- - \theta_f^-)^2 \right\rangle_f} + e^{\frac{\pi}{2}\left(\langle b \rangle_f + \langle b' \rangle_f\right)} \right) \Bigg].
\end{aligned} \tag{3.94}$$

A heavy use of symmetry considerations lead us to the expression

$$\begin{aligned}
&\left\langle S_t^2\right\rangle_f - \langle S_t\rangle_f^2 \to \frac{u^2}{\pi^2} e^{-2\pi\left(G_\theta(0)+G_\phi(0)\right)} \\
&\times \int \mathrm{d}\tau \Big\{ \cos\left[\sqrt{\pi}\left(2\phi_{1s}+2\phi_{2s}\right)\right] \cos\left[\sqrt{\pi}\left(2\theta_{1s}+2\theta_{2s}\right)\right] \left(1 - e^{-2\pi\left(G_\theta(0)+G_\phi(0)\right)}\right) \\
&\qquad + \cos\left[\sqrt{\pi}\left(2\phi_{1s}+2\phi_{2s}\right)\right] \left(1 - e^{-2\pi\left(-G_\theta(0)+G_\phi(0)\right)}\right) \\
&\qquad - \cos\left[\sqrt{\pi}\left(2\theta_{1s}+2\theta_{2s}\right)\right] \left(1 - e^{-2\pi\left(G_\theta(0)-G_\phi(0)\right)}\right) \\
&- \left(1 - \frac{1}{2}\left(\frac{\partial\phi_{1s}}{\partial\tau} + \frac{\partial\phi_{2s}}{\partial\tau}\right)^2 - \frac{1}{2}\left(\frac{\partial\theta_{1s}}{\partial\tau} + \frac{\partial\theta_{2s}}{\partial\tau}\right)^2\right) \left(1 - e^{-2\pi\left(-G_\theta(0)-G_\phi(0)\right)}\right) \Big\} \\
&\qquad = \frac{u^2}{\pi^2} e^{-\left(K+\frac{1}{K}\right)\ln b} \\
&\times \int \mathrm{d}\tau \Big\{ \cos\left[\sqrt{\pi}\left(2\phi_{1s}+2\phi_{2s}\right)\right] \cos\left[\sqrt{\pi}\left(2\theta_{1s}+2\theta_{2s}\right)\right] \left(1 - e^{\left(K+\frac{1}{K}\right)\ln b}\right) \\
&\qquad + \cos\left[\sqrt{\pi}\left(2\phi_{1s}+2\phi_{2s}\right)\right] \left(1 - e^{\left(K-\frac{1}{K}\right)\ln b}\right) \\
&\qquad - \cos\left[\sqrt{\pi}\left(2\theta_{1s}+2\theta_{2s}\right)\right] \left(1 - e^{\left(-K+\frac{1}{K}\right)\ln b}\right) \\
&- \left(1 - \frac{1}{2}\left(\frac{\partial\phi_{1s}}{\partial\tau} + \frac{\partial\phi_{2s}}{\partial\tau}\right)^2 - \frac{1}{2}\left(\frac{\partial\theta_{1s}}{\partial\tau} + \frac{\partial\theta_{2s}}{\partial\tau}\right)^2\right) \left(1 - e^{-\left(K+\frac{1}{K}\right)\ln b}\right) \Big\}
\end{aligned} \tag{3.95}$$

and we are finally ready to perform the RG step by rescaling $\tau \to \tau' = \tau/b$, $\phi'(\tau') = \phi_s(\tau)$ and $\theta'(\tau') = \theta_s(\tau)$, so that the rescaled version becomes

$$\begin{aligned}
\left\langle S_t'^2\right\rangle_f - \langle S_t'\rangle_f^2 = \int \mathrm{d}\tau' \Big\{ & V_1 \cos\left[\sqrt{\pi}\left(2\phi_1' + 2\phi_2'\right)\right] \cos\left[\sqrt{\pi}\left(2\theta_1' + 2\theta_2'\right)\right] \\
& + V_2 \left(1 - \frac{1}{2}\left(\frac{\partial\phi_1'}{\partial\tau} + \frac{\partial\phi_2'}{\partial\tau}\right)^2 - \frac{1}{2}\left(\frac{\partial\theta_1'}{\partial\tau} + \frac{\partial\theta_2'}{\partial\tau}\right)^2\right) \\
& + V_\theta \cos\left[\sqrt{\pi}\left(2\theta_1' + 2\theta_2'\right)\right] + V_\phi \cos\left[\sqrt{\pi}\left(2\phi_1' + 2\phi_2'\right)\right],
\end{aligned} \tag{3.96}$$

where we have defined

$$V_1 = b\frac{u^2}{\pi^2}\left(e^{-\left(K+\frac{1}{K}\right)\ln b} - e^{-2\left(K+\frac{1}{K}\right)\ln b}\right) \tag{3.97}$$

$$V_2 = b\frac{u^2}{\pi^2}\left(1 - e^{-\left(K+\frac{1}{K}\right)\ln b}\right) \tag{3.98}$$

$$V_\theta = b\frac{u^2}{\pi^2}\left(e^{-\frac{2}{K}\ln b} - e^{-\left(K+\frac{1}{K}\right)\ln b}\right) \tag{3.99}$$

$$V_\phi = b\frac{u^2}{\pi^2}\left(e^{-\left(K+\frac{1}{K}\right)\ln b} - e^{-2K\ln b}\right). \tag{3.100}$$

The term with V_1 will be irrelevant compared to the other terms, while the V_2 term will be of higher order than the others. The two interesting terms are thus the V_θ and V_ϕ terms. The RG equation for V_θ is

$$\frac{\partial V_\theta}{\partial \ln b} = \frac{u}{\pi^2}\left((1-\frac{2}{K})e^{(1-\frac{2}{K})\ln b} - \left(1-\left(K+\frac{1}{K}\right)\right)e^{\left(1-\left(K+\frac{1}{K}\right)\right)\ln b}\right). \tag{3.101}$$

and the one for V_ϕ is

$$\frac{\partial V_\phi}{\partial \ln b} = \frac{u}{\pi^2}\left(\left(1-\left(K+\frac{1}{K}\right)\right)e^{\left(1-\left(K+\frac{1}{K}\right)\right)\ln b} - (1-2K)e^{(1-2K)\ln b}\right). \tag{3.102}$$

Since the V's and their derivatives consist of two terms each, we have to investigate when they are positive and when they are negative. Since we already know that $1-\left(K+\frac{1}{K}\right) < 0$, we have to consider three cases for each V, namely for V_ϕ

- $1-2K > 0$
- $1-\left(K+\frac{1}{K}\right) < 1-2K < 0$
- $1-2K < 1-\left(K+\frac{1}{K}\right) < 0$

and for V_θ

- $1-\frac{2}{K} > 0$
- $1-\left(K+\frac{1}{K}\right) < 1-\frac{2}{K} < 0$
- $1-\frac{2}{K} < 1-\left(K+\frac{1}{K}\right) < 0.$

Table 3.1: Signs of V_θ and its RG equations

	V_θ	$\partial V_\theta / \partial \ln b$
$1 - \frac{2}{K} > 0$	> 0	> 0
$1 - \left(K + \frac{1}{K}\right) < 1 - \frac{2}{K} < 0$	< 0	> 0
$1 - \frac{2}{K} < 1 - \left(K + \frac{1}{K}\right) < 0$	> 0	< 0

Table 3.2: Signs of V_ϕ and its RG equations

	V_ϕ	$\partial V_\phi / \partial \ln b$
$1 - 2K > 0$	< 0	< 0
$1 - \left(K + \frac{1}{K}\right) < 1 - 2K < 0$	< 0	> 0
$1 - 2K < 1 - \left(K + \frac{1}{K}\right) < 0$	> 0	< 0

The results of the investigation are given in tables 3.1 and 3.2. Table 3.2 tells us that V_ϕ becomes relevant when

$$1 - 2K > 0 \Leftrightarrow K < 1/2, \tag{3.103}$$

which means that in order for $\partial V_\theta / \partial \ln b > 0$, i.e. for V_θ to move away from the fix-point $u = 0$, K has to be smaller than $1/2$. Table 3.1 tells us that V_θ becomes relevant when

$$1 - \frac{2}{K} > 0 \Leftrightarrow K > 2. \tag{3.104}$$

We now have a condition for the tunnelling to become relevant, namely that $K < 1/2$. This corresponds to quite strong electron-electron interactions, but certainly not unreachable. In Paper I, we estimated K to be close to 0.7 in the type of HgTe quantum well device probed in the Würzburg experiments [11], with other estimates ranging from 0.55 to 0.95 [47–49]. To improve upon our estimate of K, in what follows we attempt a more careful analysis of the experimental setup.

In eq. (3.53), K was defined to be $K = \sqrt{\frac{2\pi v_F + 2g_4 - g_2}{2\pi v_F + 2g_4 + g_2}}$. To estimate the value of this, we need to know the Fermi velocity, taken to be $v_F = 5.5 \times 10^5$ m/s [11], and the coupling constants g_4 and g_2. These coupling constants stem from the low-energy Coulomb interaction, so we start by writing

$$g_4 \propto \frac{V(k=0)}{\hbar} = \frac{1}{\hbar}\int_\kappa^d \mathrm{d}x V(x) e^{i(k=0)x} = \frac{1}{\hbar}\int_\kappa^d \mathrm{d}x \frac{e^2}{4\pi\epsilon_r\epsilon_0 x} = \frac{e^2}{4\pi\hbar\epsilon_r\epsilon_0}\ln\left(\frac{d}{\kappa}\right), \quad (3.105)$$

For clarity, $\hbar$ is also included. Here, ϵ_r is the relative permittivity of the doping and insulating layers between the gate and the QW, $V(x)$ is the Coulomb potential between the electrons, while κ and d are the high- and low-energy cutoffs, respectively. The high-energy (short-distance) cutoff κ is taken to be the penetration depth of the helical edge states into the bulk of the QW [50], while the low-energy (long-distance) cutoff d is the distance from the electrons in the QW to the nearest metallic gate. To understand how this defines a long-distance cutoff for the Coulomb potential, think about an electron that feels the Coulomb force from another electron. If this other electron is as far away as the metallic gate, the electron is screened by the mirror image in the gate [51].

Prior to the renormalisation, the g_2 coupling describes the same physical process as the g_4 coupling, namely Coulomb interaction between electrons. Comparing eqs. (3.40) and (3.41), we see that g_2 is the coupling of twice as many terms as g_4, so the naked (unrenormalised) values of the coupling constants are related as $g_2 = 2g_4$. We can now write

$$K = \sqrt{\frac{2\pi v_F + 2g_4 - 2g_4}{2\pi v_F + 2g_4 + 2g_4}} = \left(1 + \frac{2g_4}{\pi v_F}\right)^{-1/2} = \left(1 + \lambda \ln\left(\frac{d}{\kappa}\right)\right)^{-1/2}, \quad (3.106)$$

where $\lambda = 2e^2/(\pi^2\epsilon_r\epsilon_0\hbar v_F)$ [49]. We take the penetration depth to be $\kappa \approx 10$ nm. In the experiment in ref. [11] the QW was separated from the top gate by several thin (≈ 10 nm) doping layers with $\epsilon_r \approx 20$ and a 110 nm thick SiO_2/Si_3N_4 superlattice layer with $\epsilon_r \approx 6$. With a weighted average of ϵ_r to approximate the screening from all layers, we end up with $\lambda \approx 1.0$ and $K \approx 0.55$ (the somewhat higher estimate in Paper I is due to an overestimate of the screening). Let us point out that by increasing the thickness of the doping and cap layers surrounding the QW and/or adding additional layers of a material with a smaller permittivity, values of K down to 0.2 can easily be obtained [49].

3.4 Conductance

In this section, we calculate the conductance of the tunnelling current. That is, we want to see what response we get from putting an electric

voltage over the point contact. The first step is to investigate what type of current is generated.

The right-moving fields are in equilibrium with a reservoir with chemical potential μ_L and the left-moving fields are in equilibrium with the other reservoir, with chemical potential μ_R. Applying a potential V over the point contact is equivalent to having $|\mu_R - \mu_L| = V$. We choose to set $\mu_L = V/2$ and $\mu_R = -V/2$. This means that we must add the term

$$\mathcal{L}_V = e \int \mathrm{d}x \left[\mu_L \left(j_{R\uparrow}(x) + j_{R\downarrow}(x)\right) + \mu_R \left(j_{L\downarrow}(x) + j_{L\uparrow}(x)\right)\right] \tag{3.107}$$

to the Lagrangian. The terms $j_{\alpha\sigma}$ denote the currents of electrons of the specified type. Using the relations $j_{L\sigma} = -\frac{1}{2\pi}\partial_x \phi_{L\sigma}$ and $j_{R\sigma} = \frac{1}{2\pi}\partial_x \phi_{R\sigma}$ and eq. (3.56), the Lagrangian can be further simplified to

$$\begin{aligned}\mathcal{L}_V &= -\frac{eV}{4\pi} \int \mathrm{d}x \left(\partial_x \phi_{R\uparrow}(x) + \partial_x \phi_{R\downarrow}(x) + \partial_x \phi_{L\uparrow}(x) + \partial_x \phi_{L\downarrow}(x)\right) \\ &= -\frac{eV}{4\pi} \int \mathrm{d}x \; \partial_x \left(\phi_1(x) + \phi_2(x)\right) = -\frac{ieV}{4\pi v} \int \mathrm{d}x \; \partial_\tau \left(\theta_1(x) + \theta_2(x)\right).\end{aligned} \tag{3.108}$$

It is here important to note that the fields in eq. (3.108) are x-dependent, i.e. defined to take values not only in $x = 0$.

It is easily seen that when $\mu_L > \mu_R$, it will be energetically favourable for the right-moving electrons to become left-moving, i.e. for the $\psi_{R\downarrow}$-fields to tunnel from the lower edge to the upper, thus becoming $\psi_{L\downarrow}$-fields, and for the $\psi_{R\uparrow}$ on the upper edge to tunnel to $\psi_{L\uparrow}$ on the lower edge. We see that this will transfer no net charge between the edges, but that it will take spin down from the lower edge to the upper and spin down from the upper edge to the lower. The electrical voltage will thus drive a spin current. We will now calculate the conductance for this current.

We calculate $I_c(t)$, the sum of the magnitudes of the charge currents of each spin tunnelling between the edges. These of course go in opposite directions and with opposite spins, so the associated spin current will be

$$I_s(t) = \frac{\hbar}{2e} I_c(t). \tag{3.109}$$

This spin current should in principle be possible to detect experimentally with a two-terminal measurement, since $I_c(t)$ will be equal to the depletion of the source-to-drain current. Note, however, that the overall spin axis may not be preserved in a realistic system. For example, an added

Rashba-type spin-orbit interaction would produce an effective precession of the spin axis. Locally, in the point contact, the tunnelling current will be a spin current, though.

Assuming the voltage to be low, the calculation can be made using the linear response formalism, as described in [52]. Assuming $V > 0$, $I_c(t)$ is the rate of change of the number of electrons in equilibrium with, for example, the left contact of the battery,

$$I_c(t) = -e\left\langle \dot{N}_L(t)\right\rangle = -ei\int_{-\infty}^{t} \mathrm{d}t' \left\langle \left[\dot{N}_L(t), H_t(t')\right]\right\rangle, \tag{3.110}$$

where $N_L = a\left(\psi^\dagger_{R\downarrow}\psi_{R\downarrow} + \psi^\dagger_{R\uparrow}\psi_{R\uparrow}\right)$ is the number operator. It commutes with the free part of the Hamiltonian, so that

$$\dot{N}_L(t) = i[H + H_t, N_L] = i[H_t, N_L]. \tag{3.111}$$

Recalling that

$$H_t = u\left(\psi^\dagger_{R\uparrow}\psi_{L\uparrow} + \psi^\dagger_{L\downarrow}\psi_{R\downarrow} + \psi^\dagger_{L\uparrow}\psi_{R\uparrow} + \psi^\dagger_{R\downarrow}\psi_{L\downarrow}\right), \tag{3.112}$$

we can calculate the commutator $[H_t, N_L]$. It is a straight-forward calculation involving no tricks, but rather lengthy, so we settle with just stating the result here:

$$\dot{N}_L = i[H, N_L] = i[H_t, N_L] = iu\left(\psi^\dagger_{L\uparrow}\psi_{R\uparrow} - \psi^\dagger_{R\uparrow}\psi_{L\uparrow} + \psi^\dagger_{L\downarrow}\psi_{R\downarrow} - \psi^\dagger_{R\downarrow}\psi_{L\downarrow}\right). \tag{3.113}$$

We also note that $[N_R, H_t]$ is obtained from $[N_L, H_t]$ by exchanging all $\uparrow\leftrightarrow\downarrow$, which means that $[N_R, H_t] = -[N_L, H_t]$.

Now, we need the time evolution of the Hamiltonian and the number operators. First of all, we can write the total Hamiltonian as

$$H_{tot} = H + H_t = H_R + H_L + H_t, \tag{3.114}$$

where H_R and H_L govern the particles in equilibrium with the right and left reservoirs respectively. These are independent, the only interaction is through the tunnelling, which is governed by H_t.

Defining $K_R = H_R - \mu_R N_R$, $K_L = H_L - \mu_L N_L$ and $K = K_R + K_L$, $H_t(t)$ is obtained according to

$$H_t(t) = e^{iHt}H_t e^{-iHt} = e^{iKt}\left(e^{it(\mu_L N_L + \mu_R N_R)}H_t e^{-it(\mu_L N_L + \mu_R N_R)}\right)e^{-iKt}. \tag{3.115}$$

We now define $\tilde{H}_t(t) \equiv e^{it(\mu_L N_L + \mu_R N_R)} H_t e^{-it(\mu_L N_L + \mu_R N_R)}$ and write

$$\begin{aligned}\tilde{H}_t(t) &= e^{it(\mu_L N_L+\mu_R N_R)} H_t e^{-it(\mu_L N_L+\mu_R N_R)} \\ &\approx (1 + it\mu_L N_L + it\mu_R N_R)\, H_t\, (-1 - it\mu_L N_L - it\mu_R N_R) \\ &\approx H_t + it\mu_L[N_L, H_t] + it\mu_R[N_R, H_t] = H_t + it(\mu_L - \mu_R)[N_L, H_t] \\ &= H_t + iteV[N_L, H_t]. \quad (3.116)\end{aligned}$$

Using (3.113) and (3.112), we can write

$$\begin{aligned}\tilde{H}_t(t) &= u\Big[\left(\psi^\dagger_{R\uparrow}\psi_{L\uparrow} + \psi^\dagger_{R\downarrow}\psi_{L\downarrow}\right)(1 + iteV) \\ &\qquad + \left(\psi^\dagger_{L\uparrow}\psi_{R\uparrow} + \psi^\dagger_{L\downarrow}\psi_{R\downarrow}\right)(1 - iteV)\Big] \\ &\approx u\Big[e^{-iteV}\left(\psi^\dagger_{L\uparrow}\psi_{R\uparrow} + \psi^\dagger_{L\downarrow}\psi_{R\downarrow}\right) + e^{iteV}\left(\psi^\dagger_{R\uparrow}\psi_{L\uparrow} + \psi^\dagger_{R\downarrow}\psi_{L\downarrow}\right)\Big]. \quad (3.117)\end{aligned}$$

The other operator that appears in (3.110), $\dot{N}_L(t)$ can be evaluated in a similar way and turns out to be

$$\widetilde{\dot{N}_L}(t) = iu\left[e^{-iteV}\left(\psi^\dagger_{L\uparrow}\psi_{R\uparrow} + \psi^\dagger_{L\downarrow}\psi_{R\downarrow}\right) - e^{iteV}\left(\psi^\dagger_{R\uparrow}\psi_{L\uparrow} + \psi^\dagger_{R\downarrow}\psi_{L\downarrow}\right)\right]. \quad (3.118)$$

We see that both $\tilde{H}_t(t)$ and $\widetilde{\dot{N}_L}(t)$ consists mainly of products of field operators. If we define $A(t) = (\psi^\dagger_{L\uparrow}(t)\psi_{R\uparrow}(t) + \psi^\dagger_{L\downarrow}(t)\psi_{R\downarrow}(t))$, where

$$\psi_{\alpha\sigma}(t) \equiv e^{iKt}\psi_{\alpha\sigma}e^{-iKt}, \quad (3.119)$$

we can rewrite the commutator in (3.110) as

$$\begin{aligned}[\dot{N}_L(t), H_t(t')] &= iu^2\Big[e^{-ieVt}A(t) - e^{ieVt}A^\dagger(t), e^{-ieVt'}A(t') + e^{ieVt'}A^\dagger(t')\Big] \\ &= iu^2\Big(e^{-ieV(t+t')}[A(t), A(t')] + e^{-ieV(t-t')}[A(t), A^\dagger(t')] \\ &\quad - e^{ieV(t-t')}[A^\dagger(t), A(t')] - e^{ieV(t+t')}[A^\dagger(t), A^\dagger(t')]\Big) \\ &= iu^2\left(e^{-ieV(t-t')}[A(t), A^\dagger(t')] - e^{ieV(t-t')}[A^\dagger(t), A(t')]\right). \quad (3.120)\end{aligned}$$

The last equality is obtained by checking that $[A(t), A(t')]$ and $[A^\dagger(t), A^\dagger(t')]$ are zero. Now, we can rewrite eq. (3.110) as

$$I_c(t) = eu^2 \int \mathrm{d}t' \Theta(t-t') \left(e^{-ieVt} \left\langle [A(t), A^\dagger(t')] \right\rangle - e^{ieVt} \left\langle [A^\dagger(t), A(t')] \right\rangle \right), \tag{3.121}$$

where $\Theta(t)$ is the Heaviside step function. We choose $t' = 0$ and introduce the retarded Green's function $G_{\mathrm{ret}}(t) = -i\Theta(t) \left\langle [A(t), A^\dagger(0)] \right\rangle$. Fourier transforming this yields

$$\tilde{G}_{\mathrm{ret}}(-eV) = \int \mathrm{d}t e^{-ieVt} G_{\mathrm{ret}}(t) \tag{3.122}$$

and eq. (3.121) becomes

$$I_c(t) = -2eu^2 \mathrm{Im}\, [\tilde{G}_{\mathrm{ret}}(-eV)]. \tag{3.123}$$

After bosonisation, the correlation functions are readily calculated to be

$$\left\langle A(t) A^\dagger(0) \right\rangle = \frac{1}{\pi} \left(\frac{a_0}{iv(t+i\delta)} \right)^{K+1/K} \tag{3.124}$$

$$\left\langle A^\dagger(0) A(t) \right\rangle = \frac{1}{\pi} \left(\frac{a_0}{iv(t-i\delta)} \right)^{K+1/K}, \tag{3.125}$$

where a_0 is the lattice constant. (A misprint replaced the i-factors in the denominators with minus signs in eq. (15) of Paper I.)

Plugging these in the commutator and performing the Fourier transform yields the final expression for the current as a function of the voltage V:

$$I_c = 2eu^2 \frac{(a_0/v)^{K+1/K}}{\Gamma(K+1/K)} (eV)^{K+1/K-1}, \tag{3.126}$$

where Γ is Euler's gamma function. This is the zero-temperature result, and (as seen in fig. 3.3) since $(K + 1/K) \geq 2$, with equality for $K = 1$ (i.e. zero interaction), the Ohmic conductance ($I \propto V$) is enhanced by the interaction.

To figure out the temperature dependence of the conduction, a conformal transformation of eqns. (3.124) and (3.125) was performed, following [53]. This was done in Euclidian (imaginary) time $\tau = it$, taking

$$v\tau \to \frac{v\beta}{2\pi} \arctan\left(\frac{2\pi\tau}{\beta v} \right), \tag{3.127}$$

where $\beta = 1/T$. The resulting temperature dependent current is

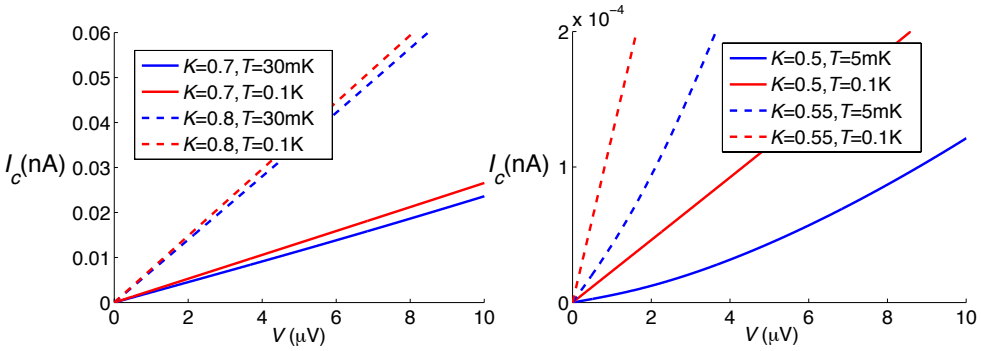

Figure 3.4: The charge tunnelling current as a function of the applied voltage for different values of K and T.

$$I_c = -2eu^2(a_0/v)^{2\Delta_K}(2\pi T)^{2\Delta_K-1} \times \mathrm{Im}\left[B(\Delta_K + ieV/2\pi T, \Delta_K - ieV/2\pi T)]\frac{\sin\left(\pi(\Delta_K - ieV/2\pi T)\right)}{\cos(\pi\Delta_K)}\right], \tag{3.128}$$

where B is the Euler beta function.

With $a_0 \approx 1$ nm, $v_F \approx 6 \times 10^5$ m/s [36, 54] and $u = 0.1v_F/a_0$, this result is plotted in fig. 3.4. Perhaps most importantly, the temperature dependence of the zero-bias differential conductance can be read off from eq. (3.128):

$$G \equiv \frac{\mathrm{d}I_c}{\mathrm{d}V}|_{V=0} \propto T^{K+1/K-2}. \tag{3.129}$$

Finally, the current/voltage characteristics resulting from putting on an ac voltage of the type $V(t) = V_0 + V_1 \sin \Omega t$ was also calculated, again following [53]. The constant V in the exponents Vt in eq. (3.121) is now changed to integrals, so that the exponents are now

$$e^{ieVt} \longrightarrow e^{-ie\int_{t'}^{t} \mathrm{d}t'' V(t'')}. \tag{3.130}$$

The result turns out be

$$I_{c,0} = 2eu^2(a/v)^{2\Delta_K} \sum_n a_n(eV_1/\Omega)(eV_0 + n\Omega)^{2\Delta_K-1}, \tag{3.131}$$

where

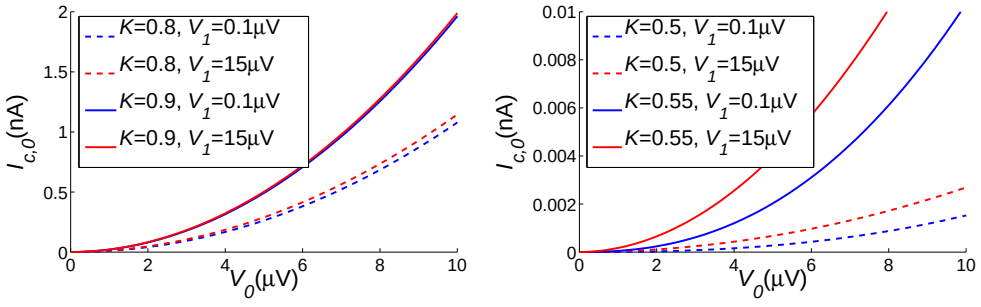

Figure 3.5: The dc component of the current as a function of the voltage V_0 for different values of K and different amplitudes V_1 of the ac voltage.

$$a_n(eV_1/\Omega) = \frac{1}{(2\pi)^2}\int_0^{2\pi}\int_0^{2\pi} dtdt' e^{in(t'-t)} e^{i\frac{eV_1}{\Omega}(\cos t' - \cos t)}. \tag{3.132}$$

This is plotted in fig. 3.5.

4

Rashba spin-orbit interaction on a quantum spin Hall edge

The connection between the spin and momentum of the electrons is perhaps the most important concept in topological insulators; indeed, the concept of a helical conductor is entirely based on this. In chapter 2, we learned that the spin-orbit coupling that splits the atomic p-orbital levels is crucial for the presence of the QSH effect in HgTe QW:s. A very large spin-orbit interaction of this type is necessary to achieve the inverted bandstructure of the material. The Rashba spin-orbit coupling is another type of spin-orbit interaction, which is present in the QW systems used in realising the QSH effect. This interaction is due to the inversion asymmetry of a QW, controllable by the gate voltage and sensitively dependent on the dopant atoms in the various materials used in the heterostructure, as well as the random bonds at the QW interface [55]. The strength of this interaction fluctuates quite rapidly as we follow the edge of the QW spatially, as sketched in fig. 4.1 [56].

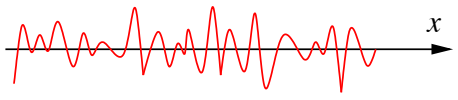

Figure 4.1: The spatially disordered Rashba coupling, $\alpha_{\mathrm{rand}}(x)$. The x variable goes along the edge of the QSH system and the length of the figure should correspond to roughly half a micron [57].

This chapter will deal with the important task of exploring the stability of the helical conductor against the disordered Rashba interaction. We will use a similar method as we did in the tunnelling approach and

model the Rashba coupling as a perturbation to the ideal QSH system, including interactions. More specifically, the Rashba coupling will be added as a perturbative Hamiltonian and we will investigate whether its coupling constant will flow to a strong coupling regime under the RG scheme or not.

Much of the exposition of this chapter follows ref. [27]. This work was published as Paper II and is a collaboration with Henrik Johannesson and George Japaridze [24].

4.1 The Rashba Hamiltonian

In heterostructures, such as quantum wells, the confinement potential, used to restrict the electrons to two-dimensional motion, and the differences of the band edges between the different materials of the heterostructure, break the inversion symmetry of the system. As a consequence, a spin-orbit type term, called the Rashba interaction [55], must be added to the Hamiltonian. In two dimensions, the Rashba term will be $H_R = \alpha(k_x\sigma_y - k_y\sigma_x)$, where α, the strength of the Rashba interaction, depends on several separate features of the QW: the applied gate electric field, the ion distribution in nearby doping layers [56], and the presence of random bonds at the two QW interfaces [58]. The gate dependence means that α is tunable and can be experimentally varied to investigate its effects. Along the one-dimensional edge, we write the Rashba Hamiltonian as [55]

$$H_R = \int \mathrm{d}x\ \alpha(x)\Psi^\dagger_\mu(x)\sigma^y_{\mu\nu}p_x\Psi_\nu(x), \tag{4.1}$$

where the μ and ν are Pauli matrix spin indices, in the sense that $\Psi_1 = \Psi_\uparrow$ and $\Psi_2 = \Psi_\downarrow$, while $\sigma^y_{12} = -i$, $\sigma^y_{21} = i$ and $\sigma^y_{11} = \sigma^y_{22} = 0$. Note that we allow the Rashba coupling in eq. (4.1) to vary with x, to encode its dependence on the spatially varying distribution of dopant ions and inhomogeneities. Let us also point out that we will make important use of the integral in the Rashba Hamiltonian H_R, so it will be more convenient for us to work with the full Hamiltonian here, rather than the Hamiltonian densities we used in the previous chapter. With $p_x = -i\partial_x$, we write

$$\begin{aligned} H_R &= \int \mathrm{d}x\ \alpha(x)\left(i\Psi^\dagger_\downarrow(-i\partial_x)\Psi_\uparrow - i\Psi^\dagger_\uparrow(-i\partial_x)\Psi_\downarrow\right) \\ &= \int \mathrm{d}x\ \alpha(x)\left(\Psi^\dagger_\downarrow\partial_x\Psi_\uparrow - \Psi^\dagger_\uparrow\partial_x\Psi_\downarrow\right). \end{aligned} \tag{4.2}$$

Since the QSH theory is helical, we know that $\Psi_\uparrow = \psi_{R\uparrow}e^{ik_F x}$ and $\Psi_\downarrow = \psi_{L\downarrow}e^{-ik_F x}$. For the purpose of describing the physics at a single edge (in contrast to the tunnelling problem in the previous chapter where two edges had to be included in the theory), the right/left indices are of course superfluous here, so we will omit them in what follows. We can thus rewrite the Rashba Hamiltonian as

$$\begin{aligned} H_R &= \int \mathrm{d}x\ \alpha(x)\left\{\psi_\downarrow^\dagger e^{ik_F x}\partial_x(\psi_\uparrow e^{ik_F x}) - \psi_\uparrow^\dagger e^{-ik_F x}\partial_x(\psi_\downarrow e^{-ik_F x})\right\} \\ &= \int \mathrm{d}x\ \alpha(x)\Big\{(ik_F\psi_\uparrow^\dagger\psi_\downarrow - \psi_\uparrow^\dagger\partial_x\psi_\downarrow)e^{-2ik_F x} \\ &\qquad + (ik_F\psi_\downarrow^\dagger\psi_\uparrow + \psi_\downarrow^\dagger\partial_x\psi_\uparrow)e^{2ik_F x}\Big\}. \end{aligned} \tag{4.3}$$

A Hamiltonian must be Hermitian, i.e. $H = H^\dagger$, or in other words $H = 1/2(H + H^\dagger)$. Using this, we obtain

$$\begin{aligned} H_R &= \frac{1}{2}(H_R + H_R^\dagger) = \frac{1}{2}\int \mathrm{d}x\ \alpha(x)\Big\{(ik_F\psi_\uparrow^\dagger\psi_\downarrow - \psi_\uparrow^\dagger\partial_x\psi_\downarrow)e^{-2ik_F x} \\ &\quad + (ik_F\psi_\downarrow^\dagger\psi_\uparrow + \psi_\downarrow^\dagger\partial_x\psi_\uparrow)e^{2ik_F x} + (-ik_F\psi_\downarrow^\dagger\psi_\uparrow - (\partial_x\psi_\downarrow^\dagger)\psi_\uparrow)e^{2ik_F x} \\ &\quad + (-ik_F\psi_\uparrow^\dagger\psi_\downarrow + (\partial_x\psi_\uparrow^\dagger)\psi_\downarrow)e^{-2ik_F x} \\ &= \frac{1}{2}\int \mathrm{d}x\ \alpha(x)\Big\{\left((\partial_x\psi_\uparrow^\dagger)\psi_\downarrow - \psi_\uparrow^\dagger\partial_x\psi_\downarrow\right)e^{-2ik_F x} \\ &\qquad - \left((\partial_x\psi_\downarrow^\dagger)\psi_\uparrow - \psi_\downarrow^\dagger\partial_x\psi_\uparrow\right)e^{2ik_F x}\Big\}. \end{aligned} \tag{4.4}$$

4.2 The theory on a lattice

Before continuing, we show that a similar expression can also be obtained by putting the theory on a lattice and do the calculations from there. From here on, we change the notation so that the operator ∂_x is only assumed to act on the field right next to it. The Rashba Hamiltonian on the lattice can be expressed as

$$\begin{aligned} H_R &= \frac{1}{2}\sum_n \alpha_n c_{n,\mu}\sigma^y_{\mu\nu}p_x c_{n,\nu} + \text{H.c.} \\ &= \frac{1}{2i\kappa}\sum_n \alpha_n\left(c^\dagger_{n,\mu}\sigma^y_{\mu\nu}c_{n+1,\nu} - c^\dagger_{n,\mu}\sigma^y_{\mu\nu}c_{n,\nu}\right) + \text{H.c.} \end{aligned} \tag{4.5}$$

With $c_{n,1} = \sqrt{a_0}\psi_\uparrow(na_0)e^{ik_F na_0}$ and $c_{n,2} = \sqrt{a_0}\psi_\downarrow(na_0)e^{-ik_F na_0}$, where a_0 is the lattice constant ($x = na_0$), this can be rewritten as

$$\begin{aligned}
H_R = \frac{1}{2i}\sum_n \alpha_n \Big\{ & -i\left(e^{-ik_F a_0(2n+1)}\psi_\uparrow^\dagger(na_0)\psi_\downarrow((n+1)a_0)\right) \\
& + i\left(e^{ik_F a_0(2n+1)}\psi_\downarrow^\dagger(na_0)\psi_\uparrow((n+1)a_0)\right) \\
& + i\left(e^{-ik_F a_0 2n}\psi_\uparrow^\dagger(na_0)\psi_\downarrow(na_0)\right) - i\left(e^{ik_F a_0 2n}\psi_\downarrow^\dagger(na_0)\psi_\uparrow(na_0)\right)\Big\} + \text{H.c.} \\
= \sum_n \frac{\alpha_n}{2}\Big\{ & e^{ik_F a_0(2n+1)}\left(\psi_\downarrow^\dagger(na_0)\psi_\uparrow((n+1)a_0) - \psi_\downarrow^\dagger((n+1)a_0)\psi_\uparrow(na_0)\right) \\
& - e^{-ik_F a_0(2n+1)}\left(\psi_\uparrow^\dagger(na_0)\psi_\downarrow((n+1)a_0) - \psi_\uparrow^\dagger((n+1)a_0)\psi_\downarrow(na_0)\right) \\
& + e^{ik_F a_0 2n}\left(\psi_\downarrow^\dagger(na_0)\psi_\uparrow(na_0) - \psi_\downarrow^\dagger(na_0)\psi_\uparrow(na_0)\right) \\
& + e^{-ik_F a_0 2n}\left(\psi_\uparrow^\dagger(na_0)\psi_\downarrow(na_0) - \psi_\uparrow^\dagger(na_0)\psi_\downarrow(na_0)\right)\Big\}. \quad (4.6)
\end{aligned}$$

It is now easy to see that the two last lines, coming from the $-c_{n,\mu}^\dagger \sigma_{\mu\nu}^y c_{n,\nu}$ term of eq. (4.5), are zero. The reason they are left in the equation is that they are useful for expressing the Rashba Hamiltonian in the form of eq. (4.4). In fact, since they are zero, it is perfectly all right to change the "$2n$" in the exponentials to "$2n+1$", yielding

$$\begin{aligned}
H_R = \frac{1}{2}\sum_n \alpha_n \Big\{ & e^{ik_F a_0(2n+1)}\Big(\psi_\downarrow^\dagger(na_0)\big[\psi_\uparrow((n+1)a_0) - \psi_\uparrow(na_0)\big] \\
& - \big[\psi_\downarrow^\dagger((n+1)a_0) - \psi_\downarrow^\dagger(na_0)\big]\psi_\uparrow(na_0)\Big) \\
& - e^{-ik_F a_0(2n+1)}\Big(\psi_\uparrow^\dagger(na_0)\big[\psi_\downarrow((n+1)a_0) - \psi_\downarrow(na_0)\big] \\
& - \big[\psi_\uparrow^\dagger((n+1)a_0) - \psi_\uparrow^\dagger(na_0)\big]\psi_\downarrow(na_0)\Big)\Big\} \\
= \frac{a_0}{2}\sum_n \alpha_n \Big\{ & e^{ik_F a_0(2n+1)}\left(\psi_\downarrow^\dagger(na_0)\partial_x\psi_\uparrow(na_0) - \partial_x\psi_\downarrow^\dagger(na_0)\psi_\uparrow(na_0)\right) \\
& - e^{-ik_F a_0(2n+1)}\left(\psi_\uparrow^\dagger(na_0)\partial_x\psi_\downarrow(na_0) - \partial_x\psi_\uparrow^\dagger(na_0)\psi_\downarrow(na_0)\right)\Big\}, \quad (4.7)
\end{aligned}$$

where we have also used that $\partial_x\psi(na_0) = \frac{1}{a_0}\left(\psi((n+1)a_0) - \psi(na_0)\right)$ (since $x = na_0$). We then take the limit $a_0 \to 0$ and $n \to \infty$ and write

$$H_R = \frac{1}{2}\int \mathrm{d}x\ \alpha(x)\Big\{e^{2ik_Fx}\Big(\psi_\downarrow^\dagger(x)\partial_x\psi_\uparrow(x) - \partial_x\psi_\downarrow^\dagger(x)\psi_\uparrow(x)\Big) - e^{-2ik_Fx}\Big(\psi_\uparrow^\dagger(x)\partial_x\psi_\downarrow(x) - \partial_x\psi_\uparrow^\dagger(x)\psi_\downarrow(x)\Big)\Big\}, \tag{4.8}$$

which is identical to eq. (4.4), just as we wanted.

4.3 Lagrangian formalism and bosonisation

We will now write the Rashba coupling as

$$\alpha(x) = \langle\alpha(x)\rangle + \alpha_{\mathrm{rand}}(x) = \langle\alpha(x)\rangle + \sum_n \hat{\alpha}(k_n)e^{ik_nx}, \tag{4.9}$$

where $\langle\alpha(x)\rangle$ is the mean value of the Rashba coupling, and $\hat{\alpha}(k_n)$ are the Fourier modes of the fluctuations around this mean. The mean value of the Rashba coupling will not affect the low-energy properties of the theory, since the corresponding rapidly fluctuating terms in the integrand of H_R will average out upon integration [59]. Using the fact that $\alpha(x)$ is real, so that $\hat{\alpha}(k) = \hat{\alpha}^*(-k)$, we may write

$$\begin{aligned}
H_R &= -\frac{1}{2}\int \mathrm{d}x \sum_n \Big\{(\psi_\uparrow^\dagger\partial_x\psi_\downarrow - \partial_x\psi_\uparrow^\dagger\psi_\downarrow)\hat{\alpha}(k_n)e^{-ix(2k_F-k_n} \\
&\qquad - (\psi_\downarrow^\dagger\partial_x\psi_\uparrow - \partial_x\psi_\downarrow^\dagger\psi_\uparrow)\hat{\alpha}(k)e^{ix(2k_F+k_n)}\Big\} \\
&= -\frac{1}{2}\int \mathrm{d}x \sum_n \Big\{(\psi_\uparrow^\dagger\partial_x\psi_\downarrow - \partial_x\psi_\uparrow^\dagger\psi_\downarrow)\hat{\alpha}(-k_n)e^{-ix(2k_F+k_n)} \\
&\qquad - (\psi_\downarrow^\dagger\partial_x\psi_\uparrow - \partial_x\psi_\downarrow^\dagger\psi_\uparrow)\hat{\alpha}(k_n)e^{ix(2k_F+k_n)}\Big\} \\
&= -\frac{1}{2}\int \mathrm{d}x \sum_n \Big\{(\psi_\uparrow^\dagger\partial_x\psi_\downarrow - \partial_x\psi_\uparrow^\dagger\psi_\downarrow)\hat{\alpha}^*(k_n - 2k_F)e^{-ik_nx} \\
&\qquad - (\psi_\downarrow^\dagger\partial_x\psi_\uparrow - \partial_x\psi_\downarrow^\dagger\psi_\uparrow)\hat{\alpha}(k_n - 2k_F)e^{ik_nx}\Big\},
\end{aligned} \tag{4.10}$$

where in the last equality, we used the transformation $k_n \to k_n + 2k_F$, together with

$$\sum_n e^{ik_n x}\hat{\alpha}(k_n+2k_F) = \sum_n e^{-ik_n x}\hat{\alpha}(-k_n+2k_F) = \sum_n e^{-ik_n x}\hat{\alpha}^*(k_n-2k_F). \tag{4.11}$$

Let us now bosonise our Rashba Hamiltonian. We will use the rules from eq. (3.14) and eq. (3.13), which imply

$$\partial_x\psi_L = \frac{\eta_{L\downarrow}}{\sqrt{2\pi}}\partial_x e^{2i\sqrt{\pi}\phi_{L\downarrow}} = \eta_{L\downarrow} i\sqrt{2}\partial_x\phi_{L\downarrow} e^{2i\sqrt{\pi}\phi_{L\downarrow}} \tag{4.12}$$

$$\partial_x\psi_R = \frac{\eta_{R\uparrow}}{\sqrt{2\pi}}\partial_x e^{-2i\sqrt{\pi}\phi_{R\uparrow}} = -\eta_{R\uparrow} i\sqrt{2}\partial_x\phi_{R\uparrow} e^{-2i\sqrt{\pi}\phi_{R\uparrow}}. \tag{4.13}$$

This gives

$$\begin{aligned} H_R = &-\frac{i}{2\kappa\sqrt{\pi}}\int \mathrm{d}x \sum_n \\ &\times \Big\{\eta_{R\uparrow}\eta_{L\downarrow}(\partial_x\phi_{L\downarrow} - \partial_x\phi_{R\uparrow}) e^{2i\sqrt{\pi}(\phi_{R\uparrow}+\phi_{L\downarrow})}\hat{\alpha}^*(2k_F-k_n)e^{-ik_n x} \\ &+ \eta_{L\downarrow}\eta_{R\uparrow}(\partial_x\phi_{R\uparrow} - \partial_x\phi_{L\downarrow}) e^{-2i\sqrt{\pi}(\phi_{R\uparrow}+\phi_{L\downarrow})}\hat{\alpha}(2k_F-k_n)e^{ik_n x}\Big\} \\ = &\frac{1}{2\kappa\sqrt{\pi}}\int \mathrm{d}x \sum_n \left(\partial_x\theta e^{-i\sqrt{4\pi}\phi}\hat{\alpha}(k_n-2k_F)e^{ik_n x} + \text{H.c.}\right), \end{aligned} \tag{4.14}$$

where $\phi = \phi_{R\uparrow} + \phi_{L\downarrow}$ and $\theta = \phi_{R\uparrow} - \phi_{L\downarrow}$. Here, we used the Clifford algebra of the Klein factors, which gives ($\eta_{R\uparrow}\eta_{L\downarrow} = -\eta_{L\downarrow}\eta_{R\uparrow}$) and also $\eta_{R\sigma} = i\eta_{L\sigma}$. We see that the Hamiltonian remains Hermitian, also after we have chosen a proper representation of the Klein factors.

As we saw in the previous chapter, the Hamiltonian describing the electrons on a single edge, including forward and dispersive scattering, becomes a free Hamiltonian in the bosonic language,

$$H_0 = \frac{v}{2}\int \mathrm{d}x \left((\partial_x\phi')^2 + (\partial_x\theta')^2\right), \tag{4.15}$$

where we have defined $\phi' = \frac{1}{\sqrt{K}}\phi$ and $\theta' = \sqrt{K}\theta$. It's easy to see that we can use $\partial_x\theta'$ as our conjugate momentum, $\Pi = \partial_x\theta'$ (so that $\partial_x\theta = \Pi/\sqrt{K}$). Thus, the corresponding Lagrangian is obtained by the Legendre transformation

$$L_0 = \int \mathrm{d}x \left(\Pi\,\partial_t\phi' - H_0\right) = \int \mathrm{d}x \left(i\Pi\,\partial_\tau\phi' - \frac{v}{2}(\partial_x\phi')^2 - \frac{v}{2}\Pi^2\right), \tag{4.16}$$

while the Rashba part of the Lagrangian, $L_R = -H_R$ can be read off from eq. (4.14). We define $\mu(x) \equiv \sum_n \hat{\alpha}(k_n - 2k_F)e^{ik_n x}$ and write:

$$\begin{aligned} L_R &= -\frac{1}{2\kappa\sqrt{\pi}} \int \mathrm{d}x \sum_n \left(\partial_x \theta e^{-i\sqrt{4\pi}\phi} \hat{\alpha}(k_n - 2k_F) e^{ik_n x} + \text{H.c.} \right) \\ &= -\frac{1}{2\kappa\sqrt{\pi}} \int \mathrm{d}x \frac{1}{\sqrt{K}} \Pi \left(\mu(x) e^{-i\sqrt{4\pi K}\phi'} + \text{H.c.} \right). \end{aligned} \tag{4.17}$$

The partition function can now be evaluated by a Gaussian integration over Π:

$$\begin{aligned} \mathcal{Z} &= \int \mathcal{D}\phi' \mathcal{D}\Pi \, e^{\int \mathrm{d}\tau L} = \int \mathcal{D}\phi' \mathcal{D}\Pi \exp\Bigg[-\frac{1}{2} \int \mathrm{d}x \mathrm{d}\tau \left(v\Pi^2 + v(\partial_x \phi')^2 \right) \\ &\quad + \int \mathrm{d}x \mathrm{d}\tau \left(i\Pi \partial_\tau \phi' - \frac{1}{2a\sqrt{K\pi}} \Pi \left[\mu(x) e^{-2i\sqrt{\pi K}\phi'} + \text{H.c.} \right] \right) \Bigg] \\ &\propto \int \mathcal{D}\phi' \exp\Bigg[\int \mathrm{d}x \mathrm{d}\tau \Bigg\{ -\frac{v}{2} (\partial_x \phi')^2 \\ &\quad + \frac{1}{2v} \left(i\partial_\tau \phi' - \frac{1}{2\kappa\sqrt{K\pi}} \left[\mu(x) e^{-2i\sqrt{\pi K}\phi'} + \text{H.c.} \right] \right)^2 \Bigg\} \Bigg] \\ &= \int \mathcal{D}\phi' \exp\Bigg[\int \mathrm{d}x \mathrm{d}\tau \Bigg\{ -\frac{v}{2} (\partial_x \phi')^2 \\ &\quad + \frac{1}{2v} \left(-(\partial_\tau \phi')^2 + \frac{1}{4\kappa^2 K\pi} \left(\mu(x) e^{-i\sqrt{4\pi K}\phi'} + \text{H.c.} \right)^2 \right) \Bigg\} \Bigg]. \end{aligned} \tag{4.18}$$

In the last equality, the mixed terms from the square are left out, because they are easily shown to be zero. In fact, they are proportional to

$$\int \mathrm{d}x \mathrm{d}\tau \partial_\tau \phi e^{A\phi} = \frac{1}{A} \int \mathrm{d}x \mathrm{d}\tau \partial_\tau \left(e^{A\phi} \right) = 0, \tag{4.19}$$

where the last identity follows from having an integral over a total derivative.

The last square in eq. (4.18) is:

$$\left(\mu(x) e^{-i\sqrt{4\pi K}\phi'} + \text{H.c.} \right)^2 = 2\mu^*(x)\mu(x) + \left(\mu^2(x) e^{-i\sqrt{16\pi K}\phi'} + \text{H.c.} \right). \tag{4.20}$$

The mixed terms, $2\mu^*(x)\mu(x)$, will only add a constant term to the action, since the ϕ's will vanish in $e^{-i\sqrt{4\pi K}\phi'}e^{i\sqrt{4\pi K}\phi'} = 1$. They will therefore not affect the RG analysis in any way, so we leave them out. If we introduce the notation

$$\xi(x) \equiv \frac{1}{4Kv\kappa}\mu^2(x) = \frac{1}{4Kv\kappa}\sum_{n,n'}\hat{\alpha}(k_n - 2k_F)\hat{\alpha}(k_{n'} - 2k_F)e^{i(k_n+k_{n'})x}, \tag{4.21}$$

the final result for the partition function can be written

$$\mathcal{Z} = \mathcal{D}\phi' e^{-\frac{1}{2K}\int \mathrm{d}x\mathrm{d}\tau\left(v(\partial_x\phi')^2 + \frac{1}{v}(\partial_\tau\phi')^2\right)} \times \exp\left[\int \mathrm{d}x\mathrm{d}\tau\frac{1}{2\kappa\pi}\left(\xi(x)e^{-i\sqrt{16\pi K}\phi'} + \text{H.c.}\right)\right]. \tag{4.22}$$

4.4 Replica renormalisation

The next step for us is to perform the renormalisation group analysis of the disordered Rashba interaction. Before diving into the calculations, we need to understand what it means to have a random term present in the Hamiltonian. A real system will only have one realisation of the random term, but if the system is large enough, it can be thought of as being built up by a large number of individual pieces, each with its own realisation of the random term. Instead of solving the problem for a specific realisation of the disorder and averaging afterwards, we thus need to average over the disorder already from the start. We will use the so-called *replica method*, described in ref. [60], to do this. In the following, we change our notation so that ϕ now denotes the rescaled field which was previously written $\phi' = \phi/\sqrt{K}$.

Generally, the average value of an observable O in a system with a random potential V is

$$\langle O\rangle_V = \frac{\int \mathcal{D}\phi O(\phi)e^{-S_V[\phi]}}{\int \mathcal{D}\phi e^{-S_V[\phi]}}, \tag{4.23}$$

where S_V is the action containing the disordered potential. Note that this is the average value with respect to a specific realisation of V. We want to average over all realisations of V. If the disorder comes with the probability distribution $p(V)$, this average is written

$$\overline{\langle O\rangle}_V = \frac{\int \mathcal{D}V p(V)\langle O\rangle_V}{\int \mathcal{D}V p(V)}. \tag{4.24}$$

In our case we have two terms like this, one the Hermitian conjugate of the other. Our action is, from eq. (4.22),

$$S_V = S_0[\phi] + \int \mathrm{d}x\mathrm{d}\tau \frac{1}{2\kappa\pi} \left(\xi(x) e^{-i\sqrt{16\pi K}\phi} + \text{H.c.} \right). \tag{4.25}$$

So, we have $V = \xi(x)$ and another term with $V^\dagger$. We need to assume a normal distribution of the disorder, in order to obtain solvable Gaussian path integrals. This is an essential part of the replica method and normally justified by the central limit theorem. In our case of the disordered Rashba coupling, it should be perfectly natural to assume this, since the fluctuations of the Rashba coupling are mainly due to the random distribution of dopant atoms and the bonds at the QW interface [61]. There is of course a possibility that the QW interface somehow has a structure that will cause a different distribution of the random bonds, but without investigating this in detail, there is no apparent reason to believe that the distribution of $\alpha(x)$ should be non-Gaussian. The Gaussian probability distribution is then

$$p(\xi(x)) = \exp\left(-\frac{1}{2D_\xi} \int \mathrm{d}x \xi^*(x)\xi(x) \right). \tag{4.26}$$

Here, D_ξ is defined by $\overline{\xi^*(x)\xi(x')} = D_\xi \delta(x - x')$. It will be important for us to be able to calculate a numerical value for D_ξ. For this, we use the expression $D_\xi = n_i V_0^2$, where n_i is the composite density of the dopant ions and interface bonds that produce the randomness in the Rashba coupling and V_0 can be thought of as the amplitude, or "strength", of one of these sources for the Rashba coupling [40]. In our case, we take the amplitude to be proportional to the standard deviation of ξ, $V_0 = \kappa\sqrt{\overline{\xi^*(x)\xi(x)}}$, and write

$$D_\xi = n_i \left(\kappa \sqrt{\overline{\xi^*(x)\xi(x)}} \right)^2 = n_i \kappa \, \overline{\xi^*(x)\xi(x)}. \tag{4.27}$$

Remembering $\xi(x)$ from eq. (4.21), the mean is

$$\begin{aligned}\overline{\xi^*(x)\xi(x)} &= \frac{1}{16K^2v^2\kappa^2}\overline{\sum_{n,n'}\hat{\alpha}^*(k_n-2k_F)\hat{\alpha}^*(k_{n'}-2k_F)e^{-i(k_n+k_{n'})x}\dots} \\ &\quad \overline{\dots\sum_{m,m'}\hat{\alpha}(k_m-2k_F)\hat{\alpha}(k_{m'}-2k_F)e^{i(k_m+k_{m'})x}} \\ &= \frac{1}{16K^2v^2\kappa^2}\overline{\sum_{n,n'}\hat{\alpha}(-k_n)\hat{\alpha}(-k_{n'})e^{-i(k_n+k_{n'})}e^{-i4k_Fx}\dots} \\ &\quad \overline{\dots\sum_{m,m'}\hat{\alpha}(k_m)\hat{\alpha}(k_{m'})e^{i(k_n+k_{n'})}e^{i4k_Fx}} \\ &= \frac{1}{16K^2v^2\kappa^2}\overline{\alpha^4_{\text{rand}}(x)}, \quad (4.28)\end{aligned}$$

which gives

$$D_\xi = \frac{n_i}{16K^2v^2\kappa}\overline{\alpha^4_{\text{rand}}(x)}. \quad (4.29)$$

Now, the difficulty of evaluating eq. (4.23) lies in the denominator and this is where the replica method comes in. The denominator can be written

$$\frac{1}{\int\mathcal{D}\phi e^{-S_V[\phi]}} = \left(\int\mathcal{D}\phi e^{-S_V[\phi]}\right)^{n-1}, \quad (4.30)$$

if $n=0$. If we instead let n be an arbitrary integer >2, this becomes

$$\left(\int\mathcal{D}\phi e^{-S_V[\phi]}\right)^{n-1} = \left(\int\mathcal{D}\phi_2 e^{-S_V[\phi_2]}\right)\dots\left(\int\mathcal{D}\phi_n e^{-S_V[\phi_n]}\right), \quad (4.31)$$

so that the average now can be rewritten without a denominator:

$$\begin{aligned}\langle O\rangle_V &= \left(\int\mathcal{D}\phi_1 O(\phi_1)e^{-S_V[\phi_1]}\right)\left(\int\mathcal{D}\phi_2 e^{-S_V[\phi_2]}\right)\dots\left(\int\mathcal{D}\phi_n e^{-S_V[\phi_n]}\right) \\ &= \int\mathcal{D}\phi_1\mathcal{D}\phi_2\dots\mathcal{D}\phi_n O(\phi_1)e^{-\sum_{a=1}^n S_V(\phi_a)}. \quad (4.32)\end{aligned}$$

This is equivalent to eq. (4.23) if we continue the integer n to a real continuous parameter and take $n\to 0$ in the end. Knowing when the limit $n\to 0$ is valid is a delicate matter, however. Without going into details about this, it can be shown that the limit is valid as long as the

disorder is treated perturbatively, and there are actually only a few cases wen the replica method is known to fail [62].

We can now use Gaussian integration over $V = \xi(x)$ to evaluate eq. (4.24) and at the same time insert eq. (4.32):

$$\begin{aligned}
\overline{\langle O\rangle}_V &= \frac{1}{\int \mathcal{D}V p(V)} \int \mathcal{D}V p(V) \int \mathcal{D}\phi_1 \mathcal{D}\phi_2 \dots \mathcal{D}\phi_n O(\phi_1) e^{-\sum_{a=1}^n S_V(\phi_a)} \\
&= \frac{1}{\int \mathcal{D}\xi e^{-\frac{1}{2D_\xi}\int \mathrm{d}x \xi^2(x)}} \int \mathcal{D}\xi e^{-\frac{1}{2D_\xi}\int \mathrm{d}x \xi^2(x)} \\
&\quad \times \int \mathcal{D}\phi_1 \dots \mathcal{D}\phi_n O(\phi_1) e^{-\sum_{a=1}^n S_V(\phi_a)} \\
&= \int \mathcal{D}\phi_1 \dots \mathcal{D}\phi_n O(\phi_1) \exp\Bigg[- \sum_{a=1}^n S_0(\phi_a) \\
&\quad + \frac{D_\xi}{2(2\kappa\pi)^2} \sum_{a=1,b=1}^n \int \mathrm{d}x \mathrm{d}\tau \mathrm{d}\tau' \left(e^{-i\sqrt{16\pi K}\phi_a(x,\tau)} e^{i\sqrt{16\pi K}\phi_b(x,\tau')} + \text{H.c.} \right) \Bigg] \\
&= \int \mathcal{D}\phi_1 \dots \mathcal{D}\phi_n O(\phi_1) \exp\Bigg[- \sum_{a=1}^n S_0(\phi_a) \\
&\quad + \frac{D_\xi}{2(2\kappa\pi)^2} \sum_{a=1,b=1}^n \int \mathrm{d}x \mathrm{d}\tau \mathrm{d}\tau' \left(e^{-i\sqrt{16\pi K}(\phi_a(x,\tau) - \phi_b(x,\tau'))} + \text{H.c.} \right) \Bigg] \\
&= \int \mathcal{D}\phi_1 \dots \mathcal{D}\phi_n O(\phi_1) \exp\Bigg[- \sum_{a=1}^n S_0(\phi_a) \\
&\quad + \frac{D_\xi}{2(2\kappa\pi)^2} \sum_{a=1,b=1}^n \int \mathrm{d}x \mathrm{d}\tau \mathrm{d}\tau' 2\cos\left(\sqrt{16\pi K}\left(\phi_a(x,\tau) - \phi_b(x,\tau')\right)\right) \Bigg].
\end{aligned} \tag{4.33}$$

We have thus found an effective action of the problem,

$$\begin{aligned}
S_{\text{eff}} &= \frac{1}{2} \sum_a \int \mathrm{d}x \mathrm{d}\tau \left[\frac{1}{v} (\partial_\tau \phi_a)^2 + v (\partial_x \phi_a)^2 \right] \\
&\quad - \frac{D_\xi}{(2\pi\kappa)^2} \sum_{a,b} \int \mathrm{d}x \mathrm{d}\tau \mathrm{d}\tau' \cos\left[\sqrt{16\pi K}\left(\phi_a(x,\tau) - \phi_b(x,\tau')\right)\right],
\end{aligned} \tag{4.34}$$

where $a, b = 1, \dots, n$ are the replica indices.

Since we ultimately need to take the limit $n \to 0$, it is not possible to see directly from eq. (4.34) that this action leads to a localisation of the

electrons. For a discussion about how the localisation arises from this, see refs. [63] and [64]. For now, we will have to settle with trusting that the electrons will localise when the disorder part of eq. (4.34) becomes dominant.

From here, we employ the RG scheme. In the previous chapter, we used the scaling parameter b, so that the flow of (x, τ) was $(x, \tau) \to (x, \tau)/b$ as b grew from 1 and up. In the case at hand, it will be more convenient to work with $l \equiv \ln b$, so we let (x, τ) flow with l as $(x, \tau) \to (x, \tau)e^{-l}$. The scaling equations become:

$$\frac{\partial \tilde{D}_\xi}{\partial l} = (3 - 8K)\tilde{D}_\xi \tag{4.35}$$

$$\frac{\partial v}{\partial l} = -2vK\tilde{D}_\xi \tag{4.36}$$

$$\frac{\partial K}{\partial l} = -2K^2\tilde{D}_\xi, \tag{4.37}$$

where we have defined the dimensionless parameter [60]

$$\tilde{D}_\xi \equiv \frac{2\kappa}{\pi v^2} D_\xi. \tag{4.38}$$

(On page 3 of Paper II, a factor κ is missing in the definition of D_ξ, the quantity which we call $\tilde{D}_\xi$ here, due to a misprint. Furthermore, the quantity D_ξ in the first equation of that page should be the same as the D_ξ we use here, without the tilde.) We notice that we now have a renormalisation of both the disorder strength $\tilde{D}_\xi$, the renormalised velocity v and the Luttinger parameter K. The equations show that when $K < 3/8$, D_ξ will become relevant, and the system will turn into what is known as an Anderson-type localised state [4]. The value $K = 3/8$ was identified in refs. [65, 66] as the critical value below which correlated backscattering (a second-order process, involving the scattering of four particles) in the presence of quenched disorder may cause localisation of the helical edge modes. We have thus found an exact microscopic realisation of this type of process.

This does not mean, however, that the edge electrons necessarily localise. Since the short-length cutoff (e.g. the penetration depth of the edge states or the lattice spacing) grows, or equivalently, the high-momentum cutoff gets lowered, we cannot take the RG arbitrarily far. When the short-length cutoff is of the order of the system size, we have to stop the renormalisation. Only if the disorder strength becomes large, i.e. $\tilde{D}_\xi$ becomes of the order unity before reaching the bounds of the system will the system localise. When we perform the renormalisation, letting l

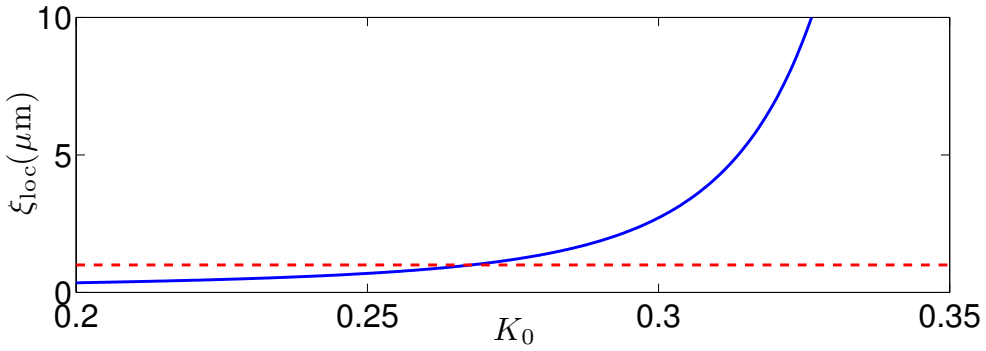

Figure 4.2: The edge localisation length ξ_{loc} for different values of the interaction parameter K_0. The dashed line marks the length of a micron-sized HgTe QW sample.

grow larger, the spatial coordinate x goes like xe^{-l}. We define l^* to be the value of l where the system localises, i.e. where $\tilde{D}_\xi \sim 1$, remembering the possibility that we cannot take l this far without making the short-length cutoff larger than the system itself. When we have renormalised this far, the electrons cannot move, and so the *localisation length*, $\xi_{\mathrm{loc}}(l)$, defined as the maximum spatial extension a wavefunction can have without decaying, is of the order of the lattice spacing. Since all lengths, including the localisation length, scale with the RG flow as $x \to xe^{-l}$, we can use this information to deduce the true, unrenormalised, localisation length ξ_{loc} of the system.

The last sentence of the previous paragraph can be formalised as

$$\xi_{\mathrm{loc}} e^{-l^*} = \kappa, \tag{4.39}$$

and hence the true localisation length is $\xi_{\mathrm{loc}} = \kappa e^{l^*}$ [60]. It is crucial for us to know this, because if the localisation length exceeds the length of our sample, it is impossible for us to renormalise all the way to localisation, and the effect will never appear. So, to find out whether Anderson localisation is present in the sample or not, we must inquire about the relation between ξ_{loc} and the length of the sample.

In order to calculate the value of the localisation length, we need to know a few things about our system. First, we define K_0 to be the naked, unrenormalised value of K, i.e. the value that we start with in the renormalisation of K. We calculate the localisation length as a function of K_0. An estimation of K_0 relevant for the HgTe QW:s was made already in section 3.2.2 and v can be estimated in a similar way with the aid of eq. (3.52). However, in order to find starting values for $\tilde{D}_\xi$ on which to do RG, we need numbers also for n_i and $\hat{\alpha}^4(k)$. We take $n_i \approx 10^9/\mathrm{m}$ [36]

and use that for a QW with zinc-blende lattice structure [56],

$$\sqrt{\overline{\alpha^2_{\text{rand}}(x)}} \approx \overline{\alpha(x)}. \tag{4.40}$$

We can then write $\overline{\alpha^4_{\text{rand}}(x)}$ from eq. (4.29) as

$$\overline{\alpha^4_{\text{rand}}(x)} = 3\left(\overline{\alpha^2_{\text{rand}}(x)}\right)^2 = 3\left(\sqrt{\overline{\alpha^2_{\text{rand}}(x)}}\right)^4 \approx 3\left(\overline{\alpha(x)}\right)^4, \tag{4.41}$$

where the first equality is a general statement about Gaussian distributed stochastic variables f, namely $\langle f^4\rangle = 3\langle f^2\rangle^2$. When estimating the average $\langle\alpha(x)\rangle$, we will take as its value the size of the effective bulk Rashba coupling as the edge bands meet the Γ_6 band in the bulk. We have to take into account that the bulk value of the Rashba coupling is k-dependent, because of the specific curvature of the Γ_6 band. This value is estimated to $\hbar\langle\alpha(x)\rangle \approx 5\times 10^{-11}$ eVm [67].

With numbers on our parameters, we are now ready to calculate the localisation length. The result is given in fig. 4.2, where a plot of the localisation length vs. K_0, the naked value of K, is shown. The calculation was performed by solving the RG equations numerically for different values of K_0 and let the value of D_ξ flow until $D_\xi(l^*) \sim 1$. The obtained value of l^* was then used to calculate ξ_{loc} as a function of K_0. We see that the edge of a micron-sized QSH sample localises for $K_0 \lesssim 0.25$. In order to probe this experimentally, we thus need values of K_0 somewhat smaller than what was estimated for the HgTe samples used in the experiments that have been performed so far [11]. However, the screening in a QW can be controlled by varying the thickness of the insulating layer between the well and the metallic gate and this will affect the value of K_0 according to eq. (3.106). As mentioned in chapter 3, values of K_0 down to 0.2 should be possible to achieve [68].

When $\xi_{\text{loc}} < L$, the size of the system, the edge electrons are localised as long as the temperature doesn't exceed $\approx \hbar/(k_B\xi_{\text{loc}})$, with an exponential decrease of the conductivity for lower temperatures [60]. The actual experiments are typically carried out at temperatures between 30 mK and 2 K [11], so at these temperatures the edge should remain an insulator.

Before concluding this section, let us mention that the problem of a spatially dependent Rashba potential in a helical conductor was recently revisited by Crépin et al. in ref. [69]. In this reference the Rashba interaction is localized at a single point ("Rashba impurity"). It was shown in agreement with our result that the generation of an effective two-particle backscattering term from the Rashba interaction is indeed

only present if electron-electron interactions are present. In addition to our result, they found a cross-over for the temperature dependence of the conductance at $K = 1/2$, with different temperature dependences in the $K < 1/2$ and $K > 1/2$ regions respectively. Surprisingly, their results showed that the effect of the Rashba coupling, the generation of the two-particle backscattering, vanishes not only at $K = 1$, but also at $K = 1/2$.

4.5 Periodic modulation of the Rashba coupling

Let us now consider the possibility to tune the Rashba coupling by hand, to induce a periodically modulated coupling. The problem was first raised by Wang in the context of an ordinary one-dimensional conductor ("nanowire"), suggesting that a sequence of equally spaced nanosized gates applied on top of the wire can be used to produce a Rashba coupling periodic in space [70] . Since the gates can be controlled at will, this would result in a switch for turning on and off the electrical current in the wire. Wang's proposal was later expanded to include effects from electron-electron interactions, as well as from the geometry of the device, but still for an ordinary non-helical conductor [59, 71]. In the following we explore how the scenario plays out for a helical conductor.

Instead of the disordered $\alpha(x)$ examined so far, we thus consider the case where we force the Rashba coupling to take the periodic form

$$\alpha(x) = A\cos(Qx). \tag{4.42}$$

We assume that the density of the electrons, and thereby k_F, can be tuned via a backgate, so that for a given periodic distance $2\pi/Q$ of the equally spaced nanogates we have $Q = 2k_F$, corresponding to a wavelength of about $5 - 10$ nm in a HgTe QW [67]. Inserting $\alpha(x) = A\cos(2k_F x)$ into eq. (4.22), the action becomes

$$S[\phi] = \frac{1}{2}\int \mathrm{d}x\mathrm{d}\tau \left[\frac{1}{v}\left(\partial_\tau\phi\right)^2 + v\left(\partial_x\phi\right)^2 - \frac{A^2}{2\pi Q\kappa^2 v}\cos\left(\sqrt{16\pi K}\phi\right)\right]. \tag{4.43}$$

This is the action of the well-studied "sine-Gordon" model that we came across already in eq. (3.25), with the RG solution to be found in a number of textbooks, including Giamarchi's [40]. The reader is recommended to study this, but here we will just state the solution. The scaling equations are the famous Kosterlitz-Thouless equations,

$$\frac{\partial z_\parallel}{\partial l} = -z_\perp \tag{4.44}$$

$$\frac{\partial z_\perp}{\partial l} = -z_\parallel z_\perp. \tag{4.45}$$

In our case

$$z_\parallel = 4K - 2 \tag{4.46}$$

$$z_\perp = \frac{A^2}{\pi Q \kappa^2 v}\sqrt{CK^3}, \tag{4.47}$$

where

$$C = \frac{128\pi^2}{v^2}\int \mathrm{d}r r^3 J_0(\Lambda r) e^{-8K\int_0^\Lambda \frac{\mathrm{d}q}{q}(1-J_0(qr))}, \tag{4.48}$$

where J_0 is the 0:th order Bessel function of the first kind and Λ is the high-energy cutoff, as before.

The solution to the Kosterlitz-Thouless equations shows that the sine-Gordon term, in our case proportional to the Rashba coupling, becomes relevant for $z_\parallel < 0$, i.e. for $K_0 < 1/2$. For $K_0 < 1/2$, it is thus possible for a mass gap Δ_M to open and the system to become what is known as a Mott insulator [72]. Put simply, the physics behind Mott insulation is that for large repulsive electron-electron interaction, compared to the kinetic energy, the system will try to minimise the repulsion and localise the electrons on the lattice sites, whereas in an Anderson insulator, the electrons will localise due to scattering back and forth against random impurities. For the insulating state to be robust, the mass gap Δ_M has to be larger than the available thermal energy. In order to calculate Δ_M, we need to know where this "mass" comes from, given the effective action in eq. (4.43).

The idea is simply that the cos-term in the action,

$$-\frac{A^2}{2\pi Q\kappa^2 v}\cos\left(\sqrt{16\pi K}\phi\right) \equiv B\cos\left(\sqrt{16\pi K}\phi\right), \tag{4.49}$$

will start to govern the behaviour of the system as soon as it becomes as large as, or larger than the kinetic term. For the system to minimise its energy, it will then configure itself so that the energy contribution from this term becomes as small as possible. When B renormalises to $-\infty$ the minimum is obtained for $\phi = 0$ and the cos-term can be expanded around $\phi = 0$ to give

$$B\cos\left(\sqrt{16\pi K}\phi\right) \approx B\frac{16\pi K\phi^2}{2}. \tag{4.50}$$

In a field theory, a mass term generically has the form $\Delta_M^2\phi^2$, so the mass gap we are looking for is in our case equal to

$$\Delta_M = \sqrt{|B|8\pi K} = \frac{A}{\kappa}\sqrt{\frac{4K}{Qv}}. \tag{4.51}$$

We now have to do a calculation analogous to the one for the localisation length. Suppose we renormalise up to the point where A is of order unity, where the cos-term starts to dominate the Hamiltonian. Since this mass gap has the dimension of an energy, when we set $\hbar = 1$ it renormalises as the inverse of time, i.e.

$$\Delta_M(l) = e^l\Delta_M(l=0). \tag{4.52}$$

As in the disordered case, we define l^* to be the value of l^* for which $A(l^*) \simeq 1$. The true mass gap of the system, $\Delta_M(l=0)$, or simply Δ_M, is then obtained by just reversing the process, so that

$$\Delta_M(l=0) = e^{-l^*}\Delta_M(l^*) \simeq e^{-l^*}\frac{1}{\kappa}\sqrt{\frac{4K}{Qv}}. \tag{4.53}$$

Now, for a certain starting value of the Rashba amplitude A and a certain starting value K_0 of the Luttinger parameter, we will obtain a certain value of l^*. This l^* defines the value of the *renormalisation length* κe^{l^*}, i.e. the length we start from in order to renormalise all the way down to the lattice spacing κ. This renormalisation length must of course be at most of the same size as the size of the sample we are working with.

To carry out the analysis, we start by choosing certain values of A and the sample length L. These are chosen to be close to the ones used in the Rashba coupling strength estimates for the disordered case. As just stated, choosing a value for K_0 will now also give a value for l^*. The l^* thus obtained is then used to calculate Δ_M according to (4.53), and thus, a function $\Delta_M(K_0)$ is extracted.

Fig. 4.3 shows a plot of Δ_M as a function of K_0. Three different values of A have been chosen. The l^* was calculated as a function of K_0 and the corresponding Δ_M and $\kappa\exp(l^*)$ were then obtained. Following the plot lines, l^* increases with K_0, and the points where the renormalisation length κe^{l^*} equals the sample length in the cases of $L = 1$ μm and $L = 20$ μm are indicated with a circle and a square, respectively. The lines are terminated when the renormalisation lengths reach 20 μm,

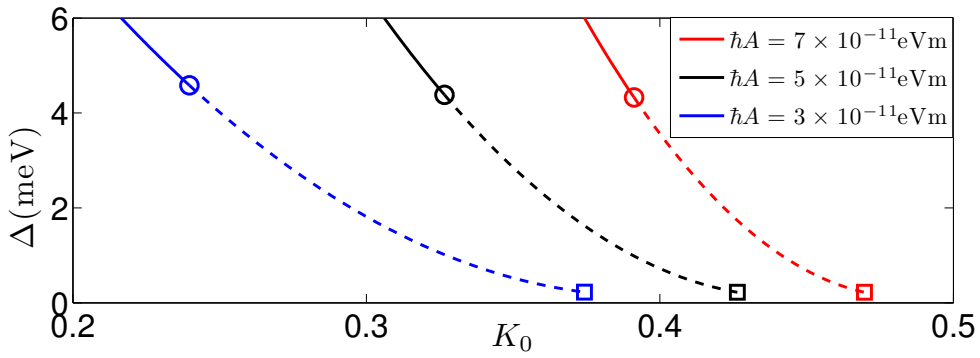

Figure 4.3: The gap Δ_M for different Rashba amplitudes $\hbar A$ and values of K_0. The circles and squares mark the smallest gaps for HgTe QW samples of length 1 μm and 20 μm, respectively.

since, as mentioned in section 2.4, at sample sizes larger than 20 μm, the experimental results by König and coworkers no longer unambigously support the existence of a quantum spin Hall state [11].

We see that for $\kappa e^{l^*} = 1$ μm, the gap size is $\Delta_M \approx 4.5$ meV for all three amplitudes, corresponding to a temperature of around 50 K. The thermally activated conductance, i.e. the conductance of electrons excited above the mass gap by the thermal energy, is given by $G = (2e^2/h)e^{-\Delta_M/k_BT}$. Thus, in order to keep the electrons in a micron-sized sample well localised, the sample must be cooled down to temperatures below 10-20 K. As previously stated, the temperatures at which these experiments are typically carried out vary between 30 mK and 1 K.

The plot in fig. 4.3 also shows the values of the electron-electron interaction (encoded by K_0) necessary for obtaining the localisation. As expected, these values vary with the size of the Rashba coupling.

5

Disorder in quasi-helical conductors

In the earlier chapters, we have analysed effects of interactions and disorder in helical liquids. The systems discussed have exclusively been quantum spin Hall edges. Helical conductors appear, however, also in quantum wires or nanotubes with strong spin-orbit interaction. A large magnetic field is needed, so time-reversal symmetry is broken in these conductors. They are thus very different from topological insulator edges and there is no topological protection of the conducting states. The very magnetic field needed to lift the right- and left-moving states of unwanted spin orientation to higher energies will also cause a certain spin overlap between the counterpropagating electrons. Since these conductors are not completely helical, we will instead call them *quasi-helical*. The most prominent examples are one-dimensional semiconductor wires in the presence of strong spin-orbit coupling and an added magnetic field [21]. We will mostly consider InAs nanowires, but GaAs and InSb wires are also conceivable [73–75]. Another example is carbon nanotubes with strong spin-orbit coupling combined with external electric fields [76].

This chapter will deal with Anderson localisation in quasi-helical conductors, due to backscattering off disordered impurities. Tuning the magnetic field will reveal metal-insulator transitions at two different field strengths. This work was submitted for publication as Paper III as a collaboration with Bernd Braunecker and George Japaridze [25].

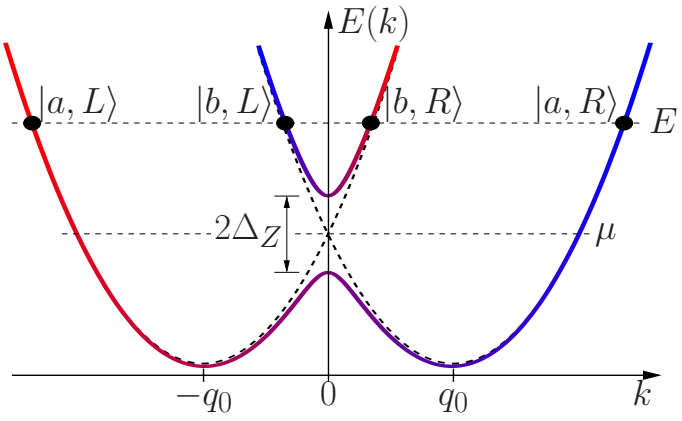

Figure 5.1: The dispersion relation of the quasihelical conductor.

5.1 Model

Consider a one-dimensional electron system with a quadratic dispersion relation. Adding a strong, uniform, Rashba spin-orbit interaction of strength α will shift the dispersion relation for the two different spins $\uparrow$ and $\downarrow$ by the wave vectors $+q_0$ and $-q_0$ respectively, where $q_0 = m\alpha/\hbar$ and m the effective mass of the electrons. If we also add a magnetic field B_x perpendicular to the spin axis, a Zeeman gap $\Delta_Z = B_x g\mu_B/2$ opens up at $k = 0$, g being the Landé factor and μ_B the Bohr magneton. The mechanism behind this is that B_x will align the spins in its direction, perpendicular to the spin z axis, and lift the degeneracy at the crossing between the $\uparrow$ and $\downarrow$ bands. (As shown below, for larger k, the effect of the Rashba interaction will dominate over the effect of the magnetic field.) This divides the system into a lower and upper band, which are labelled a and b respectively, and the resulting dispersion is shown in figure 5.1. We choose to tune the chemical potential μ to lie in the middle of the gap Δ for reasons to be discussed below.

The left- and right-movers of the low-lying band (a) have spins that are almost opposite. At large $|k|$, the spins should not be rotated by much because of the strong SOI, and if the gap Δ_Z is large enough, the higher-energy states of the b band become unavailable. Considering figure 5.1, we see that with μ in the middle of the gap, the available states around the Fermi level will then be left-movers with the spin aligned in a direction close to the positive spin z axis ($\uparrow$) (red line) and right-movers with spin close to $\downarrow$ (blue line). Thus, in the low-energy limit, the system becomes similar to a helical conductor, with the difference that the spin overlap between right- and left-movers is now non-zero.

For the b-band states to be unavailable, the gap must be larger than the available thermal energy k_BT. The larger the magnetic field, however, the larger the spin overlap between the left- and right-movers will be. Our first task will therefore be to investigate "how helical" our quasi-helical conductor can be, by calculating the sizes of the gap Δ and the spin overlaps $\langle a, L(-2q_0)|a, R(2q_0)\rangle$ at $\pm k_F = \pm 2q_0$, in terms of the applied magnetic field B_x and the Rashba strength α.

We write the Hamiltonian for the free system with an added uniform Rashba spin orbit interaction (SOI) as

$$H_{0+R} = \int \mathrm{d}x \psi^\dagger(x) \left(\frac{k^2}{2m} - \mu + \alpha \sigma_z k \right) \psi(x), \tag{5.1}$$

where now $\psi = (\psi_\uparrow, \psi_\downarrow)$ is a spinor of electron annihilation operators, $k = p/\hbar = -i\partial_x$ is the wavevector, and m is the effective mass. The three terms in this Hamiltonian are then the kinetic energy, the chemical potential and the Rashba energy. On this form, it is clear that the role of the Rashba coupling is the spin-dependent shift of the dispersion. Adding the uniform magnetic field B_x perpendicular to the spin axis gives the following term to the Hamiltonian

$$H_B = \Delta_Z \int \mathrm{d}x \psi^\dagger(x) \sigma_x \psi(x). \tag{5.2}$$

Defining $\xi_k \equiv k^2/(2m) - \mu$, the total Hamiltonian is

$$H = H_{0+R} + H_B = \int \mathrm{d}x \psi^\dagger(x) \left(\xi_k \mathbb{1} + \Delta_Z \sigma_x + \alpha k \sigma_z \right) \psi(x) \tag{5.3}$$

The matrix form of $\xi_k \mathbb{1} + \Delta_Z \sigma_x + \alpha k \sigma_z$ is

$$\begin{pmatrix} \xi_k + \alpha k & \Delta_Z \\ \Delta_Z & \xi_k - \alpha_k \end{pmatrix} \tag{5.4}$$

with the two eigenvalues

$$E_\pm(k) = \xi_k \pm \sqrt{\Delta_Z^2 + \alpha^2 k^2}. \tag{5.5}$$

We now introduce two spinor eigenvectors $\phi_\pm = (u_\pm v_\pm)^T$ for the two energy eigenvalues $E_\pm$, so that the upper band will have the electron states $|b, k\rangle = u_+ |\uparrow\rangle + v_+ |\downarrow\rangle$ and the lower band $|a, k\rangle = u_- |\uparrow\rangle + v_- |\downarrow\rangle$, allowing us to calculate the spin overlaps between states of given bands and wavevectors. We obtain the two eigenvalue equations

$$(\xi_k + \alpha_k)u_\pm + \Delta_Z v_\pm = E_\pm u_\pm \tag{5.6}$$
$$(\xi_k - \alpha_k)u_\pm + \Delta_Z v_\pm = E_\pm u_\pm. \tag{5.7}$$

This, together with the condition $|\phi_\pm| = 1 \Leftrightarrow u_\pm^2 + v_\pm^2 = 1$, gives the four eigenfunctions

$$u_\pm(k) = \sqrt{\frac{1}{2} \pm \frac{\alpha k}{2\sqrt{\Delta_Z^2 + \alpha^2 k^2}}} \tag{5.8}$$
$$v_\pm(k) = \sqrt{\frac{1}{2} \mp \frac{\alpha k}{2\sqrt{\Delta_Z^2 + \alpha^2 k^2}}}. \tag{5.9}$$

We can thus define the wavefunction $u(k) \equiv u_+(k) = v_+(-k) = u_-(-k) = -v_-(k)$ and write

$$|a, k\rangle = u(k)\,|\uparrow\rangle + u(-k)\,|\downarrow\rangle \tag{5.10}$$
$$|b, k\rangle = u(-k)\,|\uparrow\rangle - u(k)\,|\downarrow\rangle\,. \tag{5.11}$$

Already at this stage we can investigate the two limits of large B_x field and large α strength. For $B_x \gg \alpha$, we see that $u(k) \approx u(-k) \approx 1/\sqrt{2}$, so that $|a, k\rangle \approx 1/\sqrt{2}\,(|\uparrow\rangle + |\downarrow\rangle)$ and $|b, k\rangle \approx 1/\sqrt{2}\,(|\uparrow\rangle - |\downarrow\rangle)$. This is expected, since a large magnetic field will make the spins aligned in its direction, in this case perpendicular to our chosen $\uparrow$ / $\downarrow$ axis. In the opposite limit, $B_x \ll \alpha$, $u(k) \approx 1$ and $u(-k) \approx 0$, so that $|a, R\rangle \approx |\uparrow\rangle$ and $|a, L\rangle \approx |\downarrow\rangle$, R and L denoting right- and left-moving states (positive and negative k), respectively.

To investigate the "helicalness" of the quantum wire, we now calculate the spin overlap between the left- and right-movers at the Fermi level in the a band,

$$\begin{aligned}\langle a, -2q_0 | a, +2q_0\rangle &= \left[\langle\uparrow|\, u^*(-2q_0) + \langle\downarrow|\, u^*(+2q_0)\right]\left[u(2q_0)\,|\uparrow\rangle + u(-2q_0)\,|\downarrow\rangle\right] \\ &= 2u(-2q_0)u(2q_0) = 1 - \frac{4\alpha^2 q_0^2}{\Delta_Z^2 + 4\alpha^2 q_0^2}.\end{aligned} \tag{5.12}$$

The limits of strong and weak B_x behave as expected, $B_x \gg \alpha$ aligns the spins in the same direction (x), with a resulting unity overlap, while

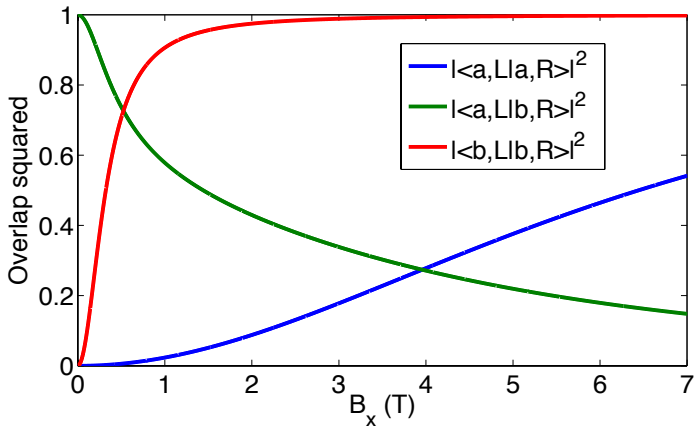

Figure 5.2: The overlap squared as a function of the magnetic field.

$B_x \ll \alpha$ keeps the spins of the left- and right-movers of the a band perpendicular, making the spin overlap zero.

To calculate the overlap for arbitrary field strengths, we need to put numbers on our parameters. We choose InAs nanowires as our test system, with $\alpha = 4 \times 10^{-11}$ eVm, g=9, $m = 0.040 m_e$ and $v_F = 2 \times 10^5$ m/s [75,77]. The overlap squared as a function of B_x is plotted in Fig. 5.2. The values chosen for the wave numbers are $k = \pm 2q_0$ for the states of the a band and $k = \pm 0.1q_0$ for the b band. At a magnetic field of about 1T, the overlap squared is about $|\langle a, L|a, R\rangle|^2 = 0.02$. This field produces the gap $\Delta = 0.26$meV, corresponding to a temperature of 3K.

5.2 Disorder

The concept of Anderson localisation caused by disorder was discussed in chapter 4. There, the spin-nonpreserving Rashba interaction was shown to cause Anderson-type localisation if disordered. Here, the Rashba interaction is assumed to be uniform, and the mechanism behind the localisation will instead be ordinary spin-preserving backscattering against randomly distributed impurities, allowed because of the finite spin overlap between left- and right-moving states. We will use a similar method as in chapter 4, starting with a bosonisation of the theory, and then finding the localisation length from the RG equations. As usual, we linearise the spectrum and integrate over the degrees of freedom between the high energy cut-off Λ and some lower lying cut-off Λ/b. Increasing b, the lower boundary of what gets integrated out will eventually approach the bottom of the upper band. In the bandgap, the number of available

states is halved, which means that we need to switch from a theory with four Fermi points to one with only two. We will thus calculate one set of RG equations for the full non-helical theory above the gap, and one for the quasi-helical theory in the gap. Upon reaching the gap, we will continue the RG flow with a new set of coupling constants applicable for the quasi-helical theory, calculated from the renormalised values of the coupling constants of the theory above the gap.

5.2.1 Theory above the gap

We want to write down and bosonise an effective Hamiltonian for each of the two cases above the gap and in the gap. The theory above the gap will be represented by a full Luttinger liquid Hamiltonian with spin, plus all the scattering potentials that we are interested in. Instead of using the a/b basis, which is the physically more transparent choice, the equations turn out much simpler if we continue using the $\uparrow$ / $\downarrow$ basis, defined by the $\uparrow$ and $\downarrow$ spins before the B_x field is added. Thus, compared to the states indicated in Fig. 5.1, we instead use $|a, L\rangle \rightarrow |\downarrow, L\rangle$, $|a, R\rangle \rightarrow |\uparrow, R\rangle$, $|b, L\rangle \rightarrow |\uparrow, L\rangle$ and $|b, R\rangle \rightarrow |\downarrow, R\rangle$. It is indeed important to keep in mind that "up" ($\uparrow$) and "down" ($\downarrow$) here refers not to the actual spins of the electrons under the influence of the B_x field, but the directions of the spins before the field was added. It would be very confusing to use the word "spin" for both the unrotated spin of our chosen basis and the actual spin, rotated by B_x. For this reason, we will use the term "prespin" for our $\uparrow$ / $\downarrow$ basis.

The free bosonic Hamiltonian, including electron-electron interactions, but before α and B_x are added, is given by

$$H_0 = \sum_{\nu=\rho,\sigma} \frac{v_\nu}{2} \int \mathrm{d}x \left[\frac{1}{K_\nu} \left(\partial_x \phi_\nu(x)\right)^2 + K_\nu \left(\partial_x \theta_\nu(x)\right)^2 \right], \tag{5.13}$$

where ϕ_ν and θ_ν are defined in eqs. (3.20)-(3.23). We assume to be away from half-filling and disregard the Umklapp scattering. Now, we need to take into account both the "prespin-preserving" and the "prespin-flipping" interactions. In contrast, we will not include actual spin-flipping backscattering against the disordered impurities in our analysis, since those processes will be much less relevant than any spin-preserving one. We need, however, to consider scattering between states that have opposite prespins in our $\uparrow$ / $\downarrow$ basis, since there will be a finite spin overlap between those states because of the B_x field. As we have seen, the role of the Rashba interaction and the perpendicular magnetic field is to shift the dispersion so that it looks like Fig. 5.1. We will assume their effect

on the interactions to be limited to adding spin-dependence to the different scattering processes. As explained in chapter 3, the g-ology coupling constants from eqs. (3.8)-(3.11) are g_1 for backward scattering, g_2 for dispersive scattering, g_3 for Umklapp and g_4 for forward scattering. The indices $_\parallel$ and $_\perp$ are used to denote whether the incoming electrons have equal or opposite prespins. For the electron-electron interactions that determine the values of K and u, i.e. the $g_{1\parallel}$, g_2 and g_4 scatterings (see Fig. 3.1), it will not matter between which bands, or within which band, the scattering takes place. Thus, the Rashba interaction will not enter into H_0. For the $g_{1\perp}$ interaction, where two electrons of opposite prespin backscatters while keeping their prespin, we see that backscattering between states of the same prespin now means scattering between left- and right-movers of two different bands only. Therefore, we need to take into account the spin overlap between the a and b states when we put $g_{1\perp}$ into our equations.

We now turn to the scattering processes between states of different prespins. Again, we will make sure that the ones we consider will be spin-preserving in terms of the actual spins. Disregarding processes that don not conserve the wavenumber k, the prespin-flip process terms in the Hamiltonian are

$$H_{1\perp f} = \int \mathrm{d}x v_F g_{1\perp f} \sum_{\sigma=\uparrow,\downarrow} \psi^\dagger_{R\sigma}\psi_{L,-\sigma}\psi^\dagger_{L,-\sigma}\psi_{R\sigma} \tag{5.14}$$

$$H_{2\perp f} = \int \mathrm{d}x v_F g_{2\perp f} \psi^\dagger_{R\uparrow}\psi_{R\downarrow}\psi^\dagger_{L\downarrow}\psi_{L\uparrow} + H.c. \tag{5.15}$$

$$H_{4\perp f} = \int \mathrm{d}x v_F g_{4\perp f} \left(\psi^\dagger_{R\uparrow}\psi_{R\downarrow}\psi^\dagger_{R\downarrow}\psi_{R\uparrow} + \psi^\dagger_{L\uparrow}\psi_{L\downarrow}\psi^\dagger_{L\downarrow}\psi_{L\uparrow}\right), \tag{5.16}$$

i.e. intraband backward scattering, interband dispersive scattering and interband forward scattering, respectively. All of these processes are equivalent to prespin-preserving processes: The $g_{1\perp}$ processes can be absorbed into the expression for $g_{2\perp}$, the $g_{2\perp f}$ processes into the $g_{1\perp}$ processes and the $g_{4\perp f}$ into the ordinary $g_{4\perp}$.

The theory of disorder scattering was briefly explained in 4, but the case at hand is somewhat more complicated in the sense that we need to be careful between which bands the scatterings take place. In the region above the gap, there will be three different ways for electrons to backscatter off the disordered impurities - within the a band, within the b band and between the a and b bands. Thus, to the Hamiltonian described above, we add a disorder Hamiltonian $H_{\mathrm{dis}} = H_{\xi aa} + H_{\xi ab} + H_{\xi bb}$ consisting of three corresponding terms describing backscattering against the impurities . They are given by

$$H_{\xi aa} = \int \mathrm{d}x \left(\xi_{aa} \psi^\dagger_{L\downarrow} \psi_{R\uparrow} + \xi^*_{aa} \psi^\dagger_{R\uparrow} \psi_{L\downarrow} \right) \tag{5.17}$$

$$H_{\xi bb} = \int \mathrm{d}x \left(\xi_{bb} \psi^\dagger_{L\uparrow} \psi_{R\downarrow} + \xi^*_{bb} \psi^\dagger_{R\downarrow} \psi_{L\uparrow} \right) \tag{5.18}$$

$$H_{\xi ab} = \sum_{\sigma=\uparrow,\downarrow} \int \mathrm{d}x \left(\xi_{ab} \psi^\dagger_{R\sigma} \psi_{L\sigma} + \xi^*_{ab} \psi^\dagger_{L\sigma} \psi_{R\sigma} \right), \tag{5.19}$$

which bosonises into

$$H_{\xi aa} = \int \mathrm{d}x \; \xi_{aa} \frac{1}{2\pi a_0} e^{-i\sqrt{\pi}(\phi_\rho + \theta_\sigma)} + H.c. \tag{5.20}$$

$$H_{\xi bb} = \int \mathrm{d}x \; \xi_{ab} \frac{1}{2\pi a_0} e^{-i\sqrt{\pi}(\phi_\rho - \theta_\sigma)} + H.c. \tag{5.21}$$

$$H_{\xi ab} = \int \mathrm{d}x \; \xi_{ab} \frac{1}{\pi a_0} e^{-i\sqrt{\pi}\phi_\rho} \cos(\sqrt{\pi}\phi_\sigma) + H.c. \tag{5.22}$$

5.2.2 Theory in the gap

Before employing the RG scheme on the effective Hamiltonian that describes the physics above the bandgap, we turn to the description of the region in the gap. Here, the theory is most easily written down by just removing the bosonic fields belonging to the b band from eq. (5.13),

$$H_0 = \frac{v_H}{2} \int \mathrm{d}x \left[\frac{1}{K_H} \left(\partial_x \varphi(x) \right)^2 + K_H \left(\partial_x \theta(x) \right)^2 \right], \tag{5.23}$$

where now $\varphi = \phi_{R\uparrow} + \phi_{L\downarrow}$ and $\theta = \phi_{R\uparrow} - \phi_{L\downarrow}$. The result is a quasi-helical Luttinger liquid, where opposite prespins belong to opposite directions. Since we have linearised the spectrum around the two Fermi points at $k = \pm 2q_0$, where the spin overlaps are very small, it is a good approximation to treat the theory in the gap as a helical liquid. In practice, this means that we may set some of the g-ology coupling constants to zero. The values of K_H and v_H can be expressed in terms of K_ν and v_ν, which is crucial for our two-step RG scheme since we need to be able to use the renormalised values of K_ν and v_ν when switching from the spinful LL above the gap to the helical liquid in the gap. The derivation is found in appendix A and the resulting expressions are

$$K_H = \sqrt{\frac{K_\rho(K_\rho K_\sigma v_\rho + v_\sigma)}{K_\sigma(K_\rho K_\sigma v_\sigma + v_\rho)}} \tag{5.24}$$

$$v_H = \frac{1}{2}\sqrt{v_\rho^2 + v_\sigma^2 + v_\rho v_\sigma \left(K_\rho K_\sigma + \frac{1}{K_\rho K_\sigma}\right)}. \tag{5.25}$$

5.2.3 RG equations

We are now ready to renormalise the theory. To set up the formalism, we will primarily follow ref. [60]. The disorder of the randomly distributed impurities is expressed by a random potential with Gaussian distribution. The amplitude for scattering between the branches $i, j = a, b$ is described by the dimensionless disorder strength $\tilde{D}_{ij}$, which is proportional to the square of the strength of each individual scattering potential, which in turn is proportional to the square of the overlap between the two branches, $|\langle i|j\rangle|^2$. Thus, if we denote the disorder strength for scattering between states with perfect spin overlap by $\tilde{D}$, we have $\tilde{D}_{ij} = \tilde{D}|\langle i|j\rangle|^4$. The renormalisation of $\tilde{D}_{ij}$ depends in the spinful LL on K_ρ, K_σ and $g_{1\perp}$, which in turn depend on v_ρ and v_σ, so we need the scaling equations for those parameters as well. In addition, we need to take into account the renormalisation of the magnetic gap. The reason is that we switch theories when the bottom of the upper band is reached by renormalisation and coincides with the lower cutoff Λ/b, so the increase of the gap by RG will affect our results. There are three competing effects at work. If the magnetic field is low enough, the amplitude $\tilde{D}_{ab}$ for scattering off impurities from one branch to the other will grow large before Λ/b reaches the gap, causing Anderson localisation. For larger magnetic fields, Λ/b will reach the gap before $\tilde{D}_{ab}$ grows large, and we continue with the renormalisation of $\tilde{D}_{aa}$ in the gap. For intermediate magnetic field strengths, the overlap between the right- and left-movers in the quasi-helical liquid is small, which will make $\tilde{D}_{aa} \propto |\langle a|a\rangle|^4$ small. In turn, this means that the localisation length for Anderson localisation caused by aa backscattering off impurities will be large. As long as it is larger than the sample length, which we will denote $\mathcal{L}$, the quasi-helical conductor will remain metallic. Finally, when B_x is large enough, the overlap $\langle aL|aR\rangle$, and thereby the disorder strength $\tilde{D}_{aa}$, will be large enough to cause localisation.

There are a couple of problems we need to deal with before continuing with this two-step RG approach. Since the overlap integrals depend on k, the problem is no longer scale invariant, in the sense that the coupling constants will depend on the energy scale we consider, even without renormalisation. To address this problem, we calculate the overlaps at

some fixed value of k and stick to them. The scatterings we consider during the RG are scatterings between one of the Fermi points and other points at high energies, determined by the Λ/b parameters. In Paper III it is shown that the overlaps don not vary too much with the energy scale, and we found that taking the overlaps at halfway to the high-energy cutoff is a good estimate of the influence of the overlaps on the theory [25]. The second issue is that it looks as though we might neglect the fact that we renormalise even over the bottom of the b band when switching from the full Luttinger liquid theory above the gap to the quasi-helical theory in the gap. This could have been a problem due to the curvature of the band bottom, since we linearise the theory in order to do bosonisation. Normally, the linearisation is a good approximation for the low-energy physics around the Fermi points, but since it seems that we need to integrate over a part of the theory where this approximation is potentially far away from the actual curved band bottom of the b band, one might fear that the approximation is instead far off. However, also the gap Δ_Z renormalises and grows under RG, which means that we will reach the bottom of the upper band and switch theories before reaching the potentially problematic part.

Next, the task will be to derive the RG equations and investigate the behaviours in the different regions. We will use the replica method described in chapter 4, and start with writing down the replicated parts of the action that are due to the three different backscattering processes we are interested in. The bosonised version of the Hamiltonians are given in eqs. (5.20)-(5.22). These yield the replicated actions

$$S_{\xi aa} = -\frac{D_{\xi aa}}{4(\pi a_0)^2} \sum_{i,j} \int \mathrm{d}x \mathrm{d}\tau \mathrm{d}\tau' e^{-i\sqrt{\pi}(\phi_\rho^i(x,\tau) - \phi_\rho^j(x,\tau') + \theta_\sigma^i(x,\tau) - \theta_\sigma^j(x,\tau'))} + H.c., \tag{5.26}$$

$$S_{\xi bb} = -\frac{D_{\xi bb}}{4(\pi a_0)^2} \sum_{i,j} \int \mathrm{d}x \mathrm{d}\tau \mathrm{d}\tau' e^{-i\sqrt{\pi}(\phi_\rho^i(x,\tau) - \phi_\rho^j(x,\tau') - \theta_\sigma^i(x,\tau) + \theta_\sigma^j(x,\tau'))} + H.c. \tag{5.27}$$

and

$$S_{\xi ab} = -\frac{D_{\xi ab}}{(\pi a_0)^2}\sum_{i,j}\int \mathrm{d}x\mathrm{d}\tau\mathrm{d}\tau' e^{-i\sqrt{\pi}(\phi_\rho^i(x,\tau)-\phi_\rho^j(x,\tau'))} \times \cos\left(\sqrt{\pi}\phi_\sigma^i(x,\tau)\right)\cos\left(\sqrt{\pi}\phi_\sigma^j(x,\tau')\right) + H.c.$$
$$= -\frac{2D_{\xi ab}}{(\pi a_0)^2}\sum_{i,j}\int \mathrm{d}x\mathrm{d}\tau\mathrm{d}\tau' \cos\left(\sqrt{\pi}(\phi_\rho^i(x,\tau)-\phi_\rho^j(x,\tau'))\right) \times \cos\left(\sqrt{\pi}\phi_\sigma^i(x,\tau)\right)\cos\left(\sqrt{\pi}\phi_\sigma^j(x,\tau')\right), \quad (5.28)$$

where i and j are the replica indices to be summed over. We will not need the replica indices in what follows, since we will perform the expansion in $D_{\xi ab}$ to first order only. In previous chapters, the RG analyses have been performed directly on the action, but in this case it will be easier to use the following correlation functions instead:

$$R_{\phi_\rho}(r_1 - r_2) = \left\langle e^{i\sqrt{\pi}\phi_\rho(r_1)}e^{-i\sqrt{\pi}\phi_\rho(r_2)}\right\rangle \quad (5.29)$$
$$R_{\phi_\sigma}(r_1 - r_2) = \left\langle e^{i\sqrt{\pi}\phi_\sigma(r_1)}e^{-i\sqrt{\pi}\phi_\sigma(r_2)}\right\rangle \quad (5.30)$$
$$R_{\theta_\sigma}(r_1 - r_2) = \left\langle e^{i\sqrt{\pi}\theta_\sigma(r_1)}e^{-i\sqrt{\pi}\theta_\sigma(r_2)}\right\rangle, \quad (5.31)$$

where $r_i = (x_i, \tau_i)$. These correlation functions are to be taken with respect to the full action $S = S_0 + S_{g\perp} + S_{\xi ab+aa+bb} + S_\Delta$. The definition of the correlation function is

$$\langle A\rangle = \frac{1}{Z}\int \mathcal{D}\phi_1\mathcal{D}\phi_2 \ldots A e^{-S[\phi_1,\phi_2\ldots]}, \quad (5.32)$$

where Z is the partition function. The fields integrated over may of course also include the dual θ fields. If we write $S = S_0 + S_{g_{1\perp}} + S_{\xi ab+aa+bb} + S_\Delta$ and $\exp(-S) = \exp(-S_0)\exp(-S_{g_{1\perp}} - S_{\xi ab+aa+bb} - S_\Delta)$, we can Taylor expand the second exponent to

$$e^{-S} = e^{-S_0}\left(1 - S_{g_{1\perp}} - S_{\xi ab+aa+bb} + S_{g_{1\perp}}^2 + S_{\xi ab+aa+bb}S_{g_{1\perp}} + \ldots\right), \quad (5.33)$$

where we have neglected the Δ part of the action, since its RG equations have already been calculated elsewhere and the crossterms can be shown to yield nothing new. Since D_ξ is already second order in ξ, the S_ξ^2 terms are omitted. With this,

$$\begin{aligned}\langle A\rangle \approx \frac{1}{Z}\int \mathcal{D}\phi_1\mathcal{D}\phi_2\ldots Ae^{-S_0} \\ \times\left(1-S_{g_{1\perp}}-S_{\xi ab+aa+bb}+S_{g_{1\perp}}^2+S_{\xi ab+aa+bb}S_{g_{1\perp}}\right) \\ =\left\langle A\left(1-S_{g_{1\perp}}-S_{\xi ab+aa+bb}+S_{g_{1\perp}}^2+S_{\xi ab+aa+bb}S_{g_{1\perp}}\right)\right\rangle_0, \quad (5.34)\end{aligned}$$

where the 0 index means that we are taking the correlation function with respect to S_0. We are thus left with a series of correlation functions to calculate, each much less complicated than the original ones. The actual calculation are unfortunately a bit too lengthy to fit in this thesis, so we will here just outline the method and state the results. Once the correlation functions are calculated, we arrive at new, effective version of R_{ϕ_ρ}, R_{ϕ_σ} and R_{ϕ_σ} from eqs. (5.29)-(5.31). It then only remains to do the rescaling and extract the RG equations:

$$\partial_l K_\rho = -v_\rho K_\rho^2(2\tilde{D}_{ab}+\tilde{D}_{aa})/4v_\sigma \quad (5.35)$$
$$\partial_l K_\sigma = -K_\sigma^2(\tilde{D}_{ab}+y^2)/2+\tilde{D}_{aa}/4 \quad (5.36)$$
$$\partial_l y = (2-2K_\sigma)y-\tilde{D}_{ab} \quad (5.37)$$
$$\partial_l \tilde{D}_{aa} = (3-K_\rho-K_\sigma^{-1})\tilde{D}_{aa} \quad (5.38)$$
$$\partial_l \tilde{D}_{bb} = (3-K_\rho-K_\sigma^{-1})\tilde{D}_{bb} \quad (5.39)$$
$$\partial_l \tilde{D}_{ab} = (3-K_\rho-K_\sigma-y)\tilde{D}_{ab} \quad (5.40)$$
$$\partial_l v_\rho = -K_\rho v_\rho^2(2\tilde{D}_{ab}+\tilde{D}_{aa})/4v_\sigma \quad (5.41)$$
$$\partial_l v_\sigma = -v_\sigma K_\sigma \tilde{D}_{ab}/2-v_\sigma K_\sigma^{-3}\tilde{D}_{aa}/4 \quad (5.42)$$
$$\partial_l \delta(l) = \left[2-(K_\rho+K_\sigma^{-1})/2\right]\delta \quad (5.43)$$

above the gap, where we have defined the dimensionless gap parameter $\delta(l)=\Delta_Z(l)/E(l)$, where $E(l)=\hbar v_F/\kappa(l)$, where $\kappa(l)=\kappa e^l$. The RG equations in the gap are

$$\partial_l K_a = -K_a^2\tilde{D}_{aa}/2, \quad (5.44)$$
$$\partial_l \tilde{D}_{aa} = (3-2K_a)\tilde{D}_{aa}, \quad (5.45)$$
$$\partial_l v_a = -v_a K_a \tilde{D}_{aa}/2. \quad (5.46)$$

5.3 Results

To extract the consequences of the RG equations in eqs. (5.35)-(5.43) and (5.44)-(5.46), we consider an experimentally accessible system. We

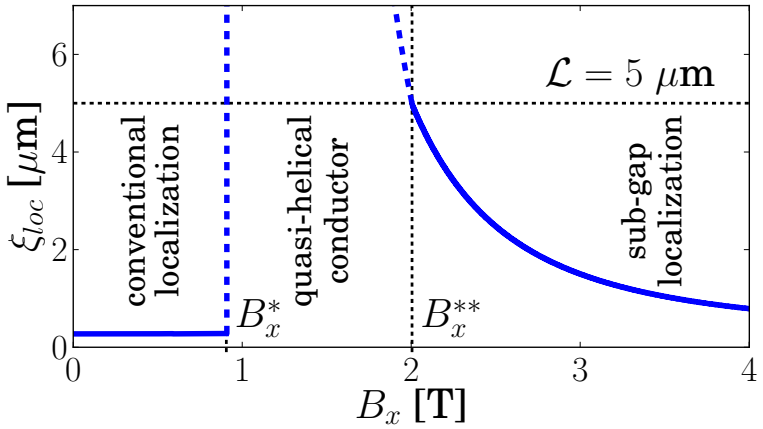

Figure 5.3: The localisation length of an InAs nanowire with system length 5μm as a function of B_x for $\tilde{D} = 0.01$. We find one metal-insulator transition at $B_x \approx 0.9$T and one at $B_x \approx 2$T. The figure is from Paper III.

choose, as before, an InAs nanowire. To carry out the analysis we need to add some more parameters to the ones given earlier. The length of the system is taken to be $L = 5\mu$m, $K_\rho = 0.5$, $K_\sigma = 1$, $v_\rho = v_F/K_\rho$, $v_\sigma = v_F/K_\sigma$ and $y = 0.1|\langle a, L|b, R\rangle|^2$. Finally, we take the short length cutoff $\kappa = 15$ nm [75, 77]

With these parameters, we renormalise the theory above the gap with eqs. (5.35)-(5.43). If any of the $\tilde{D}$ parameters become of the order unity, the system is localised and we stop the renormalisation. If the cutoff Λ/b, which becomes smaller during RG, meets the bandgap, which grows under RG, we switch to the helical theory in the gap. Here we use RG equations (5.44)-(5.46) with new values of v_H and K_H determined from the renormalised values of v_ρ, v_σ, K_ρ and K_σ according to eqs. (5.24) and (5.25). We continue the renormalisation until either the a band gets localised due to the $\tilde{D}_a a$ disorder scattering, or the renormalisation exceeds the size of the sample.

The RG flow yield the localisation lengths plotted in Fig. 5.3. For low B_x fields, the localisation length is short due to disorder backscatterings between the a and b band, the states of which have a large spin overlap at low fields. At a certain value $B_x = B_x^*$, the magnetic gap is large enough for the gap to be reached by RG before $\tilde{D}_{ab}$ grows large enough to localise the electrons. For stronger field $B_x > B_x^{**}$, the localisation length is again small, since the large spin overlap between the counterpropagating electrons will here make the $\tilde{D}_{aa}$ disorder amplitude large. We have thus

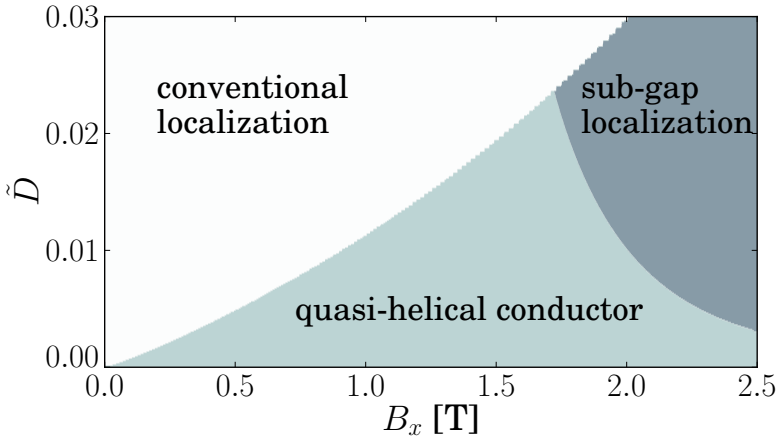

Figure 5.4: A phase diagram depicting the three different phases for different values of the disorder strength and the magnetic field. The figure comes from Paper III.

found a region $B_x^* < B_x < B_x^{**}$ where a quasi-helical conductor phase can be sustained.

We can reformulate the results as a phase diagram (see Fig. 5.4), where we show the boundaries between the three different phases as functions of the non-overlap disorder strength and the magnetic field. The figure reveals that there exists a threshold value below which a sweep of the magnetic field from low to high will result in two metal-insulator transitions, first from an insulating state to a quasi-helical liquid state, and then, at higher fields, back again. Above this threshold, however, the system will remain an insulator for any value of B_x (for the InAs nanowire at hand, this threshold value is estimated to $\tilde{D} \approx 0.023$).

6

Kondo and Rashba effects on a quantum spin Hall edge

Chapter 4 discussed the effect of adding a Rashba spin-orbit interaction at a quantum spin Hall edge. It was shown that in combination with dispersive electron-electron interaction, the Rashba interaction may cause localisation of the edge electrons if it is disordered. Now, we want to ask ourselves what the effect would be of adding a combination of a uniform Rashba interaction and a Kondo type impurity on the edge. The work presented in this chapter was published as Paper IV and is a collaboration with Erik Eriksson, Girish Sharma and Henrik Johannesson [26].

6.1 Kondo physics

The temperature dependence of the electrical resistivity in an ordinary metal shows a linear increase with temperature. The main cause of resistance is that conduction electrons gets scattered by the atoms in the metal, and the more the atoms vibrate, the more difficult it becomes for the electrons to travel through the metal unscattered. As the temperature is lowered, the linear behaviour eventually crosses over to a power-law dependence on temperature, with the leading term determined by what type of scattering process dominates (electron-phonon, electron-electron etc.). As the temperature is lowered further, the resistivity eventually levels off to a constant due to non-magnetic impurity scattering (unless the material becomes superconducting). In 1934, however, it was discovered by de Haas et al. that adding magnetic impurities to a metal will change the temperature dependence of the resistivity so that a minimum appears at a certain temperature [78]. The mechanism

behind this increase in resistivity with lowered temperature remained a mystery until Kondo was able to explain the phenomenon theoretically in 1964 [79]. Using ordinary perturbation theory, Kondo showed that spin exchange between the magnetic impurities and the conduction electrons contributes an extra term $J\ln[k_BT/(D-E_F)]$ to the resistivity, J being the coupling between the impurity spin and the electron spin, D a high-energy cut-off and E_F the Fermi energy. For positive J (antiferromagnetic case - energy is minimised when the two spins lie in opposite directions), $J\ln[k_BT/(D-E_F)]$ diverges as T approaches zero, making the perturbative result invalid. The temperature where this happens is known as the *Kondo temperature*, T_K, and it follows that Kondo's result is valid only for $T > T_K$. To give an estimate of T_K, Kondo assumed the perturbation theory to break down when

$$J\ln[k_BT_K/(D-E_F)] \approx 1 \Leftrightarrow T_K \approx \frac{(D-E_F)}{k_B}e^{1/J}, \tag{6.1}$$

where J is chosen dimensionless. The problem of describing the physics below T_K is known as the Kondo problem. It turned out to be a very difficult quantum many-particle problem which required the development of novel theoretical tools and concepts for its solution. To mention the most important: Anderson's pioneering "poor-man's scaling" theory [80], Wilson's renormalisation group [43], the exact Bethe Ansatz theories by Andrei [81] and Wiegmann [82], and the deep and powerful conformal field theory formulation by Affleck and Ludwig [83]. Moreover, as became clear in retrospect from Wilson's renormalisation group approach, the Kondo model in fact defines an asymptotically free theory: T_K is a dynamically generated energy scale below which the electrons interact strongly with the impurity spin and gets screened away. In contrast, at temperatures above T_K the interaction is weak, and therefore the physics can be accessed perturbatively.

For the rest of the chapter, we will investigate the effect of the combination of a Kondo-type magnetic impurity and a uniform Rashba SOI on the edge of a QSH system. The focus will be both on the Kondo temperature and how the edge conductance is influenced by the impurity, and especially, how both of these features are affected by the Rashba interaction. The electrical controllability of the Rashba strength in a quantum well, via a gate voltage, then may provide a tool for experimental control of Kondo physics in helical conductors.

6.2 Model

As in chapter 4, the electrons on the edge are modelled by the spinor $\Psi = (\psi_\uparrow, \psi_\downarrow)^T$, where the edge is assumed to be helical, so that $\psi_\uparrow$ and $\psi_\downarrow$ annihilates electrons with opposite spins and momenta. To add to the the helical free Hamiltonian, including dispersive and forward scatterings, we need the Hamiltonians for the Rashba and Kondo interactions, respectively. The Rashba Hamiltonian is given by eq. (4.1), while the Kondo interaction can be written

$$H_K = \Psi^\dagger(0)(J_x\sigma^x S^x + J_y\sigma^y S^y + J_z\sigma^z S^z)\Psi(0), \tag{6.2}$$

where σ^i and S^i are Pauli matrices in the spin spaces of the conduction electrons and the impurity spin, respectively. The J_x, J_y and J_z are the couplings between the two different spins along the three spatial axes. As it is written now, all three can in principle be different, but for a magnetic impurity at a 2D quantum well interface, as we shall study here, one expects $J_x = J_y > J_z$ [84].

Assuming for simplicity a uniform Rashba interaction along the edge, eq. (4.1) takes the form

$$H_R = -i\alpha \int \mathrm{d}x \Psi^\dagger(x)\sigma^y\partial_x\Psi(x). \tag{6.3}$$

If we neglect electron-electron interactions to begin with (they will be added later on), our total edge Hamiltonian can thus be written

$$\begin{aligned} H = -iv_F \int \mathrm{d}x \Psi^\dagger(x)\sigma^z\partial_x\Psi(x) - i\alpha \int \mathrm{d}x \Psi^\dagger(x)\sigma^y\partial_x\Psi(x) \\ + \Psi^\dagger(0)(J_x\sigma^x S^x + J_y\sigma^y S^y + J_z\sigma^z S^z)\Psi(0). \end{aligned} \tag{6.4}$$

The spinors can be rotated into $\Psi' = e^{-i\sigma^x\theta/2}\Psi$ in order to absorb the entire Rashba term in the kinetic part of the Hamiltonian [85]. We want the quantisation axis of the impurity spin to be the same as for the bulk electron spin, so the impurity spin is also rotated into $\mathbf{S}' = e^{-iS^x\theta/2}\mathbf{S}e^{iS^x\theta/2}$. The new spin quantisation axis z' is thus rotated by the angle θ from the z-axis. This turns $H_0 + H_R + H_K$ into $H_0' + H_K'$, with

$$H_0' = v_\alpha \int \mathrm{d}x \Psi'^\dagger(x)(-i\sigma^{z'}\partial_x)\Psi'(x) \tag{6.5}$$

$$H_K' = \Psi'^\dagger(0)\Big(J_x\sigma^x S^x + J_y'\sigma^{y'}S^{y'} + J_z'\sigma^{z'}S^{z'} + J_E(\sigma^{y'}S^{z'} + \sigma^{z'}S^{y'})\Big)\Psi'(0), \tag{6.6}$$

with the following definitions:

$$J_y' = J_y \cos^2\theta + J_z \sin^2\theta \tag{6.7}$$
$$J_z' = J_z \cos^2\theta + J_y \sin^2\theta \tag{6.8}$$
$$J_E = (J_y - J_z)\cos\theta \sin\theta \tag{6.9}$$
$$v_\alpha = \sqrt{v_F^2 + \alpha^2}. \tag{6.10}$$

The relationship between the Rashba rotated velocity v_α and the Rashba rotation angle θ is then expressed through $\cos\theta = v_F/v_\alpha$ and $\sin\theta = \alpha/v_\alpha$. As we can see, the Rashba interaction leaves the J_x coupling intact, while mixing the J_y and J_z couplings. This means that for non-zero Rashba coupling α, even if we start with the two Kondo couplings perpendicular to the spin axis equal, $J_x = J_y = J_\perp$, we will end up with an effective Kondo Hamiltonian with three different couplings J_x, J_y' and J_z'. In other words, as expected, spin along the quantisation axes is no longer conserved. In addition, unless $J_y = J_z$, a new non-collinear term $J_E(\sigma^{y'} S^{z'} + \sigma^{z'} S^{y'})$ is produced. The role of this term will be discussed later.

We will now approach the problem by using bosonisation and RG techniques. Once the RG equations have been derived, we can use them to find out when the couplings between the impurity spin and the conduction electrons grow large and start to dominate the theory. The temperature corresponding to the energy scale where this happens is interpreted as the Kondo temperature discussed above.

6.3 Bosonisation

The next step is to bosonise $H_0' + H_K'$, but from now on we drop the primes and simply write $H_0 + H_K$ (i.e. the new $H_0 + H_K$ is equal to the old $H_0 + H_R + H_K$). Similarly, we write Ψ instead of Ψ'. We start by looking at H_K in eq. (6.6). The Pauli matrices acting on the spinors there can be written

$$\Psi^\dagger \sigma_x \Psi = \psi_\uparrow^\dagger \psi_\downarrow + \psi_\downarrow^\dagger \psi_\uparrow \tag{6.11}$$
$$\Psi^\dagger \sigma_y \Psi = -i\psi_\uparrow^\dagger \psi_\downarrow + i\psi_\downarrow^\dagger \psi_\uparrow \tag{6.12}$$
$$\Psi^\dagger \sigma_z \Psi = \psi_\uparrow^\dagger \psi_\uparrow - \psi_\downarrow^\dagger \psi_\downarrow. \tag{6.13}$$

We bosonise H_K by using the bosonisation rules from eq. (3.13) and eq. (3.14) (where now the chiral index can be ignored). We will also need the bosonisation relation for the density fluctuations $\rho_{\uparrow/\downarrow}$ from eq. (3.18).

With thus obtain

$$\Psi^\dagger \sigma_x \Psi = \frac{1}{\pi a_0} \cos[2\sqrt{\pi}\varphi] \tag{6.14}$$

$$\Psi^\dagger \sigma_y \Psi = \frac{1}{\pi a_0} \sin[2\sqrt{\pi}\varphi] \tag{6.15}$$

$$\Psi^\dagger \sigma_z \Psi = \frac{i}{\sqrt{\pi}}(\partial_z + \partial_{\bar{z}})\varphi = \frac{1}{v\sqrt{\pi}}\partial_t \varphi = \frac{i}{v\sqrt{\pi}}\partial_\tau \varphi. \tag{6.16}$$

The bosonised Kondo Hamiltonian is thus

$$H_K = \frac{A}{a_0} \cos[2\sqrt{\pi}\varphi(\tau)] + \frac{B}{a_0} \sin[2\sqrt{\pi}\varphi(\tau)] + \frac{i}{v} C \partial_\tau \varphi(\tau), \tag{6.17}$$

where $A = J_x S^x/\pi$, $B = (J'_y S^{y'} + J_E S^{z'})/\pi$ and $C = (J'_z S^{z'} + J_E S^{y'})/\sqrt{\pi}$.

Turning to the kinetic part of the Hamiltonian, H_0, things will work out just like before. We also want to add electron-electron interactions at this stage. As we know by now, the interactions allowed by time-reversal symmetry, away from half-filling, are forward and dispersive scattering. The partition function then becomes

$$Z = \int \mathcal{D}\varphi(\tau) \exp\left[-\frac{1}{\beta} \sum_n \frac{|\omega_n|}{K} |\varphi(\omega_n)|^2 - \int \mathrm{d}\tau \mathcal{L}_K[\varphi(\tau)] \right] \tag{6.18}$$

6.4 Effective action

As in section 3.3, we divide our fields into a slow (s) and a fast (f) part, $\varphi(\tau) = \varphi_s(\tau) + \varphi_f(\tau)$, and the effective action can then be written

$$e^{-S_{\text{eff}}[\varphi_s]} = e^{-S_s[\varphi_s]} \left\langle e^{-S_K[\varphi_s, \varphi_f]} \right\rangle_f = e^{-S_s[\varphi_s]} e^{\langle S_K \rangle_f - \frac{1}{2}\left(\left\langle S_K^2 \right\rangle_f - \langle S_K \rangle_f^2 \right)}. \tag{6.19}$$

We will now bring the effective action in eq. (6.19) on a form suitable for an RG analysis. Let us start with the first order term in the cumulant expansion,

$$\langle S_K \rangle_f = \int \mathrm{d}\tau \Bigg[\left\langle \frac{A}{a_0} \cos[2\sqrt{\pi}\varphi(\tau)] \right\rangle + \left\langle \frac{B}{a_0} \sin[2\sqrt{\pi}\varphi(\tau)] \right\rangle + \left\langle \frac{iC}{v} \partial_\tau \varphi(\tau) \right\rangle \Bigg]. \tag{6.20}$$

We see that the last of these terms will not renormalise to first order, since $\langle \partial_\tau \varphi_f(\tau) \rangle = 0$, so that $\langle \partial_\tau \varphi \rangle = \partial_\tau \varphi_s$. The first term is

$$\begin{aligned}
&\int \mathrm{d}\tau \left\langle \frac{A}{a_0} \cos[2\sqrt{\pi}\varphi(\tau)] \right\rangle \\
&\quad = \frac{A}{2a_0} \int \mathrm{d}\tau \Bigg\{ e^{2i\sqrt{\pi}\varphi_s} \\
&\quad \times \int \mathcal{D}\varphi_f \exp\left[\int_f \frac{\mathrm{d}\omega}{2\pi} \left(2i\sqrt{\pi} e^{-i\omega\tau} \varphi_f(\omega) - \frac{|\omega|}{K} |\varphi_f|^2 \right) \right] + H.c. \Bigg\} \\
&\quad = \frac{A}{2a_0} \int \mathrm{d}\tau \left\{ e^{2i\sqrt{\pi}\varphi_s} \exp\left[- \int_f \frac{\mathrm{d}\omega}{2\pi} \frac{\pi K}{|\omega|} \right] + H.c. \right\} \\
&\quad = e^{-\frac{K}{2}\int_f \frac{\mathrm{d}\omega}{|\omega|}} \frac{A}{a_0} \int \mathrm{d}\tau \cos\left[2\sqrt{\pi}\varphi_s \right].
\end{aligned} \tag{6.21}$$

Similarly, the second term in eq. (6.20) is

$$\begin{aligned}
&\int \mathrm{d}\tau \left\langle \frac{B}{a_0} \sin[2\sqrt{\pi}\varphi(\tau)] \right\rangle \\
&\quad = \frac{B}{2ia_0} \int \mathrm{d}\tau \Bigg\{ e^{2i\sqrt{\pi}\varphi_s} \\
&\quad \times \int \mathcal{D}\varphi_f \exp\left[\int_f \frac{\mathrm{d}\omega}{2\pi} \left(2i\sqrt{\pi} e^{-i\omega\tau} \varphi_f(\omega) - \frac{|\omega|}{K} |\varphi_f|^2 \right) \right] - H.c. \Bigg\} \\
&\quad = \frac{B}{2ia_0} \int \mathrm{d}\tau \left\{ e^{2i\sqrt{\pi}\varphi_s} \exp\left[- \int_f \frac{\mathrm{d}\omega}{2\pi} \frac{\pi K}{|\omega|} \right] - H.c. \right\} \\
&\quad = e^{-\frac{K}{2}\int_f \frac{\mathrm{d}\omega}{|\omega|}} \frac{B}{a_0} \int \mathrm{d}\tau \sin\left[2\sqrt{\pi}\varphi_s \right].
\end{aligned} \tag{6.22}$$

Next, we calculate the second order terms of the cumulant expansion in eq. (6.19). We start with

$$
\begin{aligned}
-\frac{1}{2}\left(\left\langle S_K^2\right\rangle_f - \langle S_K\rangle_f^2\right) = -\frac{1}{2}\int \mathrm{d}\tau\mathrm{d}\tau' \Bigg\{ & \\
\frac{A^2}{a_0^2}\Big(\big\langle\cos[2\sqrt{\pi}\varphi(\tau)]\cos[2\sqrt{\pi}\varphi(\tau')]\big\rangle - \big\langle\cos[2\sqrt{\pi}\varphi(\tau)]\big\rangle\big\langle\cos[2\sqrt{\pi}\varphi(\tau')]\big\rangle\Big) & \\
+\frac{B^2}{a_0^2}\Big(\big\langle\sin[2\sqrt{\pi}\varphi(\tau)]\sin[2\sqrt{\pi}\varphi(\tau')]\big\rangle - \big\langle\sin[2\sqrt{\pi}\varphi(\tau)]\big\rangle\big\langle\sin[2\sqrt{\pi}\varphi(\tau')]\big\rangle\Big) & \\
-\frac{C^2}{v^2}\left(\langle\partial_\tau\varphi(\tau)\partial_{\tau'}\varphi(\tau')\rangle - \langle\partial_\tau\varphi(\tau)\rangle\langle\partial_{\tau'}\varphi(\tau')\rangle\right) & \\
+\frac{AB}{a_0^2}\Big(\big\langle\cos[2\sqrt{\pi}\varphi(\tau)]\sin[2\sqrt{\pi}\varphi(\tau')]\big\rangle - \big\langle\cos[2\sqrt{\pi}\varphi(\tau)]\big\rangle\big\langle\sin[2\sqrt{\pi}\varphi(\tau')]\big\rangle\Big) & \\
+\frac{iAC}{a_0 v}\left(\big\langle\cos[2\sqrt{\pi}\varphi(\tau)]\partial_{\tau'}\varphi(\tau')\big\rangle - \big\langle\cos[2\sqrt{\pi}\varphi(\tau)]\big\rangle\langle\partial_{\tau'}\varphi(\tau')\rangle\right) & \\
+\frac{iBC}{a_0 v}\left(\big\langle\sin[2\sqrt{\pi}\varphi(\tau)]\partial_{\tau'}\varphi(\tau')\big\rangle - \big\langle\sin[2\sqrt{\pi}\varphi(\tau)]\big\rangle\langle\partial_{\tau'}\varphi(\tau')\rangle\right) & \\
+\frac{BA}{a_0^2}\ldots + \frac{iCA}{a_0 v}\ldots + \frac{iCB}{a_0 v}\ldots \Bigg\}. &
\end{aligned}
\tag{6.23}
$$

We will treat all nine terms in order. The last three terms, proportional to BA, CA and CB, are the same as the ones proportional to AB, AC and BC respectively, but with the τ- and τ'-dependent factors in switched positions. In eq. (6.6), the different terms were written as $J_a\sigma^b S^c$, for some a, b and c, and a product of two of these terms is then a product of two J coupling constants, two Pauli matrices σ in the electron spin space and two Pauli matrices S in the impurity spin space. The anticommutation rules for the Pauli matrices are $\{\sigma^a, \sigma^b\} = \delta_{ab}$, which means that most of the terms proportional to AB will be equal to the ones proportional to BA and so on. This is shown explicitly in Appendix B, where the derivation of the second-order RG equations are carried out.

The full set of RG equations are

$$\frac{\partial J_x(l)}{\partial l} = (1-K)J_x(l) + \frac{K}{v\pi}\left(J'_y(l)J'_z(l) - J_{E1}(l)J_{E2}(l)\right) \tag{6.24}$$
$$\frac{\partial J'_y(l)}{\partial l} = (1-K)J'_y(l) + \frac{K}{v\pi}J_x(l)J'_z(l) \tag{6.25}$$
$$\frac{\partial J'_z(l)}{\partial l} = \frac{K}{v\pi}J_x(l)J'_y(l) \tag{6.26}$$
$$\frac{\partial J_{E1}(l)}{\partial l} = (1-K)J_{E1}(l) - \frac{K}{v\pi}J_x(l)J_{E2}(l) \tag{6.27}$$
$$\frac{\partial J_{E2}(l)}{\partial l} = -\frac{K}{v\pi}J_x(l)J_{E1}(l). \tag{6.28}$$

6.5 The Kondo temperature

To extract the Kondo temperature T_K, we need to see at what energy scale any of the coupling constants becomes large, so that the perturbative approach breaks down. By "large", we mean large compared to the kinetic part of the theory, so we want to compare the size of the coupling constants J with $\pi v/K$. When any J has grown to the size of $\pi v/K$, we check how far the flow parameter l has run and simply read off the corresponding thermal energy scale $k_BT = De^{-l}$.

6.5.1 Weak interaction limit

In the weak interaction limit, $K \approx 1$, and so the RG equations reduce to

$$\frac{\partial J_x}{\partial l} = \frac{K}{v\pi}\left(J'_yJ'_z - J_E^2\right) \tag{6.29}$$
$$\frac{\partial J'_y}{\partial l} = \frac{K}{v\pi}J_xJ'_z \tag{6.30}$$
$$\frac{\partial J'_z}{\partial l} = \frac{K}{v\pi}J_xJ'_y \tag{6.31}$$
$$\frac{\partial J_E}{\partial l} = -\frac{K}{v\pi}J_xJ_E, \tag{6.32}$$

where now J_E no longer separates into J_{E1} and J_{E2} by the flow. With this set of equations, the Kondo temperature turns out to be

$$T_K \approx D\exp\left(-\frac{\pi v}{J_x(0)}\frac{\operatorname{arcsinh}(\zeta)}{\zeta}\right), \tag{6.33}$$

where $\zeta = \sqrt{(J'_z(0)/J_x(0))^2 - 1}$ accounts for the anisotropy between the Kondo couplings paralell and perpendicular to the spin axis [49].

6.5.2 Strong interaction limit

In the strong interaction limit, with $K \ll 1$, the RG equations decouple and reduce to

$$\frac{\partial J_x}{\partial l} = (1-K)J_x \tag{6.34}$$

$$\frac{\partial J_{y'}}{\partial l} = (1-K)J_{y'} \tag{6.35}$$

$$\frac{\partial J_{E1}}{\partial l} = (1-K)J_{E1}. \tag{6.36}$$

The solution to each equation is simply $J(l) = J(0)e^{(1-K)l}$, for $J = J_x, J'_y$ and J_{E1} respectively. If we now insert $l = \ln(D/T)$ into the solution, and solve the equation $J(l) = \pi v/K$, we obtain that

$$T_K \approx D\left(\frac{JK}{\pi v}\right)^{1/(1-K)}, \tag{6.37}$$

and so the proper expression for T_K in the small K limit is $T_K \approx D(J_{max}K/(\pi v))^{(1/(1-K))}$, where $J_{\max}$ denotes the largest $J(0)$.

6.5.3 General case

The system of scaling equations (B.62) can also be solved numerically for any value of the interaction parameter K. Doing this will yield a value of l where one of the coupling constants will grow to the size of $\pi v/K$, which in turn gives the Kondo temperature as $T_K = De^{-l}/k_B$. When $J_x = J_y \geq J_z$ (which includes the case of an isotropic spin exchange) one obtains the Kondo temperatures shown in figure 6.1. For a given K_0, T_K decreases with increasing θ, an effect that is mostly due to the increase of v with θ. Turning to the case of an anisotropic Kondo effect with large J_z, i.e. $J_x = J_y < J_z$, the result is different, as shown in figure 6.2. It is now possible for the absolute value of the J_{E1} coupling to grow large and dominate the other couplings. Before discussing the implications of this possibility, let us calculate the conditions for it. By inspection of eq. (B.62), we see that the stronger the electron-electron interaction, the more likely it is for J_E to grow large in comparison to the other J:s. Given that all three of the l-dependent couplings in the strong-interaction limit share the same scaling equation, the one that grows large first, thereby determining the Kondo temperature, will be the one with the largest initial, or "bare", value. The bare values for the coupling constants, $J(l = 0)$, depend on the unrotated coupling constants

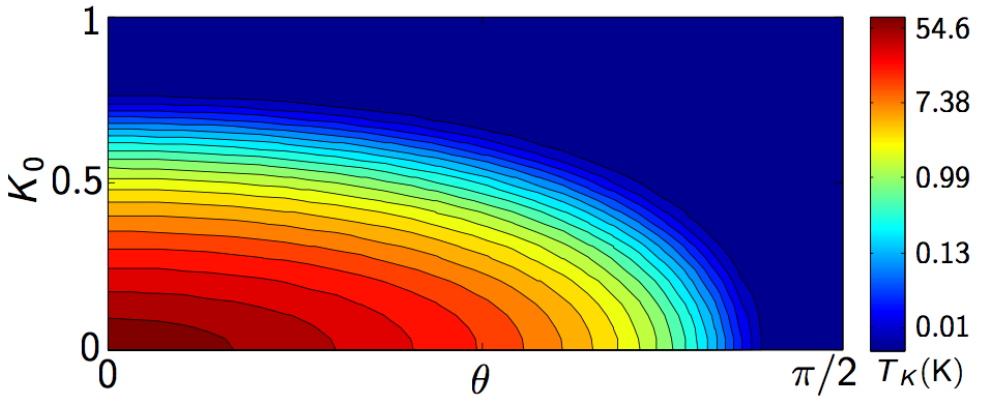

Figure 6.1: The Kondo temperature T_K as a function of the Rashba angle θ and the ordinary Luttinger liquid parameter K_0. The T_K scale is logarithmic and red and blue colour indicates high and low T_K, respectively. $J_x = J_y \geq J_z$ (here, $J_x/a_0 = J_z/a_0 = 10\text{meV}$)

$J_x = J_y (= J_\perp)$ and J_z and the Rashba angle θ as given in eqs.(6.7)-(6.9). From this, we see that for $|J_{E1}|$ to be larger than J_x and $J_{y'}$, we need J_z to be larger than $J_\perp$, making J_{E1} negative. With $J_z > J_\perp$, we also have $J_{y'} > J_x$. The two possibilities are then that $J_{y'}$ or $|J_{E1}|$ will be dominating. The condition for $|J_{E1}| > J_{y'}$ is

$$|J_{E1}| > J_{y'} \Leftrightarrow -J_{E1} > J_{y'} \tag{6.38}$$

$$(J_z - J_\perp)\cos\theta\sin\theta > J_\perp \cos^2\theta + J_z \sin^2\theta \tag{6.39}$$

$$J_z(\cos\theta\sin\theta - \sin^2\theta) > J_\perp(\cos\theta\sin\theta + \cos^2\theta) \tag{6.40}$$

$$J_z \frac{\cos\theta\sin\theta - \sin^2\theta}{\cos\theta\sin\theta + \cos^2\theta} > J_\perp. \tag{6.41}$$

The function $(\cos\theta\sin\theta - \sin^2\theta)/(\cos\theta\sin\theta + \cos^2\theta)$ reaches its maximum value of approximately 0.17 at $\theta = \pi/8$. This means that if we can produce a material with $J_z > 6J_\perp$, there might be a region in the $\theta - K_0$ plane, centered around $\theta = \pi/8$, where J_{E1} will dominate the physics, threatening to wipe out the expected Kondo regime. In Fig. 6.2, the numeric T_K calculation has been carried out with $J_z = 10J_x$. The area where J_{E1} becomes large first is shaded in the figure. This shaded area will grow with growing $J_z/J_\perp$.

Earlier, we briefly touched upon the physical explanation for the Kondo temperature, i.e. the temperature below which the perturbation theory breaks down. We stated that the impurity spin will be screened by the conduction electrons, and indeed, eq. (6.6) tells us that when any

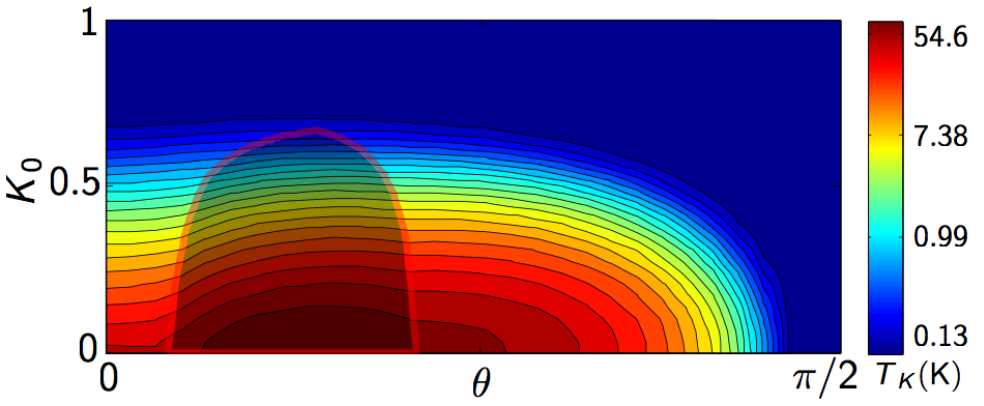

Figure 6.2: The Kondo temperature T_K as a function of the Rashba angle θ and the ordinary Luttinger liquid parameter K_0. The T_K scale is logarithmic and red and blue colour indicates high and low T_K, respectively. $J_x = J_y < J_z$ (here, $J_x/a_0 = 5$ meV and $J_z/a_0 = 50$ meV). In the shaded area, J_{E1} dominates the perturbative RG flow, hence obstructing singlet formation.

of J'_x, J'_y and J'_z grow large, the $\sigma^i S^i$ terms will make it energetically favourable for the spins to form singlets. However, the $J_{E1}\sigma^{y'} S^{z'}$ term will not favour spin singlets, which means that in the shaded area of Fig. 6.2, the Kondo screening will be obstructed and a higher conductance than with a collinear Kondo coupling can be expected.

6.6 Conductance

For the rest of the chapter, we will treat the correction to the conductance due to the Kondo impurity. Most of the analysis and calculations, some of which are quite tricky and demanding, were carried out by one of my co-authors on Paper IV, my fellow student Erik Eriksson. For completeness, the basic elements of the calculation, as well as the main results, are briefly presented here.

In the low-temperature regime, the results of ref. [49] will hold and the Rashba interaction will not affect the conductance. For $K > 1/4$, two-particle backscattering is irrelevant and at $T = 0$, no correction δG to the conductance is expected. With increased temperature, while still in the $T \ll T_K$ regime, contributions to δG from correlated two-particle backscattering (2PB) and inelastic single-particle scattering will occur. For strong electron-electron interaction, $K < 1/4$, the 2PB will be relevant and cause a crossover from weak to strong coupling at a

temperature $T_{bs} \approx D g_{bs}^{1/(1-4K)}$ [86]. This will make the conductance drop to zero at $T = 0$.

For temperatures larger than both the Kondo temperature and T_{bs}, the amplitudes for the Kondo interaction, the 2PB and the inelastic scattering remain weak. We can therefore obtain transport properties perturbatively. Though the conductance will be affected by both 2PB and inelastic scattering, these scatterings will in turn be unaffected by the Rashba interaction. Our interest is therefore solely in the contribution to δG from the Kondo interaction, which does become affected by the Rashba interaction.

The current operator is given by

$$I = \frac{e}{2}\partial_t \left(\psi_\uparrow^\dagger \psi_\uparrow - \psi_\downarrow^\dagger \psi_\downarrow \right), \tag{6.42}$$

or in the Rashba rotated basis,

$$I = \frac{e}{2}\partial_t \left(\Psi'^\dagger (\cos\theta \sigma^{z'} - \sin\theta \sigma^{y'}) \Psi' \right). \tag{6.43}$$

The part of the current operator that is due to the Kondo impurity can be shown to be

$$\begin{aligned}
\delta I = {} & \frac{ie}{4\pi a_0} \left(J_x + J_y' \right) \cos\theta \left(e^{i\left(2\sqrt{\pi K} - \lambda\right)\varphi(0)} S^+ - e^{-i\left(2\sqrt{\pi K} - \lambda\right)\varphi(0)} S^- \right) \\
& + \frac{ie}{4\pi a_0} \left(J_x - J_y' \right) \cos\theta \left(e^{i\left(2\sqrt{\pi K} + \lambda\right)\varphi(0)} S^- - e^{-i\left(2\sqrt{\pi K} + \lambda\right)\varphi(0)} S^+ \right) \\
& - \frac{e}{4\pi a_0} J_E \cos\theta e^{2i\sqrt{\pi K}\varphi(0)} S^z + \frac{e}{2\pi a_0 \sqrt{\pi K}} J_x \sin\theta : \partial_x \vartheta(0) e^{-i\sqrt{\pi}\lambda\varphi(0)}
\end{aligned} \tag{6.44}$$

in its bosonised form. In eq. (6.44), $\lambda = J_z'/(\pi v\sqrt{K})$ and the combined Pauli matrices in the impurity spin space are defined as $S^\pm = \left(S^x \pm i S^{y'}\right)$. The field conjugate to φ is denoted ϑ to distinguish it from the Rashba angle θ.

Using the Kubo formula will give the Kondo contribution to the conductivity as

$$\begin{aligned}\delta G &= \frac{1}{\omega}\int_0^\omega \mathrm{d}t e^{i\omega t}\left\langle\left[\delta I^\dagger(t),\delta I(0)\right]\right\rangle \\ &= -\left(\frac{e}{2}\left(J_x+J_y'\right)\cos\theta\right)^2 F\left(2\sqrt{K}-\lambda\right)\left(\frac{2\pi T}{D}\right)^{2\left(\sqrt{K}-\lambda/2\right)^2-2} \\ &\quad -\left(\frac{e}{2}\left(J_x-J_y'\right)\cos\theta\right)^2 F\left(2\sqrt{K}+\lambda\right)\left(\frac{2\pi T}{D}\right)^{2\left(\sqrt{K}+\lambda/2\right)^2-2} \\ &\quad -\left(\frac{e}{2}J_E\cos\theta\right)^2 F\left(2\sqrt{K}\right)\left(\frac{2\pi T}{D}\right)^{2K-2} - \left(\frac{e}{\pi\sqrt{K}}J_x\sin\theta\right)^2\tilde{F}(\lambda),\end{aligned} \tag{6.45}$$

where

$$F(x) = \frac{\left(\Gamma(x^2/4)\right)^2}{4\pi v^2\Gamma(x^2/2)} \tag{6.46}$$

and $\tilde{F}$ is a T-independent function of J_x, λ and K.

As pointed out in ref. [87], the Kubo formula rests on a perturbation expansion which in our case means that eq. (6.45) is only valid for $J^2 \ll \omega$. To study the dc limit $\omega \ll J^2 \ll T$ we will use a a semiclassical rate equation approximation where we assign classical probabilities for the states. For details, the reader is referred to Paper IV, and we will here merely state the result for the conductance correction in this limit:

$$\delta G = -\frac{e^2\cos^2\theta}{2T}\frac{4\gamma_0\gamma_0' + \left(\gamma_0+\gamma_0'\right)\left(\gamma_0^E+\tilde{\gamma}_0^E\right)+\tilde{\gamma}_0^E\gamma_0^E}{\gamma_0+\gamma_0'+\tilde{\gamma}_0^E}, \tag{6.47}$$

with the rates

$$\gamma_0 = \left(J_x + J_y'\right)^2 \frac{\left(\Gamma\left[(\sqrt{K}-\lambda/2)^2\right]\right)^2}{16\pi^2 a_0 v \Gamma\left[2(\sqrt{K}-\lambda/2)^2\right]} \left(\frac{2\pi T}{D}\right)^{2\left(\sqrt{K}-\lambda/2\right)^2-1} \tag{6.48}$$

$$\gamma_0' = \left(J_x - J_y'\right)^2 \frac{\left(\Gamma\left[(\sqrt{K}+\lambda/2)^2\right]\right)^2}{16\pi^2 a_0 v \Gamma\left[2(\sqrt{K}+\lambda/2)^2\right]} \left(\frac{2\pi T}{D}\right)^{2\left(\sqrt{K}+\lambda/2\right)^2-1} \tag{6.49}$$

$$\gamma_0^E = J_E^2 \frac{\left(\Gamma\left[K\right]\right)^2}{16\pi^2 a_0 v \Gamma\left[2K\right]} \left(\frac{2\pi T}{D}\right)^{2K-1} \tag{6.50}$$

$$\tilde{\gamma}_0^E = J_E^2 \frac{\tilde{F}(\lambda)}{4} \left(\frac{2\pi T}{D}\right)^{\lambda^2/2+1}. \tag{6.51}$$

Finally, to explore the dependence of the conductance on the Rashba interaction, we use the same formalism as in the calculation of the tunnelling conductance in section 3.4. The result for $\delta I = I - G_0 V$, G_0 being the quantum conductance e^2/h, is

$$\delta I \approx -e \sum_{j=-1}^{+1} \mathrm{Im}\Bigg\{ B\left(\frac{K_j + ieV}{2\pi T}, \frac{K_j - ieV}{2\pi T}\right) \times C_j \left(\frac{T}{D}\right)^{2K_j-1} \frac{\sin\left(\pi K_j - ieV/2T\right)}{\cos(\pi K_j)} \Bigg\}, \tag{6.52}$$

where we have defined $K_j \equiv (\sqrt{2} - j\lambda/2)^2$, $C_{\pm 1} \equiv c_\pm (J_x \pm J_y')^2$ and $C_0 \equiv c_0 J_E^2$, with $c_{\pm,0}$ constants depending on K, λ and θ.

With this we want to explore the Rashba dependence of δI, with experimentally relevant numbers for our parameters. We choose to consider an Mn^{2+} ion close to the edge of a HgTe QW [88]. Our calculation is based on a spin-1/2 impurity and it can be shown that the Mn^{2+}, though having spin $S = 5/2$, will at the quantum well interface have its higher spin components frozen out, leaving behind a spin-1/2 doublet [89]. The reader is referred to Paper IV for the estimates of the values of the Kondo couplings J_x, J_y and J_z and the Rashba strength α. We put $a_0 \approx 0.5$ nm [90], $v_F \approx 5.0 \times 10^5$ m/s [11] and $D \approx 300$ meV knigexp. The temperature dependence of the Kondo couplings can be estimated by performing an RG analysis of the coupling constants in eq. (6.52), renormalising until $l = \ln(D/T)$ reaches the chosen temperature

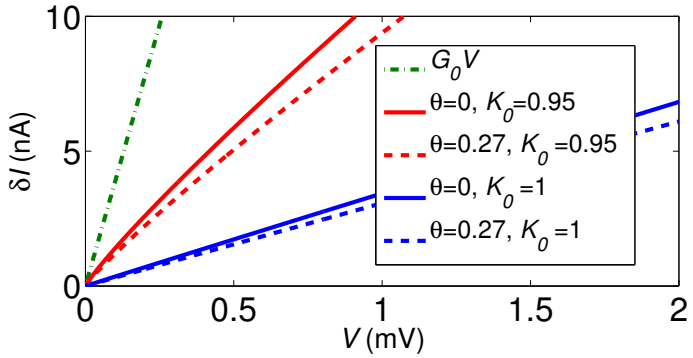

Figure 6.3

(here, $T = 30$ mK is chosen). The resulting $\delta I - V$ characteristic is plotted in Fig. 6.3.

7

Conclusions

In this thesis we have discussed aspects of some of the most novel and interesting developments in one-dimensional quantum physics. Helical conductors provide an excellent arena for the study of physics at the mesoscopic scale driven by relativistic spin-orbit interactions. In particular, we have had the opportunity to investigate some interesting aspects of effects from electron-electron interactions and disordered impurity scatterings in these spin-filtered one-dimensional conductors. Intriguing as they may be by themselves, theoretical investigations of new physics are predictions about the outcomes of experimental research, and in all of the cases studied in this thesis we have also made suggestions for experimental tests of our results.

We have shown that electron-electron interactions play a very important role in the physics of a one-dimensional helical conductor. For example, the tunnelling of edge electrons through a point-contact created by a gate voltage was shown to depend heavily on the strength of the dispersive scattering of the electrons in the system. Similarly, the ability for a disordered Rashba interaction to localise the edge states, and thereby destroying the quantum spin Hall state, was also found to depend on the dispersive scattering, in addition to the strength of the Rashba fluctuations themselves. In the case of a periodically modulated Rashba interaction along the edge, we showed that a localisation can occur already at moderate electron-electron interactions. This suggests that a gate-controlled modulated Rashba interaction may be used in a future device to switch the edge current on and off. The difference in interaction strength at which the two types of localisation occur opens up the intriguing possibility to study the transition between a Mott insulating phase, caused by the periodic Rashba modulation and the Anderson-

localised phase due to the interplay between a strong electron-electron interaction and a disordered Rashba interaction.

In our study of a magnetic impurity at a quantum spin Hall edge, we have also shown that in the case of combined Rashba and Kondo interactions, the Kondo temperature has a strong dependence on the magnitude of the Rashba interaction, electrically controllable by a gate voltage. The ability to control the Kondo effect experimentally may turn out to be an important tool in the further understanding of these systems. We also found a non-collinear interaction between the edge electrons and the impurity spin, which for certain configurations of the anisotropy of the Kondo couplings and the strengths of the electron-electron interactions and the Rashba coupling may cause a blocking of the Kondo effect. Finally, in the study of Anderson localisation in quasi-helical conductors, we were able to predict two metal-insulator transitions at different strengths of a magnetic field applied parallel to the conductor. This surprising result means that even a conductor which is localised at low magnetic fields can undergo a transition into a quasi-helical state at some finite magnetic field strength. The intermediate quasi-helical state was shown to be present even at quite strong disorder, an important finding for future manufacturing of quantum wires to be used as quasi-helical conductors.

The dispersive interaction between electrons plays a main role in all of the situations considered. This sets the quantum spin Hall insulators apart from ordinary quantum Hall systems, where by time-reversal symmetry breaking the dispersive scattering channel is killed off. Our results vividly show the importance of including a careful analysis of the dispersive electron interaction in the analysis of this new class of materials.

The subject of topological insulators is still new, and is developing rapidly. Many challenges lie ahead, perhaps especially in the area of interaction and disorder effects, the very subjects of this thesis. There are also many new materials that await a more thorough theoretical treatment, as well as a need for theoretical predictions for possible new topological insulators. Other fascinating areas that have are now beginning to draw attention are those involving heterostructures and interfaces between different kinds of topological materials.materials. Here much of the the inspiration draws from prospects to find zero-mode Majorana fermions when a helical conductor is in proximity to a superconductor. For a review of this, see ref. [91].

Experimentally, there are many challenges, in creating samples of different materials that can be experimentally tested for various features of topological insulators, in coming up with methods of measuring these, but also in inventing effective methods for manufacturing good samples

so that the reproducibility of experiments can be improved. There is still a long way to go before dissipationless edge currents can be exploited in small and energy-cheap devices.

The idea of using magnetic fields to produce quasi-helical conductors in quantum wires and carbon nanotubes is also something that may become increasingly important. Although there is no topological protection of the quasi-helical states, these conductors could still be used for spin-filtered transport [21]. More intriguingly, they could also offer the possibility for Cooper pair splitting [92], and, if in contact with a superconductor, they may be used to realise Majorana bound states at their ends [91, 93, 94], just as predicted for the quantum spin Hall edges, but experimentally much more easily available.

To conclude, helical conductors are physically interesting and potentially useful systems, where many things remain to be explored. The study of interaction and disorder in these conductors, the central topic of this thesis, is important for furthering our understanding of spin-orbit driven physics and to pave the way for the possible use of this type of conductors in future device technology.

A

Transformation between theories

In this appendix, the derivation of the transformation between the renormalised velocities and Luttinger liquid parameters of the theories above and in the gap are derived. We will go through the differences between the two theories, starting with the different g-ology coupling constants g_1, g_2 and g_4.

- For g_1, we will have both $g_{1\perp}$ and $g_{1\parallel}$ in the spinful LL. As is shown in ref. [40], one can permute the operators to put $g_{1\parallel}$ equal to $-g_{2\parallel}$, so that we can take it into account by changing $g_{2\parallel}$ to $g_{2\parallel} - g_{1\parallel}$ in the dispersion part of the Hamiltonian. In the helical LL, there is no backscattering allowed, and it is also not possible to have dispersive scattering of two electrons with the same spin. Thus, in the helical case, $g_{1\parallel} = g_{2\parallel} = 0$. When it comes to $g_{1\perp}$, the corresponding interaction is represented by a sine-Gordon term, present only in the spinful LL.

- For g_2, we just stated that $g_{2\parallel}$ will be combined with $g_{1\parallel}$ in the spinful LL, and put to zero in the helical LL. However, $g_{2\perp}$ is non-zero in both theories.

- For g_4, we have both $g_{4\perp}$ and $g_{4\parallel}$ in the spinful LL, but only $g_{4\parallel}$ in the helical LL. Electrons moving in the same direction have equal spins, so $g_{4\perp} = 0$ in the helical LL.

As explained before, when constructing the bosonised Hamiltonian, the main idea is to absorb the "g-ology" interactions in the K and u

parameters, with the exception of $g_{1\perp}$, thereby constructing a free bosonic theory from an interacting fermionic one. For this purpose, it is useful to define charge and spin versions of the coupling constants for dispersive and forward scattering:

$$g_\rho = g_{1\parallel} - g_{2\parallel} - g_{2\perp} \tag{A.1}$$
$$g_\sigma = g_{1\parallel} - g_{2\parallel} + g_{2\perp} \tag{A.2}$$
$$g_{4\rho} = g_{4\parallel} + g_{4\perp} \tag{A.3}$$
$$g_{4\sigma} = g_{4\parallel} - g_{4\perp}. \tag{A.4}$$

In the helical LL, $g_\rho = -g_\sigma$ and $g_{4\rho} = g_{4\sigma}$, since only $g_{2\perp}$ and $g_{4\parallel}$ are non-zero. We can connect the two theories by expressing this fact as

$$g_{2\perp} = \frac{g_\sigma - g_\rho}{2} \tag{A.5}$$
$$g_{4\parallel} = \frac{g_{4\rho} + g_{4\sigma}}{2}. \tag{A.6}$$

Next, we write down the definitions of K and u that allows us to use a free bosonic theory in the presence of forward and dispersive scatterings (plus spin parallel backward scattering):

$$K_\rho = \sqrt{\frac{1 + y_{4\rho}/2 + y_\rho/2}{1 + y_{4\rho}/2 - y_\rho/2}} \tag{A.7}$$
$$K_\sigma = \sqrt{\frac{1 + y_{4\sigma}/2 + y_\sigma/2}{1 + y_{4\sigma}/2 - y_\sigma/2}} \tag{A.8}$$
$$v_\rho = v_F\sqrt{(1 + y_{4\rho}/2)^2 - (y_\rho/2)^2} \tag{A.9}$$
$$v_\sigma = v_F\sqrt{(1 + y_{4\sigma}/2)^2 - (y_\sigma/2)^2}, \tag{A.10}$$

where we have defined $y \equiv g/(\pi v_F)$. The corresponding parameters in the helical theory are

$$K_H = \sqrt{\frac{1 + y_{4\perp}/2 + y_\rho/2}{1 + y_{4\rho}/2 - y_\rho/2}} = \sqrt{\frac{1 + \frac{y_{4\rho}+y_{4\sigma}}{4} - \frac{y_\sigma - y_\rho}{4}}{1 + \frac{y_{4\rho}+y_{4\sigma}}{4} + \frac{y_\sigma - y_\rho}{4}}} \tag{A.11}$$

$$v_H = v_F\sqrt{(1 + y_{4\parallel}/2)^2 - (y_{2\perp}/2)^2} = v_F\sqrt{\left(1 + \frac{y_{4\rho} + y_{4\sigma}}{4}\right)^2 - \left(\frac{y_\sigma - y_\rho}{4}\right)^2}, \tag{A.12}$$

where (A.5) and (A.6) was used. In order to write K_H and v_H as functions of $K_{\rho,\sigma}$ and $v_{\rho,\sigma}$, we first need to write down the y:s in terms of $K_{\rho,\sigma}$ and $v_{\rho,\sigma}$. The proper expressions are found to be

$$y_\rho = \frac{\pm(v_\rho - K_\rho^2 v_\rho)}{K_\rho v_F} \tag{A.13}$$

$$y_\sigma = \frac{\pm(v_\sigma - K_\sigma^2 v_\sigma)}{K_\sigma v_F} \tag{A.14}$$

$$v_\rho = \frac{\pm(v_\rho + K_\rho^2 v_\rho) - 2K_\rho v_F}{K_\rho v_F} \tag{A.15}$$

$$v_\sigma = \frac{\pm(v_\sigma + K_\sigma^2 v_\sigma) - 2K_\sigma v_F}{K_\sigma v_F}. \tag{A.16}$$

What remains is just to write

$$\begin{aligned} K_H &= \sqrt{\frac{4 + y_{4\rho} + y_{4\sigma} - y_\sigma + y_\rho}{4 + y_{4\rho} + y_{4\sigma} + y_\sigma - y_\rho}} \\ &= \Bigg[\Bigg(4 + \frac{1}{K_\rho v_F}\left(\pm(v_\rho + K_\rho^2 v_\rho) - 2K_\rho v_F\right) + \frac{1}{K_\sigma v_F}\left(\pm(v_\sigma + K_\sigma^2 v_\sigma) - 2K_\sigma v_F\right) \\ &\qquad - \frac{\pm(v_\sigma - K_\sigma^2 v_\sigma)}{K_\sigma v_F} + \frac{\pm(v_\rho - K_\rho^2 v_\rho)}{K_\rho v_F}\Bigg) \\ &\Bigg/ \Bigg(4 + \frac{1}{K_\rho v_F}\left(\pm(v_\rho + K_\rho^2 v_\rho) - 2K_\rho v_F\right) + \frac{1}{K_\sigma v_F}\left(\pm(v_\sigma + K_\sigma^2 v_\sigma) - 2K_\sigma v_F\right) \\ &\qquad + \frac{\pm(v_\sigma - K_\sigma^2 v_\sigma)}{K_\sigma v_F} - \frac{\pm(v_\rho - K_\rho^2 v_\rho)}{K_\rho v_F}\Bigg)\Bigg]^{1/2} \\ &= \sqrt{\frac{K_\rho(K_\rho K_\sigma v_\rho + v_\sigma)}{K_\sigma(K_\rho K_\sigma v_\sigma + v_\rho)}}, \end{aligned} \tag{A.17}$$

where the last equality is obtained by noting that we must choose all $\pm$ postive in order for K_H to make physical sense. Similarly for v_H,

$$
\begin{aligned}
v_H &= v_F \sqrt{\left(1 + \frac{y_{4\rho} + y_{4\sigma}}{4}\right)^2 - \left(\frac{y_\sigma - y_\rho}{4}\right)^2} \\
&= \frac{v_F}{2} \sqrt{\frac{(K_\rho K_\sigma v_\rho + v_\sigma)(v_\rho + K_\rho K_\sigma v_\sigma)}{K_\rho K_\sigma v_F^2}} \\
&= \frac{1}{2} \sqrt{u_\rho^2 + u_\sigma^2 + v_\rho v_\sigma \left(K_\rho K_\sigma + \frac{1}{K_\rho K_\sigma}\right)}. \quad \text{(A.18)}
\end{aligned}
$$

B

Derivation of the second order RG equations for the Kondo couplings

This Appendix is devoted to the calculation of the second order RG equations for the Kondo couplings in chapter 6. Our starting point is the second-order cumulant expansion

$$
\begin{aligned}
-\frac{1}{2}\left(\left\langle S_K^2\right\rangle_f-\langle S_K\rangle_f^2\right)=-\frac{1}{2}\int \mathrm{d}\tau\mathrm{d}\tau'\Bigg\{ & \\
\frac{A^2}{a_0^2}\left(\left\langle\cos[2\sqrt{\pi}\varphi(\tau)]\cos[2\sqrt{\pi}\varphi(\tau')]\right\rangle-\left\langle\cos[2\sqrt{\pi}\varphi(\tau)]\right\rangle\left\langle\cos[2\sqrt{\pi}\varphi(\tau')]\right\rangle\right) & \\
+\frac{B^2}{a_0^2}\left(\left\langle\sin[2\sqrt{\pi}\varphi(\tau)]\sin[2\sqrt{\pi}\varphi(\tau')]\right\rangle-\left\langle\sin[2\sqrt{\pi}\varphi(\tau)]\right\rangle\left\langle\sin[2\sqrt{\pi}\varphi(\tau')]\right\rangle\right) & \\
-\frac{C^2}{v^2}\left(\langle\partial_\tau\varphi(\tau)\partial_{\tau'}\varphi(\tau')\rangle-\langle\partial_\tau\varphi(\tau)\rangle\langle\partial_{\tau'}\varphi(\tau')\rangle\right) & \\
+\frac{AB}{a_0^2}\left(\left\langle\cos[2\sqrt{\pi}\varphi(\tau)]\sin[2\sqrt{\pi}\varphi(\tau')]\right\rangle-\left\langle\cos[2\sqrt{\pi}\varphi(\tau)]\right\rangle\left\langle\sin[2\sqrt{\pi}\varphi(\tau')]\right\rangle\right) & \\
+\frac{iAC}{a_0v}\left(\left\langle\cos[2\sqrt{\pi}\varphi(\tau)]\partial_{\tau'}\varphi(\tau')\right\rangle-\left\langle\cos[2\sqrt{\pi}\varphi(\tau)]\right\rangle\langle\partial_{\tau'}\varphi(\tau')\rangle\right) & \\
+\frac{iBC}{a_0v}\left(\left\langle\sin[2\sqrt{\pi}\varphi(\tau)]\partial_{\tau'}\varphi(\tau')\right\rangle-\left\langle\sin[2\sqrt{\pi}\varphi(\tau)]\right\rangle\langle\partial_{\tau'}\varphi(\tau')\rangle\right) & \\
+\frac{BA}{a_0^2}\ldots+\frac{iCA}{a_0v}\ldots+\frac{iCB}{a_0v}\ldots\Bigg\} & \quad \text{(B.1)}
\end{aligned}
$$

of eq. (6.19).

B.1 The cumulant expansion

We start with the term proportional to A^2 and work our way through all nine terms.

B.1.1 First term (A^2)

The term proportional to A^2 is

$$
\begin{aligned}
&-\frac{1}{2}\int \mathrm{d}\tau\mathrm{d}\tau' \frac{A^2}{a_0^2}\Big(\big\langle \cos[2\sqrt{\pi}\varphi(\tau)]\cos[2\sqrt{\pi}\varphi(\tau')]\big\rangle \\
&\qquad\qquad - \big\langle \cos[2\sqrt{\pi}\varphi(\tau)]\big\rangle \big\langle \cos[2\sqrt{\pi}\varphi(\tau')]\big\rangle \Big) \\
&\quad = -\frac{1}{2}\int \mathrm{d}\tau\mathrm{d}\tau' \frac{A^2}{4a_0^2}\Bigg[\Big(e^{2i\sqrt{\pi}(\varphi_s(\tau)+\varphi_s(\tau'))} \Big\langle e^{2i\sqrt{\pi}\left(\varphi_f(\tau)+\varphi_f(\tau')\right)}\Big\rangle \\
&\qquad + e^{2i\sqrt{\pi}(\varphi_s(\tau)-\varphi_s(\tau'))} \Big\langle e^{2i\sqrt{\pi}\left(\varphi_f(\tau)-\varphi_f(\tau')\right)}\Big\rangle + H.c.\Big) \\
&\qquad - \Big(e^{2i\sqrt{\pi}(\varphi_s(\tau)+\varphi_s(\tau'))} \Big\langle e^{2i\sqrt{\pi}\varphi_f(\tau)}\Big\rangle \Big\langle e^{2i\sqrt{\pi}\varphi_f(\tau')}\Big\rangle \\
&\quad + e^{2i\sqrt{\pi}(\varphi_s(\tau)-\varphi_s(\tau'))} \Big\langle e^{2i\sqrt{\pi}\varphi_f(\tau)}\Big\rangle \Big\langle e^{-2i\sqrt{\pi}\varphi_f(\tau')}\Big\rangle + H.c.\Big) \\
&= -\frac{1}{2}\int \mathrm{d}\tau\mathrm{d}\tau' \frac{A^2}{4a_0^2}\Bigg[\\
&\quad \times e^{2i\sqrt{\pi}(\varphi_s(\tau)+\varphi_s(\tau'))} \left(e^{-2\pi\left\langle \left(\varphi_f(\tau)+\varphi_f(\tau')\right)^2\right\rangle} - e^{-2\pi\left(\left\langle\varphi_f^2(\tau)\right\rangle+\left\langle\varphi_f^2(\tau')\right\rangle\right)}\right) \\
&+ e^{2i\sqrt{\pi}(\varphi_s(\tau)-\varphi_s(\tau'))} \left(e^{-2\pi\left\langle \left(\varphi_f(\tau)-\varphi_f(\tau')\right)^2\right\rangle} - e^{-2\pi\left(\left\langle\varphi_f^2(\tau)\right\rangle+\left\langle\varphi_f^2(\tau')\right\rangle\right)}\right) + H.c.\Bigg] \\
&= -\frac{1}{2}\int \mathrm{d}\tau\mathrm{d}\tau' \frac{A^2}{2a_0^2}\Bigg[\\
&\quad \times \cos\left[2\sqrt{\pi}\left(\varphi_s(\tau)+\varphi_s(\tau')\right)\right] e^{-4\pi\left\langle\varphi_f^2(\tau)\right\rangle} \left(e^{-4\pi\left\langle\varphi_f(\tau)\varphi_f(\tau')\right\rangle} - 1\right) \\
&+ \cos\left[2\sqrt{\pi}\left(\varphi_s(\tau)-\varphi_s(\tau')\right)\right] e^{-4\pi\left\langle\varphi_f^2(\tau)\right\rangle} \left(e^{+4\pi\left\langle\varphi_f(\tau)\varphi_f(\tau')\right\rangle} - 1\right)\Bigg]. \qquad \text{(B.2)}
\end{aligned}
$$

The correlation functions to be calculated are $\left\langle\varphi_f^2(\tau)\right\rangle$ and $\langle\varphi_f(\tau)\varphi_f(\tau')\rangle$. Let us begin with the second one:

$$\langle\varphi_f(\tau)\varphi(\tau')\rangle = \int \mathcal{D}\varphi_f \exp\left[-\int_f \frac{\mathrm{d}\omega}{2\pi}\frac{|\omega|}{K}|\varphi_f|^2\right]\varphi_f(\tau)\varphi(\tau')$$
$$= \int \mathcal{D}\varphi_f \exp\left[-\int_f \frac{\mathrm{d}\omega}{2\pi}\frac{|\omega|}{K}|\varphi_f|^2\right]\int_f \frac{\mathrm{d}\omega}{2\pi}e^{-i\omega\tau}\varphi(\omega)\int_f \frac{\mathrm{d}\omega'}{2\pi}e^{-i\omega'\tau'}\varphi(\omega')$$
$$= \int_f \frac{\mathrm{d}\omega\mathrm{d}\omega'}{(2\pi)^2}e^{-i(\omega\tau+\omega'\tau')}\exp\left[-\int_f \frac{\mathrm{d}\omega}{2\pi}\frac{|\omega|}{K}|\varphi_f|^2\right]\varphi(\omega)\varphi(\omega')$$
$$\propto \int_f \frac{\mathrm{d}\omega\mathrm{d}\omega'}{2\pi}e^{-i(\omega\tau+\omega'\tau')}\frac{K}{2|\omega|}\delta(\omega+\omega') = \frac{K}{2}\int_{\Lambda/b<|\omega|<\Lambda}\frac{\mathrm{d}\omega}{2\pi}e^{-i\omega(\tau-\tau')}|\omega|^{-1}$$
$$= \frac{K}{2\pi}\int_{\Lambda/b}^{\Lambda}\frac{\mathrm{d}\omega}{\omega}e^{-i\omega(\tau-\tau')}. \quad \text{(B.3)}$$

The correlation $\left\langle\varphi_f^2(\tau)\right\rangle$ is obtained from this by setting $\tau = \tau'$:

$$\left\langle\varphi_f^2(\tau)\right\rangle = \frac{K}{2\pi}\int_{\Lambda/b}^{\Lambda}\frac{\mathrm{d}\omega}{\omega} = \frac{K}{2\pi}\ln b. \quad \text{(B.4)}$$

Keeping $\tau \neq \tau'$, the result is approximately, for large $\tau-\tau'$, a generalized Bessel function of the 0:th order:

$$\frac{K}{2\pi}\int_{\Lambda/b}^{\Lambda}\frac{\mathrm{d}\omega}{\omega}e^{-i\omega(\tau-\tau')} \approx \frac{K}{2\pi}K_0\left(\frac{\Lambda(\tau-\tau')}{b}\right), \quad \text{(B.5)}$$

The Bessel function, with $K_0(1) = 0.5$, falls off exponentially for sufficiently large $\tau-\tau'$. Now, in eq. (B.2) both cosine terms are proportional to

$$\left(e^{\pm 4\pi\left\langle\varphi_f(\tau)\varphi_f(\tau')\right\rangle} - 1\right), \quad \text{(B.6)}$$

which will rapidly approach $1-1=0$ as $\Lambda(\tau-\tau')/b$ grows. A good approximation for eq. (B.2) is thus obtained by limiting $\tau-\tau'$ by an upper cutoff b/Λ, and letting $\tau \to \tau'$ in the correlation function:

$$\langle\varphi_f(\tau)\varphi_f(\tau')\rangle \approx \left\langle\varphi_f^2(\tau)\right\rangle = \frac{K}{2\pi}\ln b. \quad \text{(B.7)}$$

We also introduce the coordinates $s = \tau-\tau'$ and $T = (\tau+\tau')/2$. Then

$$\varphi_s(\tau) + \varphi_s(\tau') = \varphi_s(T+s/2) + \varphi_s(T-s/2) \approx 2\varphi_s(T), \quad \text{(B.8)}$$

for small s. Also,

$$\varphi_s(\tau) - \varphi_s(\tau') = \varphi_s(T + s/2) - \varphi_s(T - s/2) \approx s\partial_T \varphi_s(T). \tag{B.9}$$

With this, the cosines can be approximated by

$$\cos\left[2\sqrt{\pi}\left(\varphi_s(\tau) + \varphi_s(\tau')\right)\right] \approx \cos\left[4\sqrt{\pi}\left(\varphi_s(T)\right)\right] \tag{B.10}$$

and

$$\cos\left[2\sqrt{\pi}\left(\varphi_s(\tau) - \varphi_s(\tau')\right)\right] \approx 1. \tag{B.11}$$

The first second order term of the cumulant expansion is thus approximately

$$\begin{aligned}
&-\frac{1}{2}\int \mathrm{d}\tau\mathrm{d}\tau' \frac{A^2}{a_0^2}\Big(\left\langle \cos[2\sqrt{\pi}\varphi(\tau)]\cos[2\sqrt{\pi}\varphi(\tau')]\right\rangle \\
&\qquad\qquad - \left\langle \cos[2\sqrt{\pi}\varphi(\tau)]\right\rangle \left\langle \cos[2\sqrt{\pi}\varphi(\tau')]\right\rangle \Big) \\
&\approx -\frac{1}{2}\int_0^{b/\Lambda} \mathrm{d}s \int_0^{\beta} \mathrm{d}T \frac{A^2}{2a_0^2}\Big[\cos\left[4\sqrt{\pi}\varphi_s(T)\right]\left(e^{-8\pi\frac{K\ln b}{2\pi}} - e^{-4\pi\frac{K\ln b}{2\pi}}\right) \\
&\qquad\qquad + \left(1 - e^{-4\pi\frac{K\ln b}{2\pi}}\right)\Big] \\
&= -\frac{1}{2}\frac{b}{\Lambda}\frac{A^2}{2a_0^2}\int \mathrm{d}T \cos\left[4\sqrt{\pi}\varphi_s(T)\right]\left(\left(\frac{1}{b}\right)^{4K} - \left(\frac{1}{b}\right)^{2K}\right) + \text{const.},
\end{aligned} \tag{B.12}$$

where const. denotes field-independent terms. The $\cos\left[4\sqrt{\pi}\varphi_s(T)\right]$ term turns out to be RG-irrelevant, and it follows that the full A^2 term is irrelevant.

B.1.2 Second term (B^2)

The term proportional to B^2 is

$$
\begin{aligned}
&-\frac{1}{2}\int \mathrm{d}\tau\mathrm{d}\tau' \frac{B^2}{a_0^2}\Big(\big\langle \sin[2\sqrt{\pi}\varphi(\tau)]\sin[2\sqrt{\pi}\varphi(\tau')]\big\rangle \\
&\qquad\qquad - \big\langle \sin[2\sqrt{\pi}\varphi(\tau)]\big\rangle \big\langle \sin[2\sqrt{\pi}\varphi(\tau')]\big\rangle \Big) \\
&\quad = -\frac{1}{2}\int \mathrm{d}\tau\mathrm{d}\tau' \frac{B^2}{-4a_0^2}\Bigg[\Big(e^{2i\sqrt{\pi}(\varphi_s(\tau)+\varphi_s(\tau'))}\Big\langle e^{2i\sqrt{\pi}\left(\varphi_f(\tau)+\varphi_f(\tau')\right)}\Big\rangle \\
&\qquad - e^{2i\sqrt{\pi}(\varphi_s(\tau)-\varphi_s(\tau'))}\Big\langle e^{2i\sqrt{\pi}\left(\varphi_f(\tau)-\varphi_f(\tau')\right)}\Big\rangle + H.c.\Big) \\
&\qquad - \Big(e^{2i\sqrt{\pi}(\varphi_s(\tau)+\varphi_s(\tau'))}\Big\langle e^{2i\sqrt{\pi}\varphi_f(\tau)}\Big\rangle\Big\langle e^{2i\sqrt{\pi}\varphi_f(\tau')}\Big\rangle \\
&\quad - e^{2i\sqrt{\pi}(\varphi_s(\tau)-\varphi_s(\tau'))}\Big\langle e^{2i\sqrt{\pi}\varphi_f(\tau)}\Big\rangle\Big\langle e^{-2i\sqrt{\pi}\varphi_f(\tau')}\Big\rangle + H.c.\Big) \\
&= \frac{1}{2}\int \mathrm{d}\tau\mathrm{d}\tau' \frac{B^2}{4a_0^2}\Bigg[\\
&\times e^{2i\sqrt{\pi}(\varphi_s(\tau)+\varphi_s(\tau'))}\left(e^{-2\pi\left\langle\left(\varphi_f(\tau)+\varphi_f(\tau')\right)^2\right\rangle} - e^{-2\pi\left(\left\langle\varphi_f^2(\tau)\right\rangle+\left\langle\varphi_f^2(\tau')\right\rangle\right)}\right) \\
&- e^{2i\sqrt{\pi}(\varphi_s(\tau)-\varphi_s(\tau'))}\left(e^{-2\pi\left\langle\left(\varphi_f(\tau)-\varphi_f(\tau')\right)^2\right\rangle} - e^{-2\pi\left(\left\langle\varphi_f^2(\tau)\right\rangle+\left\langle\varphi_f^2(\tau')\right\rangle\right)}\right) + H.c.\Bigg] \\
&= \frac{1}{2}\int \mathrm{d}\tau\mathrm{d}\tau' \frac{B^2}{2a_0^2}\Bigg[\\
&\quad \times \cos\left[2\sqrt{\pi}\left(\varphi_s(\tau)+\varphi_s(\tau')\right)\right] e^{-4\pi\left\langle\varphi_f^2(\tau)\right\rangle}\left(e^{-4\pi\left\langle\varphi_f(\tau)\varphi_f(\tau')\right\rangle}-1\right) \\
&\quad - \cos\left[2\sqrt{\pi}\left(\varphi_s(\tau)-\varphi_s(\tau')\right)\right] e^{-4\pi\left\langle\varphi_f^2(\tau)\right\rangle}\left(e^{+4\pi\left\langle\varphi_f(\tau)\varphi_f(\tau')\right\rangle}-1\right)\Bigg].
\end{aligned}
\tag{B.13}
$$

By comparison with the A^2 term we see that this term is also irrelevant.

B.1.3 Third term (C^2)

The term proportional to C^2 vanishes, since

$$
\begin{aligned}
&\frac{1}{2}\int \mathrm{d}\tau\mathrm{d}\tau' \frac{C^2}{v^2}\left(\left\langle\partial_\tau\varphi(\tau)\partial_{\tau'}\varphi(\tau')\right\rangle - \left\langle\partial_\tau\varphi(\tau)\right\rangle\left\langle\partial_{\tau'}\varphi(\tau')\right\rangle\right) \\
&\quad = \frac{1}{2}\int \mathrm{d}\tau\mathrm{d}\tau' \frac{C^2}{v^2}\left(\partial_\tau\varphi_s(\tau)\partial_{\tau'}\varphi_s(\tau') - \partial_\tau\varphi_s(\tau)\partial_{\tau'}\varphi_s(\tau')\right) = 0.
\end{aligned}
\tag{B.14}
$$

B.1.4 Fourth term (AB)

The term proportional to AB is

$$
\begin{aligned}
&-\frac{1}{2}\int \mathrm{d}\tau\mathrm{d}\tau' \frac{AB}{a_0^2}\Big(\big\langle \cos[2\sqrt{\pi}\varphi(\tau)]\sin[2\sqrt{\pi}\varphi(\tau')]\big\rangle \\
&\qquad\qquad - \big\langle \cos[2\sqrt{\pi}\varphi(\tau)]\big\rangle \big\langle \sin[2\sqrt{\pi}\varphi(\tau')]\big\rangle \Big) \\
&\quad = -\int \mathrm{d}\tau\mathrm{d}\tau' \frac{AB}{8ia_0^2}\Bigg[\Big(e^{2i\sqrt{\pi}(\varphi_s(\tau)+\varphi_s(\tau'))} \Big\langle e^{2i\sqrt{\pi}\left(\varphi_f(\tau)+\varphi_f(\tau')\right)}\Big\rangle \\
&\qquad - e^{2i\sqrt{\pi}(\varphi_s(\tau)-\varphi_s(\tau'))} \Big\langle e^{2i\sqrt{\pi}\left(\varphi_f(\tau)-\varphi_f(\tau')\right)}\Big\rangle - H.c.\Big) \\
&\qquad - \Big(e^{2i\sqrt{\pi}(\varphi_s(\tau)+\varphi_s(\tau'))} \Big\langle e^{2i\sqrt{\pi}\varphi_f(\tau)}\Big\rangle \Big\langle e^{2i\sqrt{\pi}\varphi_f(\tau')}\Big\rangle \\
&\quad - e^{2i\sqrt{\pi}(\varphi_s(\tau)-\varphi_s(\tau'))} \Big\langle e^{2i\sqrt{\pi}\varphi_f(\tau)}\Big\rangle \Big\langle e^{-2i\sqrt{\pi}\varphi_f(\tau')}\Big\rangle - H.c.\Big) \\
&= -\int \mathrm{d}\tau\mathrm{d}\tau' \frac{AB}{8ia_0^2}\Bigg[\\
&\quad \times e^{2i\sqrt{\pi}(\varphi_s(\tau)+\varphi_s(\tau'))} \left(e^{-2\pi\left\langle \left(\varphi_f(\tau)+\varphi_f(\tau')\right)^2\right\rangle} - e^{-2\pi\left(\left\langle\varphi_f^2(\tau)\right\rangle+\left\langle\varphi_f^2(\tau')\right\rangle\right)}\right) \\
&- e^{2i\sqrt{\pi}(\varphi_s(\tau)-\varphi_s(\tau'))} \left(e^{-2\pi\left\langle \left(\varphi_f(\tau)-\varphi_f(\tau')\right)^2\right\rangle} - e^{-2\pi\left(\left\langle\varphi_f^2(\tau)\right\rangle+\left\langle\varphi_f^2(\tau')\right\rangle\right)}\right) - H.c.\Bigg] \\
&= -\int \mathrm{d}\tau\mathrm{d}\tau' \frac{AB}{4a_0^2}\Bigg[\\
&\quad \times \sin\left[2\sqrt{\pi}\left(\varphi_s(\tau)+\varphi_s(\tau')\right)\right] e^{-4\pi\left\langle\varphi_f^2(\tau)\right\rangle} \left(e^{-4\pi\left\langle\varphi_f(\tau)\varphi_f(\tau')\right\rangle} - 1\right) \\
&\quad - \sin\left[2\sqrt{\pi}\left(\varphi_s(\tau)-\varphi_s(\tau')\right)\right] e^{-4\pi\left\langle\varphi_f^2(\tau)\right\rangle} \left(e^{+4\pi\left\langle\varphi_f(\tau)\varphi_f(\tau')\right\rangle} - 1\right)\Bigg].
\end{aligned}
\tag{B.15}
$$

By comparison with the A^2 term, we see that the small-s approximation, where we let $\tau \to \tau'$ is good here too. The sines can thus be approximated as

$$
\sin\left[2\sqrt{\pi}\left(\varphi_s(\tau)+\varphi_s(\tau')\right)\right] \approx \sin\left[4\sqrt{\pi}\left(\varphi_s(T)\right)\right] \tag{B.16}
$$

and

$$
\sin\left[2\sqrt{\pi}\left(\varphi_s(\tau)-\varphi_s(\tau')\right)\right] \approx 2\sqrt{\pi}s\partial_T\varphi_s(T). \tag{B.17}
$$

The fourth second-order term of the cumulant expansion is thus approximately given by

$$
\begin{aligned}
&-\frac{1}{2}\int \mathrm{d}\tau\mathrm{d}\tau' \frac{AB}{a_0^2}\Big(\left\langle \cos[2\sqrt{\pi}\varphi(\tau)]\sin[2\sqrt{\pi}\varphi(\tau')]\right\rangle \\
&\qquad\qquad - \left\langle \cos[2\sqrt{\pi}\varphi(\tau)]\right\rangle \left\langle \sin[2\sqrt{\pi}\varphi(\tau')]\right\rangle \Big) \\
&\approx -\int_0^{b/\Lambda}\mathrm{d}s\int_0^{\beta}\mathrm{d}T\frac{AB}{4a_0^2}\Big[\sin\left[4\sqrt{\pi}\varphi_s(T)\right]\left(e^{-8\pi\frac{K\ln b}{2\pi}}-e^{-4\pi\frac{K\ln b}{2\pi}}\right) \\
&\qquad\qquad - 2\sqrt{\pi}s\partial_T\varphi_s(T)\left(1-e^{-4\pi\frac{K\ln b}{2\pi}}\right)\Big] \\
&= -\frac{AB}{4a_0^2}\int \mathrm{d}T\Big[\frac{b}{\Lambda}\sin\left[4\sqrt{\pi}\varphi_s(T)\right]\left(\left(\frac{1}{b}\right)^{4K}-\left(\frac{1}{b}\right)^{2K}\right) \\
&\qquad\qquad - 2\sqrt{\pi}\frac{b^2}{2\Lambda^2}\partial_T\varphi_s(T)\left(1-\left(\frac{1}{b}\right)^{2K}\right)\Big]. \qquad \text{(B.18)}
\end{aligned}
$$

The $\sin\left[4\sqrt{\pi}\varphi_s(T)\right]$ term can be shown to be RG-irrelevant, (just as the cos-term in eq. (B.12)), so the relevant contribution to the cumulant expansion is

$$
\frac{AB\sqrt{\pi}}{4v^2}\int \mathrm{d}T\partial_T\varphi_s(T)\left(\left(\frac{1}{b}\right)^{-2}-\left(\frac{1}{b}\right)^{2K-2}\right), \qquad \text{(B.19)}
$$

where the relation $\Lambda = v/a_0$ between the high frequency and the small distance cutoffs have been used.

Before moving to the fifth term, let us examine the term proportional to BA. First of all, $AB = J_xJ_y'S^xS^{y'}/\pi + J_xJ_ES^xS^{z'}/\pi$, which means that $BA = -AB$ since the S matrices anticommute. However, the relevant part of eq. (B.15) is

$$
\begin{aligned}
&\int \mathrm{d}\tau\mathrm{d}\tau'\frac{AB}{8ia_0^2}e^{2i\sqrt{\pi}(\varphi_s(\tau)-\varphi_s(\tau'))}e^{-4\pi\left\langle\varphi_f^2(\tau)\right\rangle}\left(e^{4\pi\left\langle\varphi_f(\tau)\varphi_f(\tau')\right\rangle}-1\right)-H.c. \\
&\qquad = \int \mathrm{d}\tau\mathrm{d}\tau'\frac{AB}{4a_0^2}\sin\left[2\sqrt{\pi}\left(\varphi_s(\tau)-\varphi_s(\tau')\right)\right]e^{-4\pi\left\langle\varphi_f^2(\tau)\right\rangle} \\
&\qquad\qquad\qquad \times\left(e^{4\pi\left\langle\varphi_f(\tau)\varphi_f(\tau')\right\rangle}-1\right), \qquad \text{(B.20)}
\end{aligned}
$$

whereas the corresponding term in the BA term is instead

$$\int \mathrm{d}\tau\mathrm{d}\tau' \frac{BA}{8ia_0^2} e^{2i\sqrt{\pi}(\varphi_s(\tau')-\varphi_s(\tau))} e^{-4\pi\left\langle\varphi_f^2(\tau)\right\rangle} \left(e^{4\pi\left\langle\varphi_f(\tau')\varphi_f(\tau)\right\rangle}-1\right) - H.c.$$
$$= -\int \mathrm{d}\tau\mathrm{d}\tau' \frac{AB}{4a_0^2} \sin\left[2\sqrt{\pi}\left(\varphi_s(\tau')-\varphi_s(\tau)\right)\right] e^{-4\pi\left\langle\varphi_f^2(\tau)\right\rangle} \times \left(e^{4\pi\left\langle\varphi_f(\tau')\varphi_f(\tau)\right\rangle}-1\right). \quad \text{(B.21)}$$

From eq. (B.9), we see that $\phi_s(\tau') - \phi_s(\tau) \approx -s\partial_T\varphi_s(T)$ and so, the equivalence to eq. (B.17) for the BA term is

$$\sin\left[2\sqrt{\pi}\left(\varphi_s(\tau')-\varphi_s(\tau)\right)\right] \approx -2\sqrt{\pi}s\partial_T\varphi_s(T). \quad \text{(B.22)}$$

Thus, the relative minus sign between eq. (B.17) and eq. (B.22) eliminates the one between AB and BA, and the two terms have been shown to be equal.

B.1.5 Fifth term (AC)

The term proportional to AC is

$$-\frac{1}{2}\int \mathrm{d}\tau\mathrm{d}\tau' \frac{iAC}{a_0 v}\left(\left\langle\cos[2\sqrt{\pi}\varphi(\tau)]\partial_{\tau'}\varphi(\tau')\right\rangle - \left\langle\cos[2\sqrt{\pi}\varphi(\tau)]\right\rangle\left\langle\partial_{\tau'}\varphi(\tau')\right\rangle\right)$$
$$= -\int \mathrm{d}\tau\mathrm{d}\tau' \frac{iAC}{2a_0 v}\Big\{ \left\langle\cos[2\sqrt{\pi}\varphi(\tau)]\right\rangle \partial_{\tau'}\varphi_s(\tau') - \left\langle\cos[2\sqrt{\pi}\varphi(\tau)]\right\rangle \partial_{\tau'}\varphi_s(\tau')$$
$$+ \left\langle\cos[2\sqrt{\pi}\varphi(\tau)]\partial_{\tau'}\varphi_f(\tau')\right\rangle - \left\langle\cos[2\sqrt{\pi}\varphi(\tau)]\right\rangle\left\langle\partial_{\tau'}\varphi_f(\tau')\right\rangle \Big\}$$
$$= -\int \mathrm{d}\tau\mathrm{d}\tau' \frac{iAC}{2a_0 v}\left\langle\cos[2\sqrt{\pi}\varphi(\tau)]\partial_{\tau'}\varphi_f(\tau')\right\rangle, \quad \text{(B.23)}$$

since $\langle\partial_\tau\varphi_f(\tau)\rangle = 0$. The correlation function can then be rewritten as

$$\begin{aligned}
\left\langle \cos[2\sqrt{\pi}\varphi_f(\tau)]\partial_{\tau'}\varphi(\tau')\right\rangle &= \lim_{\epsilon\to 0}\frac{1}{2i\epsilon\sqrt{\pi}}\partial_{\tau'}\left\langle e^{2i\epsilon\sqrt{\pi}\varphi_f(\tau')}\cos[2\sqrt{\pi}\varphi(\tau)]\right\rangle \\
&= \lim_{\epsilon\to 0}\frac{1}{4i\epsilon\sqrt{\pi}}\Big\{ e^{2i\sqrt{\pi}\varphi_s(\tau)}\partial_{\tau'}\left\langle e^{2i\epsilon\sqrt{\pi}\varphi_f(\tau')}e^{2i\sqrt{\pi}\varphi_f(\tau)}\right\rangle \\
&\quad + e^{-2i\sqrt{\pi}\varphi_s(\tau)}\partial_{\tau'}\left\langle e^{2i\epsilon\sqrt{\pi}\varphi_f(\tau')}e^{-2i\sqrt{\pi}\varphi_f(\tau)}\right\rangle\Big\} \\
&= \lim_{\epsilon\to 0}\frac{1}{4i\epsilon\sqrt{\pi}}\Big\{ e^{2i\sqrt{\pi}\varphi_s(\tau)}\partial_{\tau'}e^{-2\pi\left\langle\left(\epsilon\varphi_f(\tau')+\varphi_f(\tau)\right)^2\right\rangle} \\
&\quad + e^{-2i\sqrt{\pi}\varphi_s(\tau)}\partial_{\tau'}e^{-2\pi\left\langle\left(\epsilon\varphi_f(\tau')-\varphi_f(\tau)\right)^2\right\rangle}\Big\} \\
= \lim_{\epsilon\to 0}\frac{1}{4i\epsilon\sqrt{\pi}}\Big\{ &(-4\pi\epsilon)\partial_{\tau'}\left\langle\varphi_f(\tau')\varphi_f(\tau)\right\rangle e^{2i\sqrt{\pi}\varphi_s(\tau)}e^{-2\pi\left(\left\langle\varphi_f^2(\tau)\right\rangle+2\epsilon\left\langle\varphi_f(\tau')\varphi_f(\tau)\right\rangle\right)} \\
&+ (4\pi\epsilon)\partial_{\tau'}\left\langle\varphi_f(\tau')\varphi_f(\tau)\right\rangle e^{-2i\sqrt{\pi}\varphi_s(\tau)}e^{-2\pi\left(\left\langle\varphi_f^2(\tau)\right\rangle-2\epsilon\left\langle\varphi_f(\tau')\varphi_f(\tau)\right\rangle\right)}\Big\} \\
&= -2\sqrt{\pi}\sin[2\sqrt{\pi}\varphi_s(\tau)]\partial_{\tau'}\left\langle\varphi_f(\tau')\varphi_f(\tau)\right\rangle e^{-2\pi\left\langle\varphi_f^2(\tau)\right\rangle}. \quad \text{(B.24)}
\end{aligned}$$

Next, we calculate the derivative of the correlation function in the last line of eq. (B.24). We make the same variable substitution as before, from τ and τ' to $s=\tau-\tau'$ and $T=(\tau+\tau')/2$. Then $G(\tau'-\tau)=\langle\varphi_f(\tau')\varphi_f(\tau)\rangle$ is a function of s and the derivative is

$$\frac{\partial}{\partial\tau'}=\frac{\partial}{\partial s}\frac{\partial s}{\partial\tau'}=-\frac{\partial}{\partial s}. \quad \text{(B.25)}$$

We can then calculate the integral over the derivative as

$$\int_0^\beta \mathrm{d}s\partial_s G(s)=G(s=\beta)-G(s=0)=-\frac{K}{2\pi}\ln b, \quad \text{(B.26)}$$

since $G(\beta)\to 0$ as $\beta\to\infty$.

Using this together with the approximation for the sine, the fifth second-order term of the cumulant expansion is

$$
\begin{aligned}
-\int \mathrm{d}\tau\mathrm{d}\tau' \frac{iAC}{2a_0 v} \left(\left\langle \cos[2\sqrt{\pi}\varphi(\tau)]\partial_{\tau'}\varphi(\tau') \right\rangle - \left\langle \cos[2\sqrt{\pi}\varphi(\tau)] \right\rangle \left\langle \partial_{\tau'}\varphi(\tau') \right\rangle \right) \\
\approx -\int \mathrm{d}s\mathrm{d}T \frac{iAC\sqrt{\pi}}{a_0 v} \sin[2\sqrt{\pi}\varphi_s(T)]\partial_s G(s) e^{-2\pi G(0)} \\
= \int \mathrm{d}T \frac{iAC\sqrt{\pi}}{a_0 v} \sin[2\sqrt{\pi}\varphi_s(T)] \frac{K}{2\pi} \ln b e^{-K\ln b} \\
= \int \mathrm{d}T \frac{iAC}{2a_0 v\sqrt{\pi}} \sin[2\sqrt{\pi}\varphi_s(T)](K\ln b) e^{-K\ln b} \\
\approx \int \mathrm{d}T \frac{iAC}{2a_0 v\sqrt{\pi}} \sin[2\sqrt{\pi}\varphi_s(T)] \left(e^{K\ln b} - 1 \right) e^{-K\ln b} \\
= \int \mathrm{d}T \frac{iAC}{2a_0 v\sqrt{\pi}} \sin[2\sqrt{\pi}\varphi_s(T)] \left(1 - \left(\frac{1}{b} \right)^K \right). \quad \text{(B.27)}
\end{aligned}
$$

Turning to the term proportional to CA instead, the derivative of the Green's function in eq. (B.24) is changed into

$$
\partial_\tau \left\langle \varphi(\tau)\varphi(\tau') \right\rangle = \partial_s \left\langle \varphi(\tau)\varphi(\tau') \right\rangle, \quad \text{(B.28)}
$$

changing the minus sign to a plus sign in eq. (B.26), thereby compensating for the minus sign when going from AC to $CA = -AC$.

B.1.6 Sixth term (BC)

Finally, the term proportional to BC is

$$
\begin{aligned}
-\frac{1}{2}\int \mathrm{d}\tau\mathrm{d}\tau' \frac{iBC}{a_0 v} \left(\left\langle \sin[2\sqrt{\pi}\varphi(\tau)]\partial_{\tau'}\varphi(\tau') \right\rangle - \left\langle \sin[2\sqrt{\pi}\varphi(\tau)] \right\rangle \left\langle \partial_{\tau'}\varphi(\tau') \right\rangle \right) \\
= -\int \mathrm{d}\tau\mathrm{d}\tau' \frac{iBC}{2a_0 v} \left\langle \sin[2\sqrt{\pi}\varphi(\tau)]\partial_{\tau'}\varphi_f(\tau') \right\rangle. \quad \text{(B.29)}
\end{aligned}
$$

The same calculation as for the AC term, with the cosine replaced by a sine, gives us

$$
\begin{aligned}
&\left\langle \sin[2\sqrt{\pi}\varphi(\tau)]\partial_{\tau'}\varphi_f(\tau') \right\rangle \\
&\qquad = 2\sqrt{\pi}\cos[2\sqrt{\pi}\varphi_s(\tau)]\partial_{\tau'} \left\langle \varphi_f(\tau')\varphi_f(\tau) \right\rangle e^{-2\pi\left\langle \varphi_f^2(\tau) \right\rangle}. \quad \text{(B.30)}
\end{aligned}
$$

We can thus approximate the last second-order term of the cumulant expansion with

$$-\int \mathrm{d}\tau\mathrm{d}\tau' \frac{iBC}{2a_0 v}\left(\left\langle \sin[2\sqrt{\pi}\varphi(\tau)]\partial_{\tau'}\varphi(\tau')\right\rangle - \left\langle \sin[2\sqrt{\pi}\varphi(\tau)]\right\rangle \left\langle \partial_{\tau'}\varphi(\tau')\right\rangle\right)$$
$$\approx -\int \mathrm{d}T \frac{iBC}{2a_0 v\sqrt{\pi}} \cos[2\sqrt{\pi}\varphi_s(T)]\left(1-\left(\frac{1}{b}\right)^K\right). \quad \text{(B.31)}$$

The CB term is equal to most of the BC terms by the same arguments as for the CA term. However, since

$$BC = \frac{1}{\pi^{3/2}}\left(J'_y J'_z S^{y'} S^{z'} + J'_y J_{E2}(S^{y'})^2 + J_{E1} J'_z (S^{z'})^2 + J_{E1} J_{E2} S^{z'} S^{y'}\right), \quad \text{(B.32)}$$

there are two terms that don't get a minus sign when replacing BC with CB. When adding the term proportional to CB to eq. (B.31), the terms with $(S^{y'})^2$ and $(S^{z'})^2$ cancel out, while the ones proportional to $S^{y'}S^{z'}$ and $S^{z'}S^{y'}$ stay.

B.2 Rescaling

The important parts of the cumulant expansion in eq. (6.19) were in Appendix B found to be

$$\langle S_K\rangle_f = \int \mathrm{d}\tau \left(\frac{1}{b}\right)^K \left(\frac{A}{a_0}\cos[2\sqrt{\pi}\varphi_s(\tau)] + \frac{B}{a_0}\sin[2\sqrt{\pi}\varphi_s(\tau)]\right) \quad \text{(B.33)}$$

and

$$-\frac{1}{2}\left(\left\langle S_K^2\right\rangle_f - \langle S_K\rangle_f^2\right) \approx \int \mathrm{d}\tau \frac{AB\sqrt{\pi}}{2v^2}\partial_\tau\varphi_s(\tau)\left(\left(\frac{1}{b}\right)^{-2} - \left(\frac{1}{b}\right)^{2K-2}\right)$$
$$-\int \mathrm{d}\tau \frac{iBC}{a_0 v\sqrt{\pi}}\cos[2\sqrt{\pi}\varphi_s(\tau)]\left(1-\left(\frac{1}{b}\right)^K\right)$$
$$+\int \mathrm{d}\tau \frac{iAC}{a_0 v\sqrt{\pi}}\sin[2\sqrt{\pi}\varphi_s(\tau)]\left(1-\left(\frac{1}{b}\right)^K\right). \quad \text{(B.34)}$$

We now perform the rescaling. When we rescale the high frequency cut-off Λ to $\Lambda' = \Lambda/b$, we must at the same time rescale the frequency parameter ω to $\omega' = \omega b$ and therefore also the imaginary time parameter τ to $\tau' = \tau/b$. We choose the rescaled fields to be $\phi'(\tau') = \phi_s(\tau)$

(and hence $\phi'(\omega') = \phi(\omega)/b$). It is important now to note that a_0, the penetration depth of the edge states, is the short distance cutoff, so that $\Lambda = v/a_0$. This means that the rescaling of Λ is *automatically* a rescaling of a_0. The rescaled cumulant expansion is thus:

$$\begin{aligned}\langle S_K\rangle_f &= \int b\mathrm{d}\tau' \left(\frac{1}{b}\right)^K \left(\frac{A}{a_0'}\cos[2\sqrt{\pi}\varphi'(\tau')] + \frac{B}{a_0'}\sin[2\sqrt{\pi}\varphi'(\tau')]\right) \\ &= \int \mathrm{d}\tau' \left(\frac{1}{b}\right)^{K-1} \left(\frac{A}{a_0'}\cos[2\sqrt{\pi K}\phi'(\tau')] + \frac{B}{a_0'}\sin[2\sqrt{\pi K}\phi'(\tau')]\right) \quad \text{(B.35)}\end{aligned}$$

and

$$\begin{aligned}-\frac{1}{2}\left(\left\langle S_K^2\right\rangle_f - \langle S_K\rangle_f^2\right) \approx{}& \int b\mathrm{d}\tau' \frac{AB\sqrt{\pi}}{2v^2}\frac{1}{b}\partial_{\tau'}\varphi'(\tau')\left(\left(\frac{1}{b}\right)^{-2} - \left(\frac{1}{b}\right)^{2K-2}\right) \\ &- \int b\mathrm{d}\tau' \frac{iBC}{a_0' v\sqrt{\pi}}\cos[2\sqrt{\pi}\varphi'(\tau')]\left(1 - \left(\frac{1}{b}\right)^K\right) \\ &+ \int b\mathrm{d}\tau' \frac{iAC}{a_0' v\sqrt{\pi}}\sin[2\sqrt{\pi}\varphi'(\tau')]\left(1 - \left(\frac{1}{b}\right)^K\right) \\ ={}& \int \mathrm{d}\tau' \frac{AB\sqrt{\pi}}{2v^2}\partial_{\tau'}\varphi'(\tau')\left(\left(\frac{1}{b}\right)^{-2} - \left(\frac{1}{b}\right)^{2K-2}\right) \\ &- \int \mathrm{d}\tau' \frac{iBC}{a_0' v\sqrt{\pi}}\cos[2\sqrt{\pi}\varphi'(\tau')]\left(\left(\frac{1}{b}\right)^{-1} - \left(\frac{1}{b}\right)^{K-1}\right) \\ &+ \int \mathrm{d}\tau' \frac{iAC}{a_0' v\sqrt{\pi}}\sin[2\sqrt{\pi}\varphi'(\tau')]\left(\left(\frac{1}{b}\right)^{-1} - \left(\frac{1}{b}\right)^{K-1}\right). \quad \text{(B.36)}\end{aligned}$$

We need to write our rescaled cumulant expansion in terms of the coupling constants, rather than the combined expressions A, B and C. The coupling constant J_E actually multiplies two different operators, $S^{z'}\sin[2\sqrt{\pi}\varphi(\tau)]$ and $S^{y'}\partial_\tau\varphi(\tau)$. We can already see that these operators renormalise differently, so we need to explicitly divide the parts containing J_E into two parts,

$$\begin{aligned}&\frac{J_E}{a_0\pi}S^{z'}\sin[2\sqrt{\pi}\varphi(\tau)] + \frac{iJ_E}{v\sqrt{\pi}}S^{y'}\partial_\tau\varphi(\tau) \\ &\qquad = \frac{J_{E1}}{a_0\pi}S^{z'}\sin[2\sqrt{\pi}\varphi(\tau)] + \frac{iJ_{E2}}{v\sqrt{\pi}}S^{y'}\partial_\tau\varphi(\tau), \quad \text{(B.37)}\end{aligned}$$

with $J_{E1} = J_{E2} = J_E$ before the rescaling. We then have:

$$A = \frac{1}{\pi} J_x S^x \tag{B.38}$$

$$B = \frac{1}{\pi}(J'_y S^{y'} + J_{E1} S^{z'}) \tag{B.39}$$

$$C = \frac{1}{\sqrt{\pi}}(J'_z S^{z'} + J_{E2} S^{y'}), \tag{B.40}$$

so that

$$\begin{aligned} AB - BA &= \frac{2}{\pi^2}\left(J_x J'_y S^x S^{y'} + J_x J_{E1} S^x S^{z'}\right) \\ &= \frac{2i}{\pi^2}\left(J_x J'_y S^{z'} - J_x J_{E1} S^{y'}\right) \end{aligned} \tag{B.41}$$

$$\begin{aligned} AC - CA &= \frac{2}{\pi^{3/2}}\left(J_x J'_z S^x S^{z'} + J_x J_{E2} S^x S^{y'}\right) \\ &= \frac{2i}{\pi^{3/2}}\left(J_x J_{E2} S^{z'} - J_x J'_z S^{y'}\right) \end{aligned} \tag{B.42}$$

$$\begin{aligned} BC - CB &= \frac{2}{\pi^{3/2}}\left(J'_y J'_z S^{y'} S^{z'} + J_{E1} J_{E2} S^{z'} S^{y'}\right) \\ &= \frac{2i}{\pi^{3/2}}\left(J'_y J'_z - J_{E1} J_{E2}\right) S^x. \end{aligned} \tag{B.43}$$

Now we can rewrite the rescaled effective action in terms of the original coupling constants. Using the cumulant expansion, we collect the results from eqs. (B.38)-(B.43) and put them into eqs. (B.33) and (B.36). We then have that

$$\begin{aligned} \langle S_K \rangle_f = \int \mathrm{d}\tau' f_1(b,K) \Bigg(&\frac{1}{a'_0 \pi} J_x S^x \cos[2\sqrt{\pi}\varphi'(\tau')] \\ &+ \frac{1}{a'_0 \pi}(J'_y S^{y'} + J_{E1} S^{z'}) \sin[2\sqrt{\pi}\varphi'(\tau')] \Bigg) \end{aligned} \tag{B.44}$$

and

$$
\begin{aligned}
-\frac{1}{2}\left(\left\langle S_K^2\right\rangle_f - \langle S_K\rangle_f^2\right) \approx & \int \mathrm{d}\tau' \frac{AB\sqrt{\pi}}{2v^2}\partial_{\tau'}\varphi'(\tau')\left(\left(\frac{1}{b}\right)^{-2} - \left(\frac{1}{b}\right)^{2K-2}\right) \\
& - \int \mathrm{d}\tau' \frac{iBC}{a_0' v\sqrt{\pi}} \cos[2\sqrt{\pi}\varphi'(\tau')]\left(\left(\frac{1}{b}\right)^{-1} - \left(\frac{1}{b}\right)^{K-1}\right) \\
& + \int \mathrm{d}\tau' \frac{i(AC-CA)}{2a_0' v\sqrt{\pi}} \sin[2\sqrt{\pi}\varphi'(\tau')]\left(\left(\frac{1}{b}\right)^{-1} - \left(\frac{1}{b}\right)^{K-1}\right). \\
= & \int \mathrm{d}\tau' \Bigg\{ i\frac{1}{2v^2\pi^{3/2}}\left(J_x J_y' S^{z'} - J_x J_{E1} S^{y'}\right)\partial_{\tau'}\varphi'(\tau') f_2(b,K) \\
& + \frac{1}{a_0' v\pi^2}\left(J_y' J_z' - J_{E1}J_{E2}\right) S^x \cos[2\sqrt{\pi}\varphi'(\tau')] f_3(b,K) \\
& - \frac{1}{a_0' v\pi^2}\left(-J_x J_z' S^{y'} + J_x J_{E2} S^{z'}\right)\sin[2\sqrt{\pi}\varphi'(\tau')] f_3(b,K)\Bigg\} \\
= & \int \mathrm{d}\tau' \frac{1}{v\pi}\Bigg\{ f_3(b,K)(J_y' J_z' - J_{E1}J_{E2}) S^x \frac{1}{a_0'\pi}\cos[2\sqrt{\pi}\varphi'(\tau')] \\
& + f_3(b,K)(J_x J_z' S^{y'} - J_x J_{E2} S^{z'})\frac{1}{a_0'\pi}\sin[2\sqrt{\pi}\varphi'(\tau')] \\
& + f_2(b,K)\frac{1}{2}\left(J_x J_y' S^{z'} - J_x J_{E1} S^{y'}\right)\frac{i}{v\sqrt{\pi}}\partial_{\tau'}\varphi'(\tau')\Bigg\}, \qquad \text{(B.45)}
\end{aligned}
$$

where

$$
f_1(b,K) = \left(\frac{1}{b}\right)^{K-1} \qquad \text{(B.46)}
$$

$$
f_2(b,K) = \left(\frac{1}{b}\right)^{-2} - \left(\frac{1}{b}\right)^{2K-2} \qquad \text{(B.47)}
$$

$$
f_3(b,K) = \left(\frac{1}{b}\right)^{-1} - \left(\frac{1}{b}\right)^{K-1}. \qquad \text{(B.48)}
$$

Next, we write $\Lambda/b = \Lambda + \delta\Lambda$, so that

$$
\frac{1}{b} = \frac{\delta\Lambda + \Lambda}{\Lambda} = 1 + \frac{\delta\Lambda}{\Lambda}. \qquad \text{(B.49)}
$$

The different factors containing $1/b$ can thus be rewritten as

$$f_1 = \left(\frac{1}{b}\right)^{K-1} = \left(1+\frac{\delta\Lambda}{\Lambda}\right)^{K-1} \approx 1+(K-1)\frac{\delta\Lambda}{\Lambda} \tag{B.50}$$

$$\begin{aligned} f_2 = \left(\frac{1}{b}\right)^{-2} - \left(\frac{1}{b}\right)^{2K-2} &= \left(1+\frac{\delta\Lambda}{\Lambda}\right)^{-2} - \left(1+\frac{\delta\Lambda}{\Lambda}\right)^{2K-2} \\ &\approx -2\frac{\delta\Lambda}{\Lambda} - (2K-2)\frac{\delta\Lambda}{\Lambda} = -2K\frac{\delta\Lambda}{\Lambda} \end{aligned} \tag{B.51}$$

$$\begin{aligned} f_3 = \left(\frac{1}{b}\right)^{-1} - \left(\frac{1}{b}\right)^{K-1} &= \left(1+\frac{\delta\Lambda}{\Lambda}\right)^{-1} - \left(1+\frac{\delta\Lambda}{\Lambda}\right)^{K-1} \\ &\approx (-1)\frac{\delta\Lambda}{\Lambda} - (K-1)\frac{\delta\Lambda}{\Lambda} = -K\frac{\delta\Lambda}{\Lambda}. \end{aligned} \tag{B.52}$$

Comparing the original action with the cumulant expansion, we are now ready to write down the rescaled coupling constants and derive their scaling equations. We see that the rescaled effective action of eqs. (B.44) and (B.45) is identical to the one belonging to the original Hamiltonian in eq. (6.17), apart from the new cutoff and the rescaled coupling constants. As $\Lambda \to \Lambda'$, the coupling constants $J_i(\Lambda) \to \tilde{J}_i = J_i(\Lambda')$ (with $J_i = J_x, J'_y, J'_z, J_{E1}$ and J_{E2}). The coupling constants are read off by comparing the original action with the effective rescaled action.

Starting with J_x, we see that the rescaled effective action of eqs. (B.44) and (B.45) is identical to the

the factor f_1 in eq. (B.50) is the difference between the rescaled effective action of eq. (B.44) and the original action that can be read off from eq. (6.17). The coupling constant

$$\begin{aligned} \tilde{J}_x = J_x(\Lambda') &= \left(1+(K-1)\frac{\delta\Lambda}{\Lambda}\right) J_x(\Lambda) - \frac{K}{v\pi}\frac{\delta\Lambda}{\Lambda}\left(J'_y J'_z - J_{E1}J_{E2}\right) \\ \Leftrightarrow \delta J_x = J_x(\Lambda') - J_x(\Lambda) &= (K-1)\frac{\delta\Lambda}{\Lambda}J_x(\Lambda) - \frac{K}{v\pi}\frac{\delta\Lambda}{\Lambda}\left(J'_y J'_z - J_{E1}J_{E2}\right) \\ \Leftrightarrow \frac{\partial J_x}{\partial l} = -\Lambda\frac{\delta J_x}{\delta\Lambda} &= (1-K)J_x(\Lambda) + \frac{K}{v\pi}\left(J'_y J'_z - J_{E1}J_{E2}\right). \end{aligned} \tag{B.53}$$

The same procedure for J'_y yields

$$\begin{aligned} \tilde{J}'_y = J'_y(\Lambda') &= \left(1+(K-1)\frac{\delta\Lambda}{\Lambda}\right) J'_y(\Lambda) - \frac{K}{v\pi}\frac{\delta\Lambda}{\Lambda}J_x J'_z \\ \Leftrightarrow \delta J'_y = J'_y(\Lambda') - J'_y(\Lambda) &= (K-1)\frac{\delta\Lambda}{\Lambda}J'_y(\Lambda) - \frac{K}{v\pi}\frac{\delta\Lambda}{\Lambda}J_x J'_z \\ \Leftrightarrow \frac{\partial J'_y}{\partial l} = -\Lambda\frac{\delta J'_y}{\delta\Lambda} &= (1-K)J'_y(\Lambda) + \frac{K}{v\pi}J_x J'_z. \end{aligned} \tag{B.54}$$

The easiest way to extract the scaling equations for J_z' is to write

$$\begin{aligned}\tilde{J}_z' = J_z'(\Lambda') &= \left(e^{2\ln b} - e^{(2-2K)\ln b}\right)\frac{K}{v\pi}\frac{1}{2K}J_xJ_y' \\ &\approx (2K\ln b)\frac{K}{v\pi}\frac{1}{2K}J_xJ_y' \\ &\Leftrightarrow \frac{\partial J_z'}{\partial l} = \frac{\partial J_z'}{\partial \ln b} = \frac{K}{v\pi}J_xJ_y'. \quad \text{(B.55)}\end{aligned}$$

Finally, we want to extract the scaling equations for J_E, i.e. J_{E1} and J_{E2}.

$$\begin{aligned}\tilde{J}_{E1} = J_{E1}(\Lambda') &= \left(1 + (K-1)\frac{\delta\Lambda}{\Lambda}\right)J_{E1}(\Lambda) + \frac{K}{v\pi}\frac{\delta\Lambda}{\Lambda}J_xJ_{E2} \\ &\Leftrightarrow \frac{\partial J_{E1}}{\partial l} = -\Lambda\frac{\delta J_{E1}}{\delta\Lambda} = (1-K)J_{E1}(\Lambda) - \frac{K}{v\pi}J_xJ_{E2} \quad \text{(B.56)}\end{aligned}$$

and

$$\begin{aligned}\tilde{J}_{E2} = J_{E2}(\Lambda') &= -\left(e^{2\ln b} - e^{(2-2K)\ln b}\right)\frac{K}{v\pi}\frac{1}{2K}J_xJ_{E1} \\ &\approx -2K\ln b\frac{K}{v\pi}\frac{1}{2K}J_xJ_y' \\ &\Leftrightarrow \frac{\partial J_{E2}}{\partial l} = \frac{\partial J_{E2}}{\partial \ln b} = -\frac{K}{v\pi}J_xJ_{E1}. \quad \text{(B.57)}\end{aligned}$$

In summary, the scaling equations are:

$$\frac{\partial J_x(l)}{\partial l} = (1-K)J_x(l) + \frac{K}{v\pi}\left(J_y'(l)J_z'(l) - J_{E1}(l)J_{E2}(l)\right) \quad \text{(B.58)}$$

$$\frac{\partial J_y'(l)}{\partial l} = (1-K)J_y'(l) + \frac{K}{v\pi}J_x(l)J_z'(l) \quad \text{(B.59)}$$

$$\frac{\partial J_z'(l)}{\partial l} = \frac{K}{v\pi}J_x(l)J_y'(l) \quad \text{(B.60)}$$

$$\frac{\partial J_{E1}(l)}{\partial l} = (1-K)J_{E1}(l) - \frac{K}{v\pi}J_x(l)J_{E2}(l) \quad \text{(B.61)}$$

$$\frac{\partial J_{E2}(l)}{\partial l} = -\frac{K}{v\pi}J_x(l)J_{E1}(l). \quad \text{(B.62)}$$

Bibliography

[1] L. D. Landau, *The theory of a fermi liquid*, Sov. Phys. JETP **3**, 920–925 (1957).

[2] S. Tomonaga, *Remarks on Bloch's method of sound waves applied to many-fermion problems*, Prog. Theor. Phys. **5**, 544–569 (1950).

[3] J. Luttinger, *An Exactly Soluble Model Of A Many-Fermion System*, J. Math. Phys. **4**, 1154–& (1963).

[4] P. W. Anderson, *Absence of diffusion in certain random lattices*, Phys. Rev. **109**, 1492 (1958).

[5] L. D. Landau and E. M. Lifschitz, *Statistical physics vol.1, 3rd edition.* Butterworth-Heinemann, 1980.

[6] D. Thouless, M. Kohmoto, M. Nightingale and M. den Nijs, *Quantized Hall conductance in a two-dimensional periodic potential*, Phys. Rev. Lett. **49**, 405 (1982).

[7] X.-G. Wen and Q. Niu, *Ground-state degeneracy of the fractional quantum Hall states in the presence of a random potential and on high-genus Riemann surfaces*, Phys. Rev. B **41**, 9377 (1990).

[8] M. Z. Hasan and C. L. Kane, *Topological insulators*, Rev. Mod. Phys. **82**, 3045 (2010).

[9] X.-L. Qi and S.-C. Zhang, *Topological insulators and superconductors*, `arXiv:1008.2026`.

[10] C. Kane and E. J. Mele, *The quantum spin Hall effect in graphene*, Phys. Rev. Lett. **95**, 226801 (2005).

[11] M. König, S. Wiedmann, C. Bruene, A. Roth, H. Buhmann, L. W. Molenkamp, X.-L. Qi and S.-C. Zhang, *Quantum spin Hall insulator state in HgTe quantum wells*, Science **318**, 766 (2007).

[12] B. A. Bernevig and S.-C. Zhang, *Toward dissipationless spin transport in semiconductors*, IBM J. Res. & Dev. **50**, 141 (2006).

[13] L. Fu and C. L. Kane, *Topological insulators with inversion symmetry*, Phys. Rev. B **76**, 045302 (2007).

[14] D. Hsieh, D. Qian, L. Wray, Y. Xia, Y. S. Hor, R. J. Cava and M. Z. Hasan, *A topological Dirac insulator in a quantum spin Hall phase*, Nature **452**, 970 (2008).

[15] Y. Xia, D. Qian, D. Hsieh, L. Wray, A. Pal, H. Lin, A. Bansil, D. Grauer, Y. S. Hor, R. J. Cava and M. Z. Hasan, *Observation of a large-gap topological-insulator class with a single Dirac cone on the surface*, Nature Physics **5**, 398 (2009).

[16] H. Zhang, C.-X. Liu, X.-L. Qi, X. Dai, Z. Fang and S.-C.-Zhang, *Topological insulators in Bi2Se3, Bi2Te3 and Sb2Te3 with a single Dirac cone on the surface*, Nature Physics **5**, 438 (2009).

[17] A. Kitaev, *Periodic table for topological insulators and superconductors*, AIP Conf. Proc. **1134**, 22 (2009).

[18] X.-L. Qi, T. Hughes, S. Raghu and S.-C. Zhang, *Time-reversal-invariant topological superconductors and superfluids in two and three dimensions*, Phys. Rev. Lett. **102**, 187001 (2009).

[19] R. Roy, *Topological superfluids with time reversal symmetry*, `arXiv:0803.2868`.

[20] A. P. Schnyder, S. Ryu, A. Furusaki and A. W. W. Ludwig, *Classification of topological insulators and superconductors in three spatial dimensions*, Phys. Rev. B **78**, 195125 (2008).

[21] P. Streda and P. Seba, *Antisymmetric spin filtering in one-dimensional electron systems with uniform spin-orbit coupling*, Phys. Rev. Lett. **90** (jun 27, 2003).

[22] B. Braunecker, C. Bena and P. Simon, *Spectral properties of Luttinger liquids: a comparative analysis of regular, helical, and spiral Luttinger liquids*, Phys. Rev. B **85** (jan 31, 2012).

[23] A. Ström and H. Johannesson, *Tunneling between edge states in a quantum spin Hall system*, Phys. Rev. Lett. **102**, 096806 (2009).

[24] A. Ström, H. Johannesson and G. I. Japaridze, *Edge dynamics in a quantum spin Hall state: effects from Rashba spin-orbit interaction*, Phys. Rev. Lett. **104**, 256804 (2010).

[25] B. Braunecker, A. Ström and G. Japaridze, *Magnetic-field switchable metal-insulator transitions in a quasi-helical conductor*, `arXiv:1206.5844`.

[26] E. Eriksson, A. Ström, G. Sharma and H. Johannesson, *Electrical control of the kondo effect in a helical edge liquid*, `arXiv:1207.3028`.

[27] A. Ström, *Interactions on the edge of a quantum spin Hall insulator* (licentiate thesis). Göteborgs universitet, 2011.

[28] M. Nakahara, *Geometry, Topology and Physics*. Institute of Physics Publishing, 2003.

[29] A. Altland and B. Simons, *Condensed matter field theory*. Cambridge University Press, 2007.

[30] D. C. Tsui, H. L. Stormer and A. C. Gossard, *Two-dimensional magnetotransport in the extreme quantum limit*, Phys. Rev. Lett. **48**, 1559 (1982).

[31] H. Kramers, *Théorie générale de la rotation paramagnétique dans les cristaux*, Proc. Acad. Sci. Amsterdam **33**, 959 (1930).

[32] Z. Wang, X.-L. Qi and S.-C. Zhang, *Equivalent topological invariants of topological insulators*, New J. Phys. **12**, 065007 (2010).

[33] S.-C. Zhang, *The Chern-Simons-Landau-Ginzburg theory of the fractional quantum Hall effect*, Int. J. Mod. Phys. B **6**, 25 (1992).

[34] S.-C. Zhang and J. Hu, *A four-dimensional generalisation of the quantum Hall effect*, Science **26**, 823 (2001).

[35] X.-L. Qi, T. L. Hughes and S.-C. Zhang, *Topological field theory of time-reversal invariant insulators*, Phys. Rev. B **78**, 195424 (2008).

[36] M. König, H. Buhmann, L. Molenkamp, T. Hughes, C.-X. Liu, X.-L. Qi and S.-C. Zhang, *The quantum spin Hall effect: theory and experiment*, J. Phys. Soc. Jpn. **77**, 031007 (2008).

[37] T. H. Andrei Bernevig and S.-C. Zhang, *Quantum spin Hall effect and topological phase transition in HgTe quantum wells*, Science **314**, 1757 (2006).

[38] A. Zee, *Quantum field theory in a nutshell*. Princeton University Press, 2003.

[39] J. Solyom, *Fermi gas-model of one-dimensional conductors*, Adv. Phys. **28**, 201–303 (1979).

[40] T. Giamarchi, *Quantum physics in one dimension*. Oxford Science Publications, 2003.

[41] D. Senechal, *An introduction to bosonization*, in *Theoretical methods for strongly correlated electrons*, D. Senechal, A.M. Tremblay and C. Bourbonnais, ed., CRM series in mathematical physics, pp. 139–186. 2004. Workshop on theoretical methods for strongly correlated electrons, Univ Montreal, Ctr. Rech. Math., Montreal, Canada, May 26-30, 1999.

[42] S. Coleman, *Quantum sine-gordon equation as the massive thirring model*, Phys. Rev. D **11**, 2088–2097 (Apr, 1975).

[43] K. Wilson, *Renormalization group - critical phenomena and Kondo problem*, reviews of modern physics **47**, 773–840 (1975).

[44] F. Dolcini, *Full electrical control of charge and spin conductance through interferometry of edge states in topological insulators*, Phys. Rev. B **83** (apr 7, 2011).

[45] M. P. Fisher and W. Zwerger, *Quantum brownian motion in a periodic potential*, Phys. Rev. B **32**, 6190 (1985).

[46] A. Furusaki and N. Nagaosa, *Single-barrier problem and Anderson localization in a one-dimensional interacting electron-system*, Phys. Rev. B **47**, 4631 (1993).

[47] J. C. Y. Teo and C. L. Kane, *Critical behavior of a point contact in a quantum spin Hall insulator*, Phys. Rev. B **79** (2009).

[48] C.-Y. Hou, E.-A. Kim and C. Chamon, *Corner Junction as a Probe of Helical Edge States*, Phys. Rev. Lett. **102** (FEB 20, 2009).

[49] J. Maciejko, C. Liu, Y. Oreg, X.-L. Qi, C. Wu and S.-C. Zhang, *Kondo effect in the helical edge liquid of the quantum spin Hall state*, Phys. Rev. Lett. **102** (jun 26, 2009).

[50] A. Roth, C. Bruene, H. Buhmann, L. W. Molenkamp, J. Maciejko, X.-L. Qi and S.-C. Zhang, *Nonlocal transport in the quantum spin Hall state*, Science **325**, 294 (2009).

[51] W. Häusler, L. Kecke and A. MacDonald, *Tomonaga-Luttinger parameters for quantum wires*, Phys. Rev. B **65**, 085104 (2002).

[52] G. D. Mahan, *Many-particle physics, 3rd edition.* Kluwer Academic/Plenum Publishers, 2000.

[53] X.-G. Wen, *Edge transport-properties of the fractional quantum Hall states and weak-impurity scattering of a one-dimensional charge-density wave*, Phys. Rev. B **44**, 5708 (1991).

[54] D. Goren, G. Asa and Y. Nemirovsky, *Barrier formation at graded HgTe/CdTe heterojunctions*, J. Appl. Phys. **80**, 5083 (1996).

[55] R. Winkler, *Spin-orbit coupling effects in two-dimensional electron and hole systems.* Springer, 2003.

[56] E. Sherman, *Minimum of spin-orbit coupling in two-dimensional structures*, Phys. Rev. B **67** (2003).

[57] E. Y. Sherman and J. Sinova, *Physical limits of the ballistic and nonballistic spin-field-effect transistor: Spin dynamics in remote-doped structures*, Phys. Rev. B **72**, 075318 (2005).

[58] L. Golub and E. Ivchenko, *Spin splitting in symmetrical SiGe quantum wells*, PHYSICAL REVIEW B **69** (MAR, 2004).

[59] G. I. Japaridze, H. Johannesson and A. Ferraz, *Metal-insulator transition in a quantum wire driven by a modulated Rashba spin-orbit coupling*, Phys. Rev. B **80**, 041308 (2009).

[60] T. Giamarchi and H. J. Schulz, *Anderson location and interactions in one-dimensional metals*, Phys. Rev. B **37**, 325 (1988).

[61] A. Efros and B. Shklovskii, *Electronic properties of doped semiconductors.* Springer, 1989.

[62] M. Mezard, G. Parisi and M. Virasoro, *Spin glass theory and beyond.* World Scientific, 1986.

[63] T. Giamarchi and P. Le Doussal, *Variational theory of elastic manifolds with correlated disorder and localization of interacting quantum particles*, Phys. Rev. B **53**, 15206 (1996).

[64] T. Giamarchi and E. Orignac, *Disordered quantum solids*, `arXiv:cond-mat/0005220`.

[65] C. Wu, B. Bernevig and S. Zhang, *Helical liquid and the edge of quantum spin Hall systems*, Phys. Rev. Lett. **96** (2006).

[66] C. Xu and J. Moore, *Stability of the quantum spin Hall effect: effects of interactions, disorder, and Z(2) topology*, Phys. Rev. B **73** (2006).

[67] M. König, C. Becker and L. Molenkamp, *Phase effects in HgTe quantum structures*, Phys. Stat. Sol. (c) **4**, 3374 (2007).

[68] M. König. *Private communication.*

[69] F. Crépin, J. C. Budich, F. Dolcini, P. Recher and B. Trautzettel, *Renormalization group approach for the scattering off a single rashba impurity in a helical liquid*, `arXiv:1205.0374`.

[70] X. Wang, *Spin transport of electrons through quantum wires with a spatially modulated Rashba spin-orbit interaction*, Phys. Rev. B **69**, 035302 (2004).

[71] M. Malard, I. Grusha, G. I. Japaridze and H. Johannesson, *Modulated Rashba interaction in a quantum wire: spin and charge dynamics*, Phys. Rev. B **84** (aug 12, 2011).

[72] N. F. Mott, *The basis of the electron theory of metals, with special reference to the transition metals*, Proc. Phys. Soc. Sect. A **62**, 416 (1949).

[73] C. H. L. Quay, T. L. Hughes, J. A. Sulpizio, L. N. Pfeiffer, K. W. Baldwin, K. W. West, D. Goldhaber-Gordon and R. de Picciotto, *Observation of a one-dimensional spin-orbit gap in a quantum wire*, NATURE PHYSICS **6**, 336–339 (MAY, 2010).

[74] B. Braunecker, P. Simon and D. Loss, *Nuclear magnetism and electron order in interacting one-dimensional conductors*, Phys. Rev. B **80** (oct, 2009).

[75] B. Braunecker, G. I. Japaridze, J. Klinovaja and D. Loss, *Spin-selective Peierls transition in interacting one-dimensional conductors with spin-orbit interaction*, Phys. Rev. B **82** (jul 29, 2010).

[76] B. Braunecker, P. Simon and D. Loss, *nuclear magnetism and electronic order in c-13 nanotubes*, Phys. Rev. Lett. **102** (mar 20, 2009).

[77] C. Fasth, A. Fuhrer, L. Samuelson, V. N. Golovach and D. Loss, *direct measurement of the spin-orbit interaction in a two-electron inas nanowire quantum dot*, Phys. Rev. Lett. **98** (jun 29, 2007).

[78] W. J. de Haas, J. de Boer and G. J. van den Berg, *The electrical resistance of gold, copper and lead at low temperatures*, Physica **1**, 1115–1124 (1934).

[79] J. Kondo, *Resistance minimum in dilute magnetic alloys*, Prog. Theor. Phys. **32**, 37–& (1964).

[80] P. W. Anderson, *Poor man's derivation of scaling laws for Kondo problem*, J. Phys. C: Solid State Physics **3**, 2436–& (1970).

[81] N. Andrei, *Diagonalization of the Kondo-Hamiltonian*, Phys. Rev. Lett. **45**, 379–382 (1980).

[82] P. B. Wiegmann JETP Letters **31**, 392 (1980).

[83] I. Affleck and A. W. W. Ludwig, *Critical-theory of overscreened Kondo fixed-points*, Nucl. Phys. B **360**, 641–696 (aug 19, 1991).

[84] R. Zitko and J. Bonca, *Kondo effect in the presence of Rashba spin-orbit interaction*, Phys. Rev. B **84** (nov 28, 2011).

[85] J. I. Väyrynen and T. Ojanen, *Electrical manipulation and measurement of spin properties of quantum spin Hall edge states*, Phys. Rev. Lett. **106** (FEB 18, 2011).

[86] C. L. Kane and M. P. A. Fisher, *Transmission through barriers and resonant tunneling in an interacting one-dimensional electron-gas*, Phys. Rev. B **46**, 15233–15262 (DEC 15, 1992).

[87] Y. Tanaka, A. Furusaki and K. A. Matveev, *conductance of a helical edge liquid coupled to a magnetic impurity*, Phys. Rev. Lett. **106** (jun 9, 2011).

[88] S. Datta, J. K. Furdyna and R. L. Gunshor, *Diluted Magnetic Semiconductor Superlattices And Heterostructures*, Superlattice Microst. **1**, 327–334 (1985).

[89] O. Ujsaghy and A. Zawadowski, *Spin-orbit-induced magnetic anisotropy for impurities in metallic samples. i. surface anisotropy*, Phys. Rev. B **57**, 11598–11608 (may 1, 1998).

[90] A. L. Efros and B. I. Shklovskii, *Electronic properties of doped semiconductors*. Springer, 1989.

[91] J. Alicea, *New directions in the pursuit of majorana fermions in solid state systems*, `arXiv:1202.1293`.

[92] K. Sato, D. Loss and Y. Tserkovniak, *Cooper-pair injection into quantum spin hall insulators*, Phys. Rev. Lett. **105**, 226401 (2010).

[93] V. Mourik, K. Zuo, S. M. Frolov, S. R. Plissard, E. P. A. M. Bakkers and L. P. Kouwenhoven, *Signatures of majorana fermions in hybrid superconductor-semiconductor nanowire devices*, `arXiv:1204:2792`.

[94] M. T. Deng, C. L. Yu, G. Y. Huang, M. Larsson, P. Caroff and H. Q. Xu, *Observation of majorana fermions in a nb-insb nanowire-nb hybrid quantum device*, `arXiv:1204.4130`.

Paper I

Tunneling between edge states in a quantum spin Hall system

Anders Ström and Henrik Johannesson
Physical Review Letters **102**, 096806 (2009).

Paper II

Edge dynamics in a quantum spin Hall state: effects from Rashba spin-orbit interaction

Anders Ström, Henrik Johannesson and George Japaridze
Physical Review Letters **104**, 256804 (2010).

Paper III

Magnetic-field switchable metal-insulator transitions in a quasi-helical conductor

Bernd Braunecker, Anders Ström and George Japaridze
arXiv:1206.5844

Paper IV

Electrical control of the Kondo effect in a helical edge liquid

Erik Eriksson, Anders Ström, Girish Sharma and Henrik Johannesson
arXiv:1207.3028